

**DOTTORATO DI RICERCA IN
Biodiversità ed Evoluzione**

Ciclo XXIV

Settore Concorsuale di riferimento: 05/B1 - Zoologia e Antropologia

Settore Scientifico-Disciplinare di afferenza: BIO/05 - Zoologia

**“Mitochondrial inheritance and germ line
determination in a bivalve species with
Doubly Uniparental Inheritance (DUI)”**

Presentata da: Dott.ssa Liliana Milani

**Coordinatore Dottorato
Prof. Barbara Mantovani**

**Relatore
Dr Marco Passamonti**

INDEX

1 – INTRODUCTION	Pp. 1-27
1.1 – Germ line determination in metazoans	1-5
1.2 – Germ line formation in Spiralia	6-7
1.3 – Mitochondria and germ line formation	8-10
1.4 – The mitochondrial bottleneck	11-13
1.5 – Doubly Uniparental Inheritance (DUI) of mitochondria	13-24
1.5.1 – Distribution of the sex-linked mtDNAs in tissues and gametes of DUI species	17-18
1.5.2 – DUI as a model system	18
1.5.3 – Mitochondrial segregation patterns in DUI species	19-21
1.5.4 – Sex-ratio distortion and DUI	21-22
1.5.5 –The W/X/Z/S system	22
1.5.6 – Novel mitochondrial ORFs can be related to DUI functioning	22-24
1.6 – The analyzed species: development and reproductive biology	24-26
1.7 – Performed analyses	27
2 – MATERIALS AND METHODS	Pp. 28-40
2.1 – Sampling and spawning induction	28-30
2.2 – TEM sample preparation	30-31
2.3 – SEM sample preparation	31

2.4 – MitoTracker staining	31-32
2.5 – SDS-PAGE and western blotting	32-33
2.6 – <i>vasa</i>-homolog	33
2.7 – Tissue processing and immunocytochemical analyses	33-35
2.7.1 – Embryos	33-34
2.7.1.2 – <i>Vasa immunostaining</i>	34
2.7.1.3 – <i>Microtubule immunostaining</i>	34
2.7.2 – Gonads	35
2.7.2.1 – <i>Microfilament staining</i>	35
2.8 – Analysis of transcripts with sex and family biases	35-36
2.9 – <i>In situ</i> hybridization	36-40
2.9.1 – Riboprobe construction	36-38
2.9.2 – Tissue fixation and section preparation	38-39
2.9.3 – Digestion, acetylation and permeabilization	39
2.9.4 – Hybridization	39-40
2.9.5 – Alkaline phosphatase color reaction	40
3 – RESULTS	Pp. 41-72
3.1 – Sperm morphology and localization of M mitochondria during embryo development	41-47
3.2 – Gonad morphology	47-50
3.3 – <i>R. philippinarum vasa</i>-homolog	51-56

3.4 – Distribution of microtubules and spermatozoon mitochondria in early embryos	56-59
3.5 – Mitochondrial genes and ORF-MUR21 expression	60-63
3.6 – Functional domains of inferred protein	64-66
3.7 – <i>In situ</i> hybridization	66-72
4 – DISCUSSION	Pp. 73-103
4.1 – Patterns of spermatozoon mitochondria distribution in early embryos of <i>R. philippinarum</i>	73-74
4.2 – Mitochondrial inheritance and mitochondrial bottleneck in <i>R. philippinarum</i>	74-78
4.3 – Mitochondrial DNA replication in <i>R. philippinarum</i> early embryo development	78-80
4.4 – Unusual and conserved features of germ cells in DUI organisms	80-81
4.5 – Vasp and germ line formation	81-83
4.6 – Spermatozoon mitochondria and male germ line formation	83-86
4.7 – “MtRPH-21”: a mitochondrial tag for sex-specific mitochondrial transmission?	86-87
4.8 – Sex-determining factors: characterization and localization	88-94
4.8.1 – The proteasomal machinery: PSA	90-91
4.8.2 – Inhibitors of Apoptosis Protein: BIRING	91-93
4.8.3 – Ubiquitin fusion proteins: ANUBL1	93-94
4.9 – Post-transcriptional regulation of sex-determining factors?	94-95

4.10 – A sex-determination model	96-97
4.11 – Ubiquitination factors in mitochondrial transmission	98-100
4.12 – Conclusions and perspectives	101-103

5 - REFERENCES	Pp. 104-127
-----------------------	-------------

6 - LIST OF PUBLISHED PAPERS	Pp. 128-129
-------------------------------------	-------------

INDEX of FIGURES & TABLES

INTRODUCTION	Pag.
Fig. 1 – Different <i>Xenopus</i> oocyte stages in which germ plasm is localized to the vegetal hemisphere.	2
Fig. 2 – Nuage in a spermatogonium (TEM).	3
Fig. 3 – Nuage in an oogonium (TEM).	3
Fig. 4 – The Balbiani body.	4
Fig. 5 – Chromatoid body in a spermatid at the initial phase of the spermiogenesis.	5
Fig. 6 – Phylogenetic relationships of Spiralia.	6
Fig. 7 – Spiral segmentation scheme.	7
Fig. 8 – (1) TEM of mitochondria–nuage complexes in spermatogonia of the sea urchin <i>Anthocidaris crassispina</i> . (2) TEM of mitochondria–nuage complexes in <i>Drosophila</i> embryos.	9
Fig. 9 – Ultrastructure of <i>Caedibacter</i> , endosymbiont related to the Rickettsiales.	10
Fig. 10 – Mitochondrial bottleneck scheme.	12
Fig. 11 – Doubly Uniparental Inheritance (DUI) of mitochondrial DNA.	14
Fig. 12 – The taxonomic position of species currently known to have DUI.	16
Fig. 13 – Distribution patterns of spermatozoon mitochondria in the DUI species <i>Mytilus edulis</i> .	20
Fig. 14 – <i>Ruditapes philippinarum</i> Adams and Reeve.	25
Fig. 15 – <i>R. philippinarum</i> testis morphology.	26

MATERIALS AND METHODS	Pag.
Fig. 16 – <i>R. philippinarum</i> specimen preparation.	28
Fig. 17 – <i>R. philippinarum</i> spawning induction.	29
Table 1 – Transcripts target of <i>in situ</i> riboprobes.	37

RESULTS	Pag.
Fig. 18 – Gamete morphological analysis by TEM.	41
Fig. 19 – Light microscopy of live <i>R. philippinarum</i> embryos during segmentation.	42-43
Fig. 20 – <i>R. philippinarum</i> embryo development (SEM).	43-44
Fig. 21 – Distribution of spermatozoon mitochondria.	45-46
Fig. 22 – Morphological analysis of female and male gonads in <i>R. philippinarum</i> (TEM).	48
Fig. 23 – Ultrastructural analysis of the Balbiani body formation in <i>R. philippinarum</i> (TEM).	49
Fig. 24 – Ultrastructural analysis of the Chromatoid body formation in <i>R. philippinarum</i> (TEM).	50
Fig. 25 – Specificity of the anti-Cvh antibody.	51
Fig. 26 – Vasa alignment.	52
Fig. 27 – Vasph domains.	53
Fig. 28 – Vasph immunolocalization with anti-Cvh during <i>R. philippinarum</i> gonad differentiation.	54-55
Fig. 29 – Vasph immunolocalization with anti-Cvh in <i>R. philippinarum</i> embryos.	56
Fig. 30 – Distribution patterns of spermatozoon mitochondria and microtubules in	57

R. philippinarum male early embryos.

Fig. 31 – Segregation scheme of spermatozoon mitochondria in DUI male embryos.	58
Fig. 32 – Ultrastructural analysis of <i>R. philippinarum</i> male early embryos.	59
Fig. 33 – <i>R. philippinarum</i> M-type mitochondrial DNA.	60
Fig. 34 – MUR21 nucleotide alignment.	61
Fig. 35 – ORF-MUR21 putative protein alignment.	62
Table 2 – Expression of coding genes of <i>R. philippinarum</i> M-type mtDNA compared with the ORF-21 expression in males.	63
Fig. 36 – Expression of coding genes of <i>R. philippinarum</i> M-type mtDNA.	63
Fig. 37 – Conserved functional domains of ORF-21 inferred protein.	64
Fig. 38 – Conserved functional domains of PSA inferred protein.	65
Fig. 39 – Conserved functional domains of BIRING inferred protein.	65
Fig. 40 – Conserved functional domains of ANUBL1 inferred protein.	66
Fig. 41 – Morphology and localization of gonadic tissue.	67
Table 3 – Means of FPKM (fragments per kilobase of exon per million fragments mapped) of analyzed transcripts.	68
Table 4 – Transcript staining in <i>R. philippinarum</i> gonadic tissue.	68
Fig. 42 – ORF-21 expression in male gonad and surrounding tissues.	69
Fig. 43 – <i>psa</i> expression in gonad and surrounding tissues.	70
Fig. 44 – <i>biring</i> expression in gonad and surrounding tissues.	71
Fig. 45 – <i>anubl1</i> expression in gonad and surrounding tissues.	72

DISCUSSION

Pag.

Fig. 48 – Proposed model for germ line mitochondria selection under DUI.	77
---	----

Fig. 49 – Proteasome complex structure.	91
Fig. 50 – Mammalian IAPs/BIRPs.	92
Fig. 51 – A simplified model for DUI and sex-determination.	96-97
Fig. 52 – Ubiquitin factors in the transmission of spermatozoon mitochondria.	100

1 – INTRODUCTION

As often happens in biology, the study of “exceptions” might be the highroad to unravel how the “rule” works. In this conception, I think the unusual mechanism of mitochondrial transmission known as DUI (Doubly Uniparental Inheritance; Skibinski et al. 1994a,b; Zouros et al. 1994a,b) would be the experimental system of choice to investigate some of the basics of biology, such as sex evolution and determination, as well as mitochondria inheritance, dynamics and functions. My PhD Thesis is focused on the characterization of germ line formation and mitochondrial inheritance in a DUI species, *Ruditapes philippinarum* (Bivalvia, Veneridae).

1.1 – Germ line determination in metazoans

The origin of Primordial Germ Cells (PGCs) is a central issue in developmental biology. In many animals, cells receiving germ plasm during the first embryonic divisions give rise to PGCs (Eddy 1975; Illmensee et al. 1976; Rongo and Lehmann 1996; Ikenishi 1998; Saffman and Lasko 1999; Wylie 1999; Matova and Cooley 2001; Becalska and Gavis 2010). The germ plasm is a specific part of the egg cytoplasm (Fig. 1), whose composition is similar in widely divergent phyla: it mainly contains proteins from conserved germ cell-specific genes and RNAs, both messenger RNAs (mRNAs) and non-coding RNAs (ncRNAs), used for translation when post-transcriptional processing reactivates after fertilization (Kloc et al. 2001; Kloc et al. 2004; Kloc and Etkin 2005).

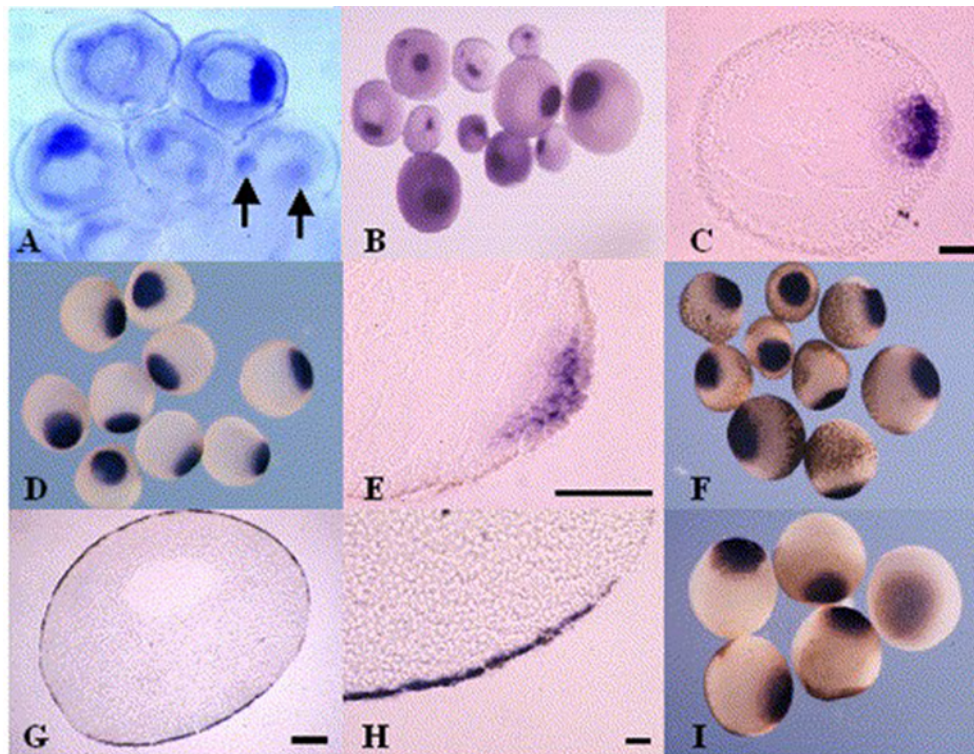


Fig. 1 – Different *Xenopus* oocyte stages in which germ plasm is localized to the vegetal hemisphere. (A-I) The germ line is here visualized by labeling a specific marker, the *DEADSouth* RNA, a member of a small sub-family of the DEAD-box RNA-dependent helicases related to eIF4A. (C,E,H) bars = 20 μ m; (G) bar = 100 μ m. (Image from MacArthur et al. 2000).

A typical component of germ plasm is the DEAD-box RNA helicase Vasa, firstly characterized in *Drosophila melanogaster* (Hay et al. 1988a,b), then isolated in many invertebrates and vertebrates (Gustafson and Wessel 2010). Inactivation of this helicase suppresses the formation of PGCs (Lasko and Ashburner 1988; Williamson and Lehmann 1996; Knaut et al. 2000; Kuznicki et al. 2000). Interestingly, the aggregation of *vasa* products in the germ plasm appears to occur either at protein or transcript level, depending on the organism (Raz 2000). Germ plasm can be identified with Transmission Electron Microscopy (TEM) by the presence of electron-dense granulofibrillar material which is called “nuage”, often positioned near the nucleus and associated with mitochondria (Matova and Cooley 2001; Kloc et al. 2004; Reunov 2006) (Figs 2 and 3).

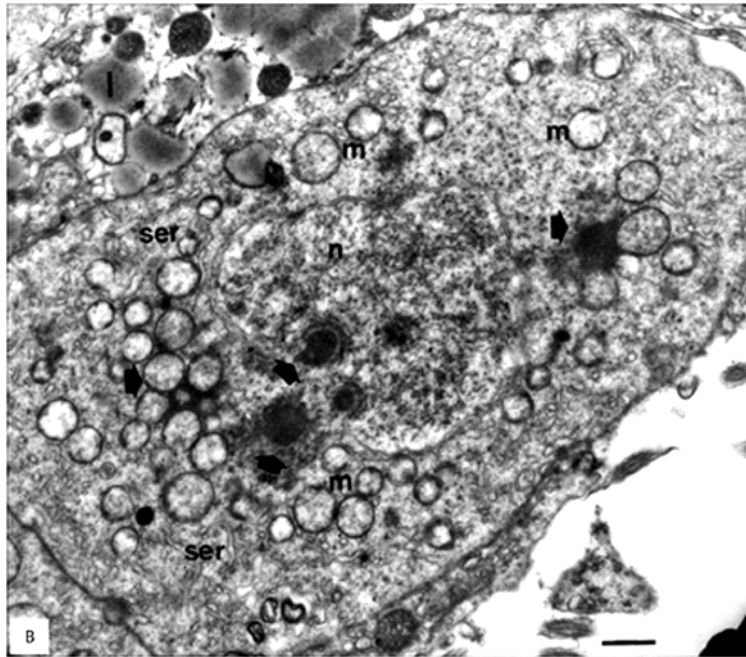


Fig. 2 – Nuage in a spermatogonium (TEM). Arrows point to nuage lodged in depressions of the nuclear envelope and dispersed in the cytoplasm, which may be associated with mitochondria; l, lipid granules of a cystic cell; m, mitochondria; ser, smooth endoplasmic reticule. Bar = 1 μ m. (Image from Abdalla and Cruz-Landim 2004).

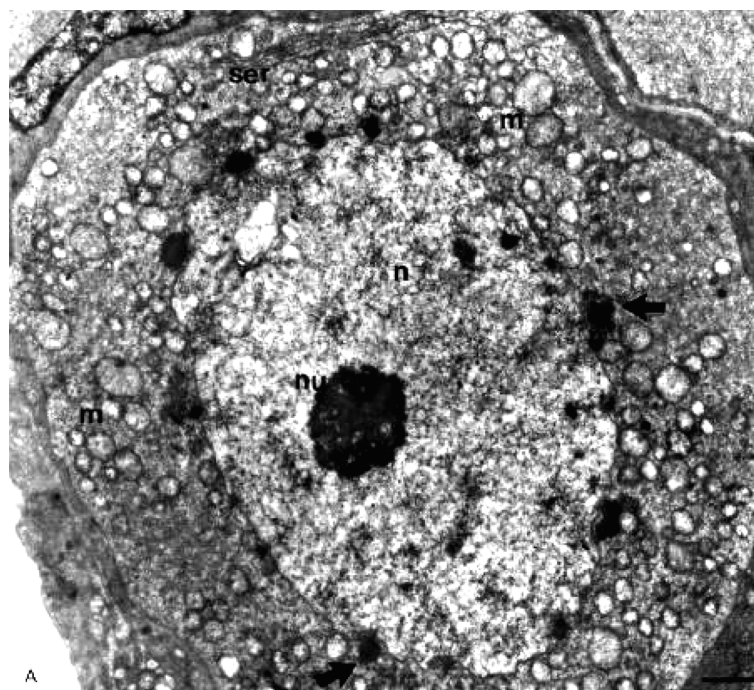


Fig. 3 – Nuage in an oogonium (TEM). Notice electrondense material (nuage; arrows) in the cytoplasmic side of the nuclear envelope, which may be associated with spherical mitochondria (m); ser, smooth endoplasmic reticule; n, nucleus; nu, nucleolus. Bar = 2 μ m. (Image from Abdalla and Cruz-Landim 2004).

The nuage stores RNAs and proteins that are produced early in oogenesis and, in oocytes, it associates with a distinctive structure known as Balbiani Body (Bb), which includes also a mitochondrial mass and Golgi complexes (Matova and Cooley 2001; Cox and Spradling 2003; Kloc et al. 2004) (Fig. 4). Subsequently, the Bb is transported in the cytoplasm area of the egg that, after fertilization, is taken up by PGCs (Kloc et al. 2004).

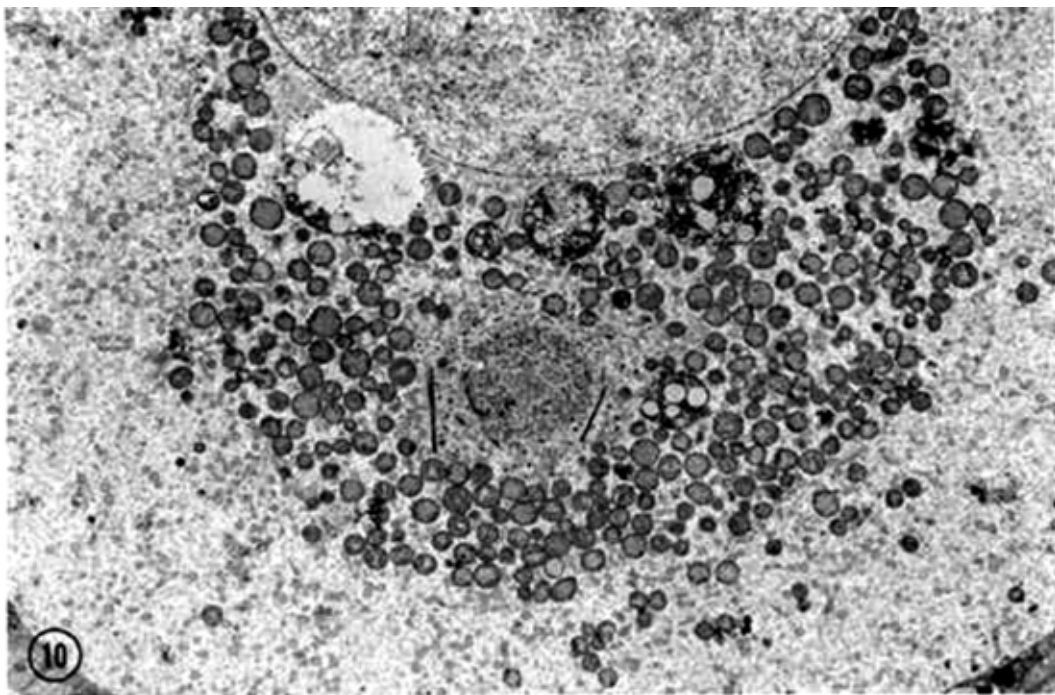


Fig. 4 – The Balbiani body. A mid-section through the Balbiani body, to show the peripheral concentration of mitochondria, the variable ballooning of compound aggregates and the cytocentrum with a dense central area surrounded by endoplasmic reticulum and coarse fibers. (Image from Hertig and Adams 1967).

In male germinal cells, the nuage is called chromatoid body (Cb), and it is typically associated with mitochondria (Russell and Frank 1978; Parvinen 2005). The Cb is first clearly seen in mid- and late pachytene spermatocytes as an inter-mitochondrial dense material (Parvinen 2005). Then, during spermiogenesis, the Cb acquires a lobular structure and it is surrounded

by a multitude of vesicles (Fig. 5), near the Golgi complex, and frequently connected by material continuities with the nucleus through nuclear pores (Parvinen 2005; Kotaja et al. 2006; Kotaja and Sassone-Corsi 2007). Later in spermiogenesis, at least in mammals, the Cb takes part in the formation of the residual body, a ring adjacent to the midpiece (the portion of the spermatozoon, between the sperm head and the axoneme, that includes the distal centriole and the mitochondria around it) (Parvinen 2005; Shang et al. 2010).

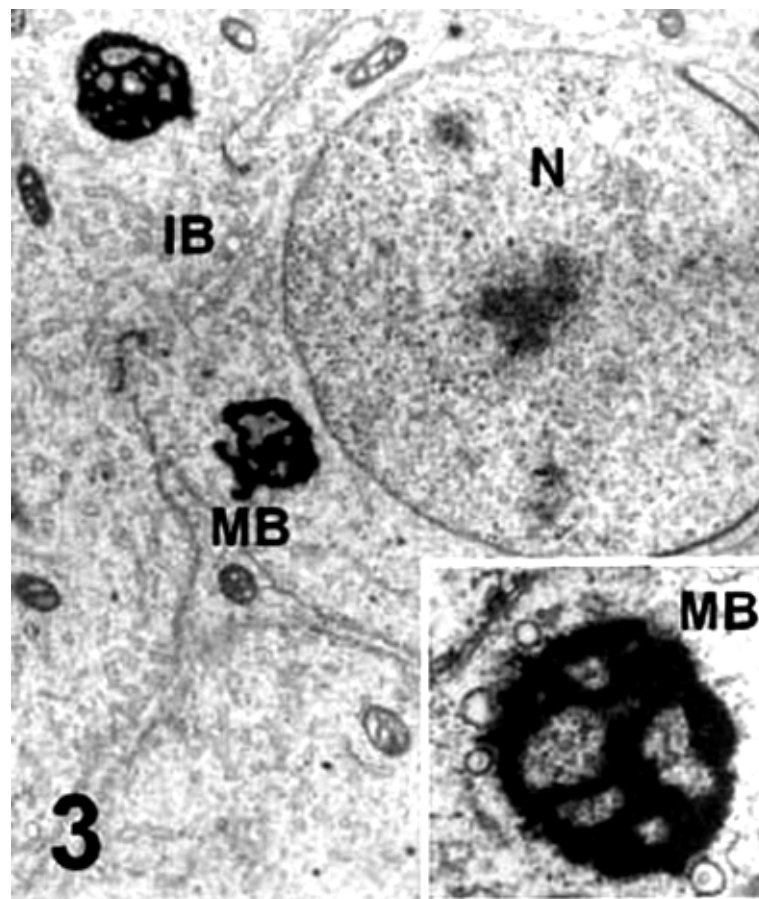


Fig. 5 – Chromatoid body in a spermatid at the initial phase of the spermiogenesis. Nucleus (N), intercellular bridge (IB), Multivesicular Body (MB = Chromatoid body). (Image from Fernandes Boaro Martins and de Carvalho Pinto e Silva 2005).

1.2 – Germ line formation in Spiralia

Like other protostomes, molluscs follow a spiralian embryonic development (Fig. 6): embryo blastomeres receive a specific content of cytoplasm, and they can be tracked through development up to the formation of organs (Hejnl 2010) (Fig. 7). PGCs arise from the 4d mesentoblast formed during the sixth cell division (Hejnl 2010, and references therein) (Fig. 7), but the mechanisms of sexual differentiation of the gonad are still unknown.

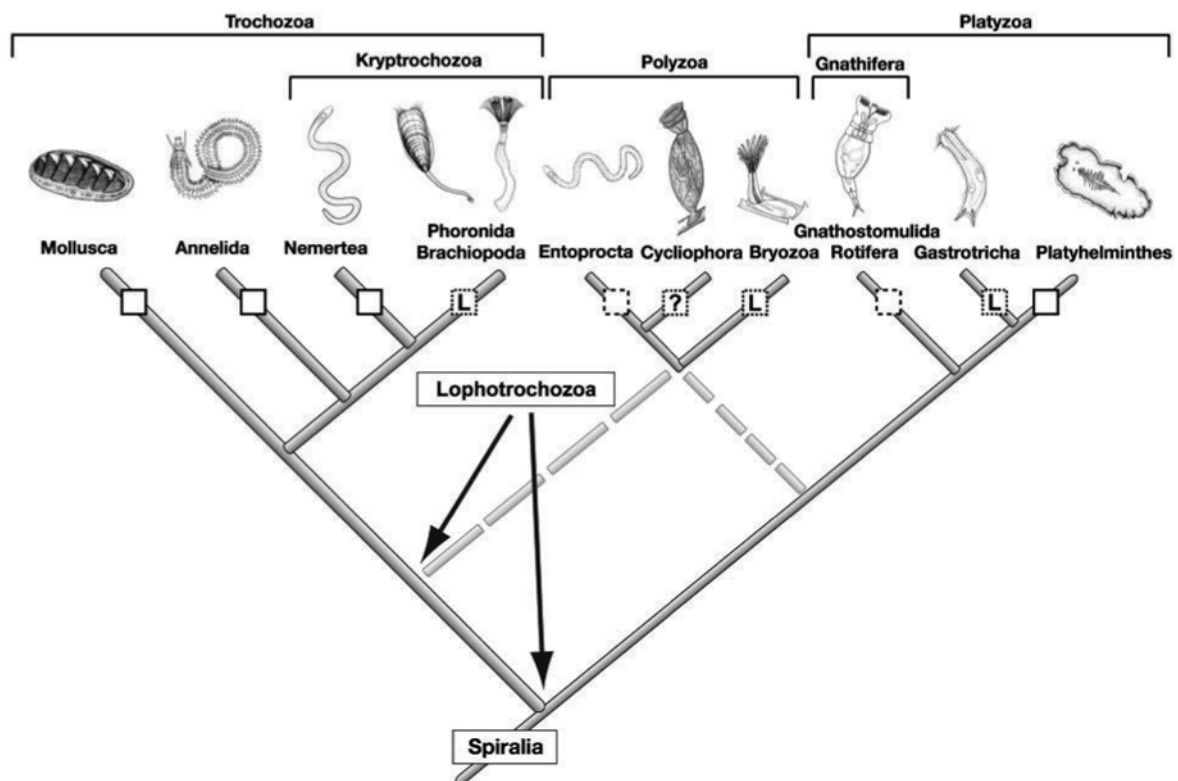


Fig. 6 – Phylogenetic relationships of Spiralia. The tree is based on recent molecular phylogenetic studies (Hejnl et al. 2010 and references therein). Taxa that gained support are named according to the literature. Taxa that show spiral cleavage are indicated by a white square. The square has a dashed outline for taxa for which reports are scarce and for which further detailed studies are necessary. A square with a dotted outline and an “L” indicate the loss of spiral cleavage. The position of the Polyzoa is not well supported, however, the application of the term “Lophotrochozoa” depends on its position, as it is indicated by the arrow. (Image from Hejnl et al. 2010).

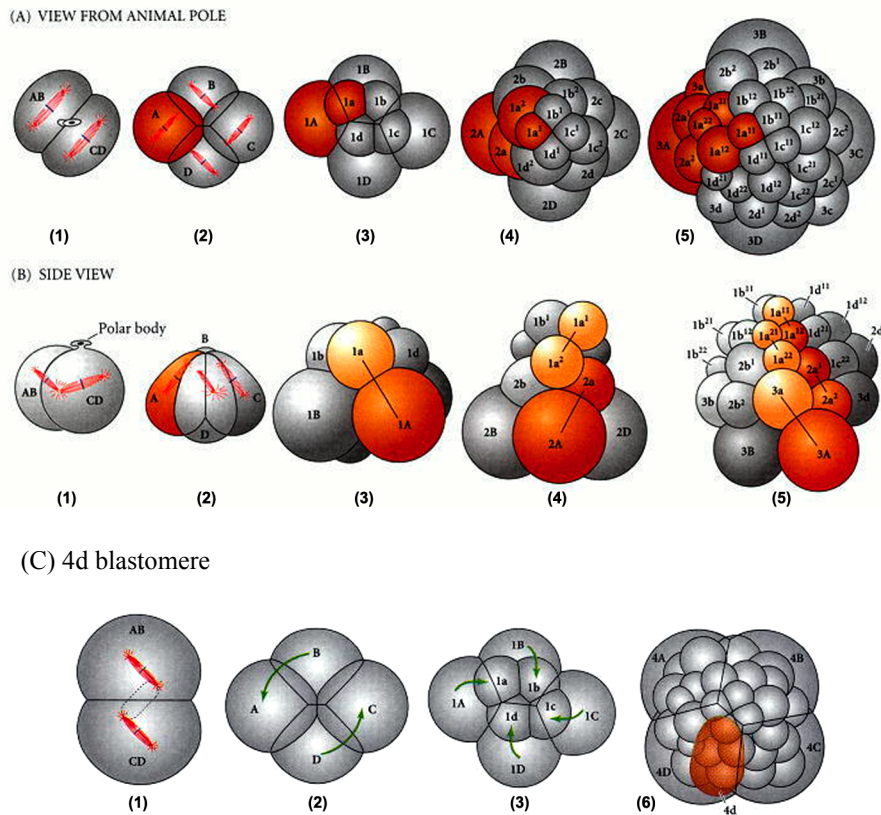


Fig. 7 – Spiral segmentation scheme. (A, B, C) The first two cleavage planes (1, 2) fall at right angles parallel to the animal–vegetal axis and divide the zygote into the A, B, C, and D quadrants. In some but not all spiralians (for example in bivalve molluscs), the D blastomere is larger than the rest. Beginning with the third round of cleavage, the A, B, C, and D blastomeres cleave off (arrows) quartets of smaller cells called micromeres at the animal pole. (A, B) Micromeres derived from A blastomere are colored in orange. In spiral cleavage, each quartet of micromeres is rotated with respect to the parent blastomere. (3) 8-cell stage, after formation of the first quartet of micromeres. (4) 16-cell stage, after formation of the second quartet of micromeres. (5) 32-cell stage after the formation of the third quartet of micromeres. (C) Formation of 4d. (6) During the formation of the fourth quartet of micromeres, three of the four vegetal macromeres divide equally; this is followed after a delay by the unequal division of a macromere which is now denominated 3D to generate a small 4D and a large 4d blastomere. The subsequent division pattern and differentiation of cells derived from 4d indicate that it is the mesentoblast. (Images from Gilbert 2000).

1.3 – Mitochondria and germ line formation

Mitochondria are semi-independent organelles, mostly known for their role in the energy metabolism of eukaryotic cells. However, their function is not limited to the production of ATP; they are involved in many processes of eukaryotic life. The above mentioned frequent colocalization of mitochondria and nuage suggests a connection between these organelles and germ line development. For example, mitochondrial ribosomes are found extramitochondrially and are required to produce proteins that are necessary for germ cell formation (Kobayashi et al. 1993; Ding et al. 1994; Iida and Kobayashi 1998; Ikenishi 1998; Kobayashi et al. 1998; Ogawa et al. 1999; Amikura et al. 2001). Moreover, evidence from TEM analysis documented the extrusion of material and cristae from mitochondria forming nuage, both in gametes during gametogenesis (Reunov et al. 2000; Reunov 2006) (Fig. 8A) and in developing embryos (Amikura et al. 2001; Isaeva and Reunov 2001; Reunov 2006) (Fig. 8B).

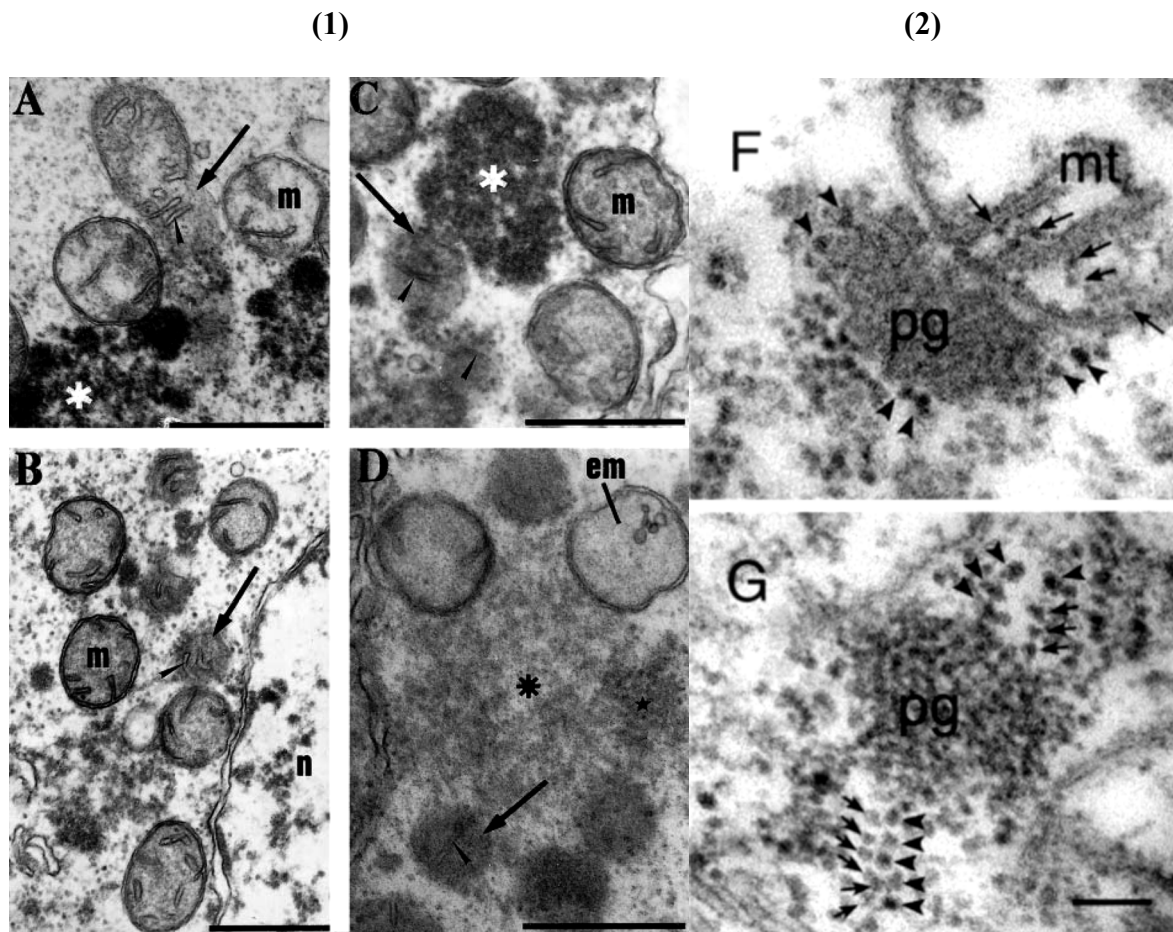


Fig. 8 – (1) TEM of mitochondria–nuage complexes in spermatogonia of the sea urchin *Anthocidaris crassispina*. (A) Mitochondrion releasing the matrix (arrow) with cristae (arrowhead) into cytoplasm; ‘asterisk’ shows nuage materials in the cytoplasm. **(B)** Electron-dense globules (arrow) with cristae (arrowhead) between mitochondria in the cytoplasm. **(C)** Cristae (arrowheads) comprising electron-dense globules (arrow) attaching to cytoplasmic nuage (asterisk). **(D)** The area of cytoplasmic nuage (asterisk) surrounded by electron-dense globules (arrow) and mitochondria; ‘arrowhead’ shows the mitochondrial cristae inside the globules; ‘star’ signifies the electron-dense globule integrating with cytoplasmic nuage; em, ‘empty’ mitochondrion; m, mitochondria; n, nucleus. Bars = 0.5 μm . (Image from Reunov et al. 2000). **(2) TEM of mitochondria–nuage complexes in *Drosophila* embryos. (F, G)** Electron micrographs of sections through polar granules. **(F)** In stage-1 embryos polar granules are intimately associated with mitochondria, and no ribosomes were found at the boundary between these organelles. Arrows point to ribosomes within a mitochondrion. **(G)** In stage-2 embryos, the smaller ribosomes (arrows) are integrated into the polar granule-polysomes. Arrowheads (F and G) point to the larger ribosomes; pg, polar granules (nuage); mt, mitochondria. Bar = 0.1 μm . (Image from Amikura et al. 2001).

Actually, in early embryos, a mitochondrial-type translation is required for germ cell formation, which is disrupted by the injection of prokaryotic translation inhibitors (Amikura et al. 2005). Another supporting clue to a role of mitochondria in germ line formation comes from their origin: they have a common ancestor with the endosymbiont Rickettsiales (Andersson et al. 1998), some of which are known to distort the sex of their host (Fig. 9).

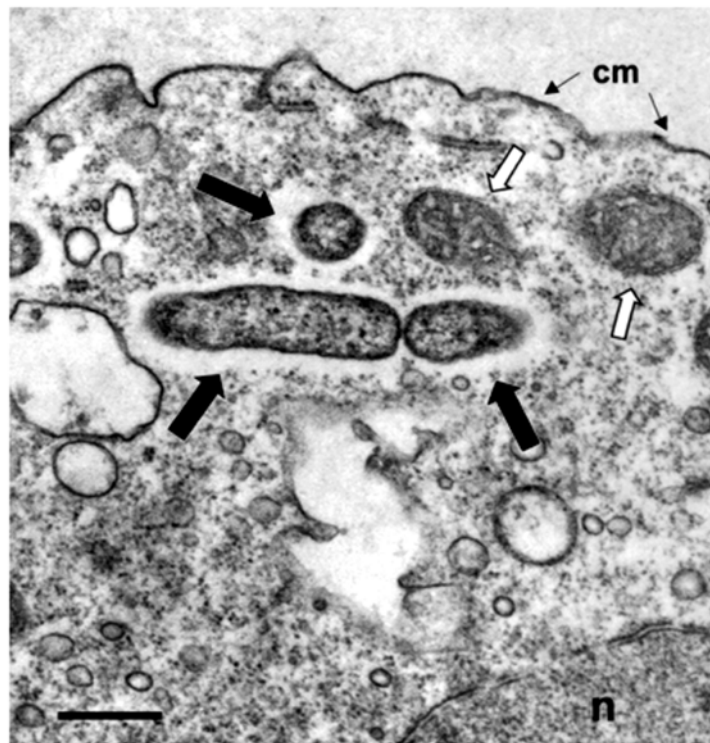


Fig. 9 – Ultrastructure of *Caedibacter*, endosymbiont related to the Rickettsiales (solid arrows) within the cytoplasm of its host, *Acanthamoeba* sp.; cm, amoebal cell membrane; n, nucleus; the open arrows indicate mitochondria. Bar = 0.5 μ m. (Image from Beier et al. 2002).

Wolbachia, for example, induces male killing, feminization, parthenogenesis, cytoplasmic incompatibility (Ebbert 1993; Hurst et al. 1997), and methylation pattern modification in gonads (Negri et al. 2009). Furthermore, depletion of mitochondrial DNA (mtDNA) results in significant changes in the methylation pattern of a number of nuclear genes, some of which are reversed by the restoration of mtDNA (Smiraglia et al. 2008).

1.4 – The mitochondrial bottleneck

Mitochondrial DNA sequence variants are known to segregate rapidly between generations, and this was explained by a very sharp reduction of mitochondrial population during germ line establishment. More precisely, Primordial Germ Cells (PGCs) are known to carry few mitochondria (around 10 per cell in mammals, Shoubridge and Wai 2007). This number increases dramatically during oogenesis, so that, for example in mammals, mature eggs may contain up to 100,000 mitochondria (Shoubridge and Wai 2007). All mitochondria of a new individual are therefore derived from the few present in PGCs, that eventually end up into the egg from which the newborn comes from (Fig. 10). However, no agreement has been reached on how SMI functions, and this issue is related to the nature of the “mitochondrial bottleneck” (Olivo et al. 1983; Laipis et al. 1988; Ashley et al. 1989).

By passing through such a narrow mitochondrial bottleneck, the embryo is largely homoplasmic, even though mtDNA is prone to mutation (Cao et al. 2007; Shoubridge and Wai 2007; Cree et al. 2008). According to some authors (see for example: Boldogh and Pon 2006; Zhou et al. 2010), the mitochondrial bottleneck could act as a selection mechanism for proper functioning by screening of mitochondrial metabolic activity: only mitochondria with a high-inner membrane potential tend to be recruited by germ line, thus deleterious mutations are eliminated each generation (Zhou et al. 2010). On the contrary, other authors (see for example Kogo et al. 2011) found that germ line mitochondria exhibit suppressed respiration, thus experiencing a lower production of reactive oxygen species. This would enable the transmission of more accurate mtDNA through generations: without undergoing the high mutational rate of somatic mitochondria, germ line mitochondria would preserve their “health”.

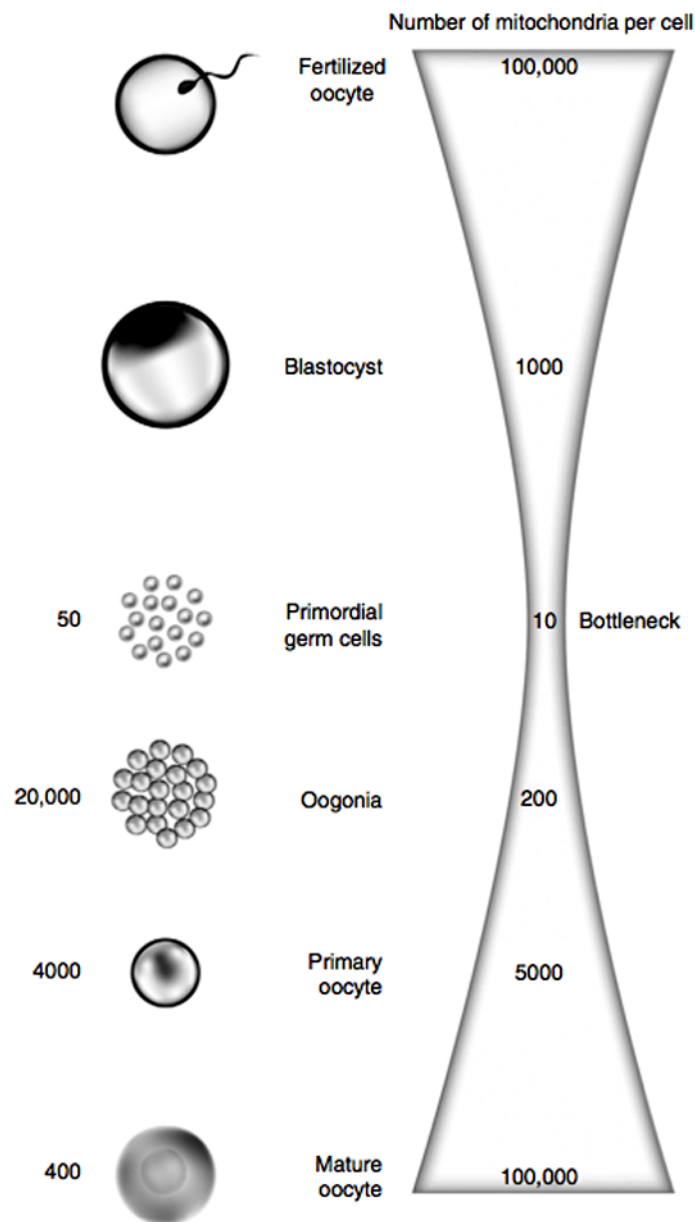


Fig. 10 – Mitochondrial bottleneck scheme. Diagrammatic representation of changes in the number of mitochondria during development of the female germ line. An estimate of the number of mitochondria is indicated at each stage of germ line development. A genetic bottleneck for the transmission of mtDNA occurs in the primordial germ cells. Development to the mature oocyte involves at least a 10,000-fold increase in the number of mitochondria. (Image from Shoubridge and Wai 2007).

The nature of the mitochondrial bottleneck is far to be understood: what is the mechanism that segregates mitochondria into PGCs? Is this a stochastic process, or rather a regulated one? (See Dumollard et al. 2007; Shoubridge and Wai 2007). The lack of clear-cut data mostly derives from the fact that, in metazoans with SMI, all mitochondria contain the same mtDNA, so it is not easy to spot the ones segregating into PGCs. This also means that it is not easy to characterize them, and follow their behavior during embryo development. Nonetheless, in oocytes of many SMI organisms two populations of mitochondria can be distinguished: one population is aggregated in the Bb and enters the embryo PGCs during development (Isaeva and Reunov 2001; Matova and Cooley 2001; Cox and Spradling 2003), while the remaining mitochondria spread in the oocyte and are transmitted to the somatic cell lineage (Tourte et al. 1984; Mignotte et al. 1987; Volodina et al. 2003). For this reason, the Bb mitochondrial population, or a part of it, may actually represent the mitochondrial bottleneck (Zhou et al. 2010).

Since all mitochondria are usually transmitted to embryos through oocytes, the bottleneck is generally believed to be under female control, but factors from spermatozoon might also be involved in mitochondrial inheritance and selection (Chuma et al. 2009). The process by which mitochondria enter the developing germ line is still unknown, but the involvement of microtubules in their general distribution was confirmed by experiments using inhibitors to microtubule polymerization (Obata and Komaru 2005; Katayama et al. 2006; Zhang et al. 2008).

1.5 – Doubly Uniparental Inheritance (DUI) of mitochondria

In metazoans, mitochondria are commonly inherited maternally, by Strictly Maternal Inheritance (SMI) (Birky 2001). However, in some bivalve molluscs, two mitochondrial lineages are present: one transmitted through females (F-type), the other through males (M-

type) (Fig. 11).

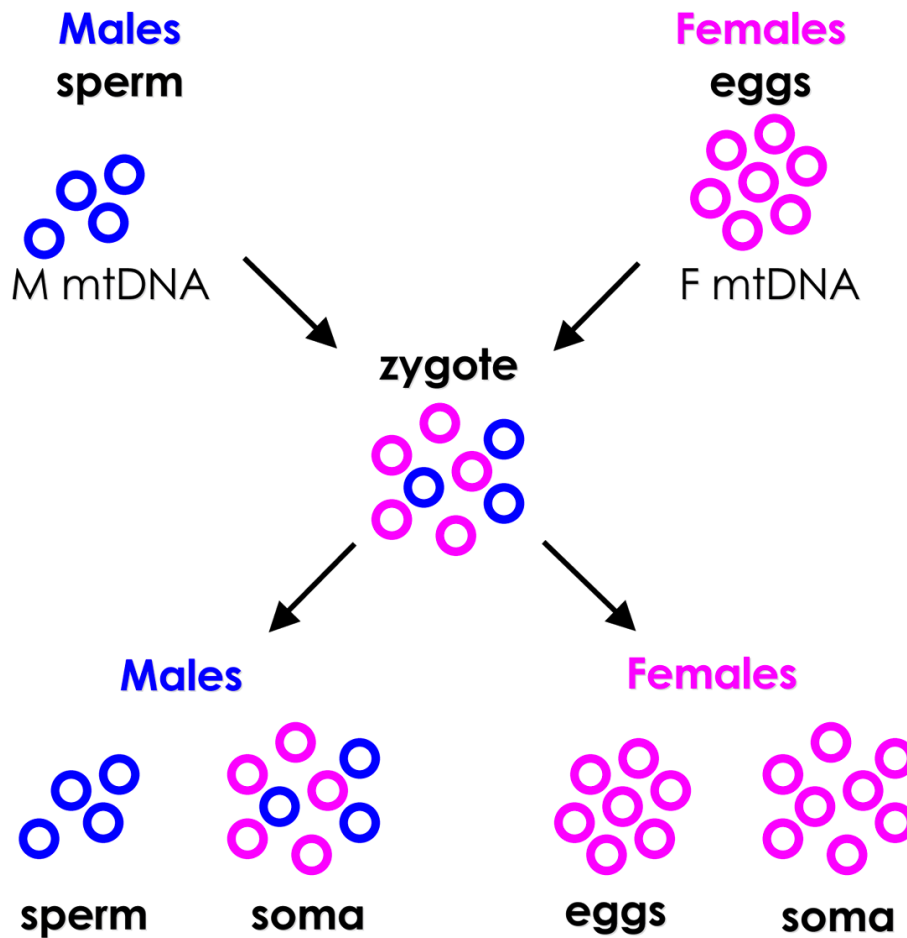


Fig. 11 – Doubly Uniparental Inheritance (DUI) of mitochondrial DNA. Eggs are homoplasmic for the F-type mitochondrial DNA, sperm for the M-type, thus the zygote is heteroplasmic. In male embryos the M-type mtDNA colonizes germ cells so that sperm will contain M-type, while male soma is heteroplasmic. In females the M-type is diluted or degraded thus eggs will contain F-type, like the female soma.

This unique system is called Doubly Uniparental Inheritance (DUI) of mitochondria (Skibinski et al. 1994a,b; Zouros et al. 1994a,b; reviewed in Breton et al. 2007; Passamonti and Ghiselli 2009). The two mtDNA variants show a high level of nucleotide sequence divergence: up to 43% (Doucet-Beaupré et al. 2010). DUI is not a case of biparental inheritance of organelles, because both male and female mitochondria are transmitted uniparentally. DUI has been found in species belonging to seven different bivalve families: Donacidae, Hyriidae, Margaritiferidae, Mytilidae, Solenidae, Unionidae, and Veneridae (Theologidis et al. 2008). Because of its wide taxonomic distribution and its scattered occurrence, there has been contention about whether DUI evolved once or many times among Bivalvia. However, because of evident analogies of DUI in all analyzed species, the soundest hypothesis is that it originated once, at the evolutionary radiation of Bivalvia, at least in the early Ordovician (leading to all Autobranchia bivalves) (Theologidis et al. 2008 and references therein; Doucet-Beaupré et al. 2010) (Fig. 12). Consequently, if DUI was the ancestral condition, reversions to standard maternal inheritance should have occurred many times, thus producing the scattered distribution of DUI, with some bivalve species not showing trace of sex-linked mtDNA heteroplasmy. However, DUI may be difficult to detect and deep analyses are needed to ascertain its presence (as discussed in Theologidis et al. 2008).

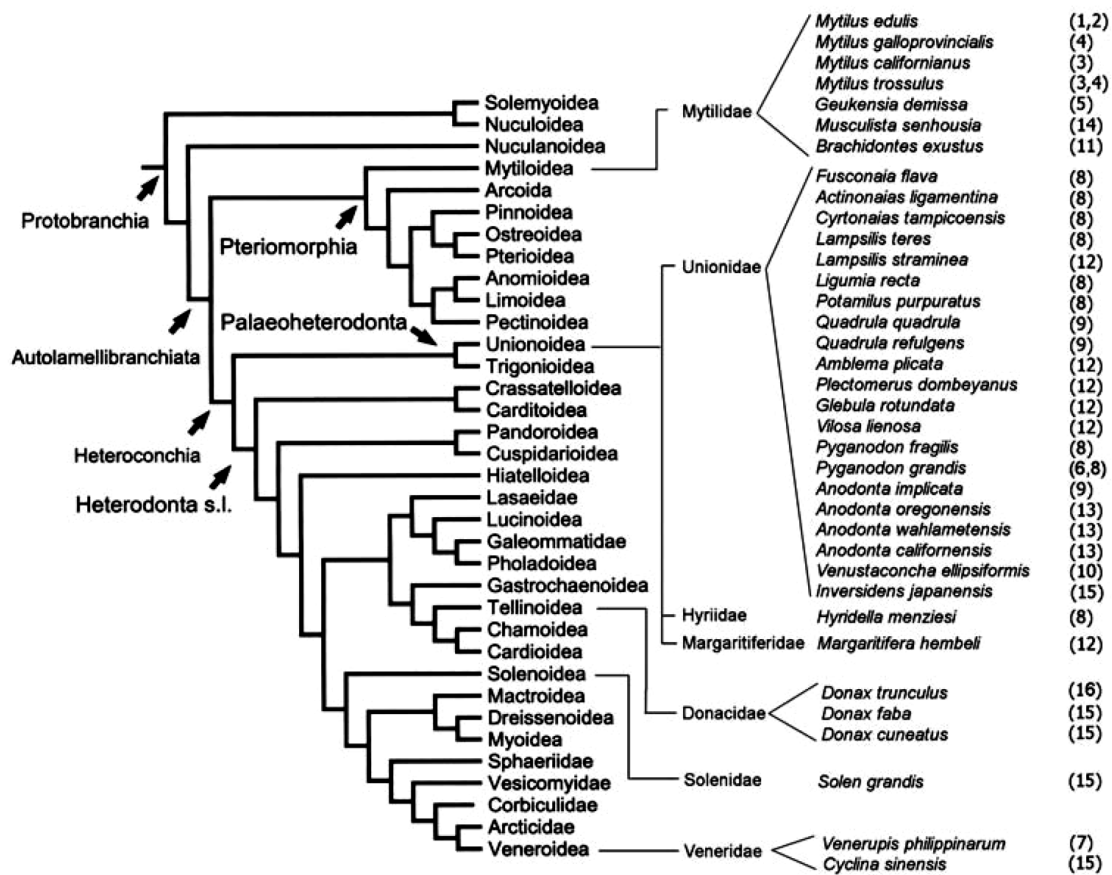


Fig. 12 – The taxonomic position of species currently known to have DUI. Taxonomic relationship of bivalve superfamilies according to Giribet and Wheeler (2002). Information about presence of DUI from references listed in the last column: (1) Zouros et al. (1994b); (2) Skibinski et al. (1994b); (3) Geller et al. (1993); (4) Rawson and Hilbish (1995); (5) Hoeh et al. (1996); (6) Liu et al. (1996); (7) Passamonti and Scali (2001); (8) Hoeh et al. (2002); (9) Curole and Kocher (2002); (10) Chakrabarti et al. (2006); (11) Lee and Ó Foighil (2004); (12) Curole and Kocher (2005); (13) Mock et al. (2004); (14) Passamonti (2007); (15) Data from GenBank. Accession numbers: *I. japonensis*: AB055624–25. *S. grandis*: AB064983–5. *D. faba* and *D. cuneatus*: AB040841–45. *C. sinensis*: AB040833–5; (16) Theologidis et al. 2008. (Image from: Theologidis et al. 2008).

1.5.1 – Distribution of the sex-linked mtDNAs in tissues and gametes of DUI species

A peculiar distribution pattern of the two mitochondrial genomes is detectable in DUI bivalves. In *Mytilus* spp. (Garrido-Ramos et al. 1998; Dalziel and Stewart 2002), as well as in *Musculista senhousia* (Passamonti 2007), mature males contain different ratios of F and M mitochondrial genomes in their tissues, with gonads containing predominantly M-type, and somatic tissues containing mainly F-type. In more detail, in *Mytilus* DUI species, the M is found in sperm and testes and it is sometimes detected in traces in male and female soma, while the F-type is found in eggs, ovaries and somatic tissues of both sexes (Garrido-Ramos et al. 1998; Dalziel and Stewart 2002). Traces of M genome were also found in unfertilized eggs of *Mytilus galloprovincialis* (Obata et al. 2007), although some kind of sperm contamination cannot be excluded in this case; in contrast, the male germ line excludes F genomes and retains M ones only (Venetis et al. 2006).

Real-Time PCR (qPCR) analyses on *Ruditapes philippinarum* Adams & Reeve (Ghiselli et al. 2011) showed that both M- and F-type mtDNA are present in male tissues, but, compared to mytilids, *R. philippinarum* males show a strong dominance of M-type mtDNA in their somatic tissues (Ghiselli et al. 2011). Also there is a strong predominance of M in male gonads, as expected for DUI, but, despite the concomitant presence of F-type in testis, *R. philippinarum* sperm never carried F-type mtDNAs, as also found in *M. galloprovincialis* by Venetis et al. (2006). In *R. philippinarum* females, M-type presence (although rare) was detected in somatic tissues, and this could be explained by a malfunctioning of the elimination mechanism of sperm mitochondria (which is also not perfect in SMI species, see paternal leakage in: Kondo et al. 1990; Shitara et al. 1998; Kvist et al. 2003; Xu 2005). Nonetheless, female gametes were always homoplasmic for F-type mitochondria. Moreover, spawned eggs of a *R. philippinarum* female having a strong predominance of M-type in the gonad were proved to contain only F-type mtDNA. These qPCR observations suggested that a strict

mechanism controlling the transmission of the mtDNA through the germ line is present in both males and females of *R. philippinarum* (Ghiselli et al. 2011).

M- and F-type expression patterns of *Mytilus galloprovincialis* were studied with *in situ* hybridization, using probes specific to M- and F-type mtDNA designed in the cytochrome b region (Obata et al. 2011). F-type mtDNA resulted to be expressed both in somatic tissues and female gonads, while M-type was not expressed in these tissues. M-type expression in male gonads was strong but limited at the early spermatogenesis. Obata et al. (2011) proposed different systems for M- and F-type tissue-specific transcriptional regulation, and different functions, with F-type being functional in somatic tissues and female gonads and M-type functioning in spermatogenetic cells only.

1.5.2 – DUI as a model system

DUI represents an ideal system for examining mitochondrial movement and effects of different mitochondrial types during development. DUI is considered to be derived from SMI: the mechanism of SMI might have evolved into DUI by modifying the molecular signals leading to degradation of spermatozoon mitochondria (M-type) (see Breton et al. 2007, and Passamonti and Ghiselli 2009, for reviews). This could be achieved through a series of molecular signals between nucleus and mitochondria, because sperm mitochondria appear to be recognized and actively transferred to the male germ line. Molecular details of such mechanisms are largely unknown but, analogous to what was observed regarding SMI (Sutovsky 1999), sperm-derived mitochondria might be labeled with a molecule similar to Ubiquitin (Kenchington et al. 2009).

1.5.3 – Mitochondrial segregation patterns in DUI species

In DUI species, during embryo development, M mitochondria have to invade the germ line of male embryos, otherwise sperm would transmit F-type mtDNA and DUI would fail. This means that M mitochondria have to be actively segregated to the male PGCs. To examine the segregation of M-type mitochondria into male PGCs, the movement of sperm mitochondria was traced in a DUI mussel, *Mytilus*. Tracing was achieved by fertilizing eggs with sperm stained with MitoTracker Green (Cao et al. 2004; Obata and Komaru 2005; Cogswell et al. 2006; Kenchington et al. 2009). In these embryos, the distribution of sperm mitochondria follows two different patterns, which seem to depend on the sex of the embryo (Fig. 13). In DUI male embryos, spermatozoon mitochondria form an aggregate (Cao et al. 2004; Obata and Komaru 2005; Cogswell et al. 2006), and, during development, this aggregate enters PGCs, as proved by the only presence of M-type mtDNA in spermatozoa (Venetis et al. 2006; Ghiselli et al. 2011).

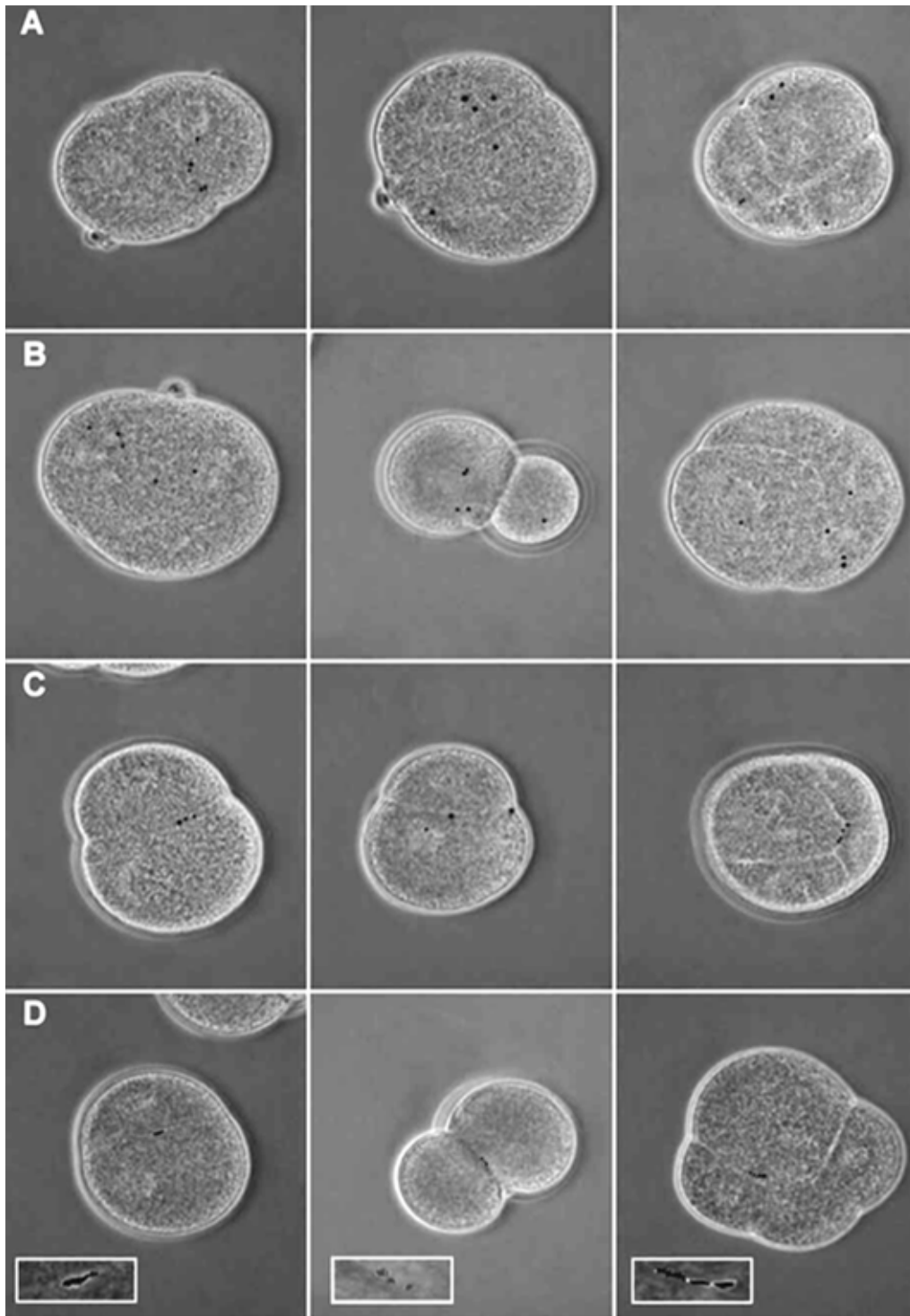


Fig. 13 – Distribution patterns of spermatozoon mitochondria in the DUI species *Mytilus edulis*. (A, B) Female-biased family. (C, D) Male-biased family. (Image from Cogswell et al. 2006).

This evidence from *Mytilus* provides an early developmental mechanism through which sperm mitochondria are segregated into the germ line of male embryos; after that, the M mitochondrial genome becomes dominant in male germ line. In DUI female embryos, sperm mitochondria are dispersed, there is no association between spermatozoon mitochondria and the first cleavage furrow, and the mitochondrial inheritance would be as in SMI species (Cao et al. 2004; Obata and Komaru 2005; Cogswell et al. 2006; Ghiselli et al. 2011; Saavedra et al. 1997; Sutherland et al. 1998).

In females, evidence for a strictly regulated mitochondrial segregation into germ line are less easy to detect because, as in SMI species, all mitochondria are F-type. However, in *R. philippinarum*, a strict selection of female mitochondria to be passed into germ line was found: eggs always carried F-type mtDNA, also in the single female in which M-type DNA was detected in gonad and somatic tissue (Ghiselli et al. 2011). This seems not to be true for *Mytilus*, in which some eggs were shown to carry also M-type mtDNA (see Obata et al. 2006).

1.5.4 – Sex-ratio distortion and DUI

Besides the two mitochondrial distribution patterns, a sex-ratio distortion was observed in DUI *Mytilus* species: females were found producing a female-biased offspring (female-biased family) and showing a majority of dispersed patterns, other females produced a male-biased progeny (male-biased family) with a majority of aggregated patterns, and others a 50:50 sex-ratio, with a balanced frequency of the two patterns (Saavedra et al. 1997; Kenchington et al. 2002; Cogswell et al. 2006). Recently, sex-ratio biased progenies were also found in the DUI species *R. philippinarum* (Ghiselli et al. 2012). The peculiar segregation pattern of spermatozoon mitochondria, correlated with the existence of sex-biased lineages, led to the hypothesis that M-type mitochondria may have an active role in gonad masculinization,

achieved through a series of specific signals between nucleus and mitochondria (Kenchington et al. 2002).

1.5.5 – The W/X/Z/S system

A model for mtDNA inheritance and sex determination in DUI species was proposed and refined by several Authors (Saavedra et al. 1997; Zouros 2000; Kenchington et al. 2002; Cao et al. 2004; Cogswell et al. 2006; Breton et al. 2007; Passamonti and Ghiselli 2009). According to this model, paternal mtDNA transmission should be affected by three nuclear genes. Factor W is expressed in males during spermatogenesis and its product labels the outer surface of sperm mitochondria, thus distinguishing them from egg mitochondria. Factor X is expressed in females. It supplies the egg with a factor that interacts with W and prevents sperm mitochondria from aggregating and segregating into PGCs, or allow their degradation. Factor Z is also expressed in females, with an active (Z) and an inactive (z) allele. It supplies the eggs with factor Z which suppresses factor X and allows sperm mitochondria to aggregate and co-segregate into the first germ cells. Sex would be determined by nuclear factors (S) with different “dosage” effect and for maleness it is required an higher dosage (Kenchington et al. 2009; Ghiselli et al. 2012).

1.5.6 – Novel mitochondrial ORFs can be related to DUI functioning

Comparative mitochondrial genomics revealed that animal mtDNAs are very conserved in terms of gene content (Boore 1999; Gissi et al. 2008). These small circular and typically intron-less molecules encode 2 ribosomal RNAs, 22 transfer RNAs and 13 protein subunits of the mitochondrial respiratory chain complexes and ATP synthase. The other subunits of the electron transport system as well as all the proteins and factors involved in other mitochondrial functions, such as mtDNA replication and mtDNA expression, are nuclear-

encoded (Boore 1999; Garesse and Vallejo 2001). One intriguing observation that emerged from sequencing studies of whole animal mtDNAs is the occurrence of numerous Open Reading Frames (ORFs) of unknown function that are present in closely related species, but for which homologues cannot be determined among more distantly related species (Saccone et al. 1987; Endo et al. 2005; Shao et al. 2006; Cameron et al. 2007; Flot and Tillier 2007; Gissi et al. 2008; Breton et al. 2009, 2011a,b). Interestingly, such lineage-specific genes were shown to be involved in key biological functions (Monchois et al. 2001; Khalturin et al. 2008; Khalturin et al. 2009). Thus, the lineage-specific ORFs occurring in animal mitochondrial genomes could potentially have functional significance. Lineage-specific mtDNA-encoded proteins are already known to play a role in sex determination in angiosperm plants exhibiting cytoplasmic male sterility (Chase 2007). Interestingly, novel lineage-specific ORFs have been also discovered in the only known animals that do not transmit their mtDNA exclusively maternally, that are DUI species.

In more detail, in DUI mussels, two novel mtDNA-encoded proteins have been shown to be mt genome-specific, one for F genome and one for M genome (Breton et al. 2009; Breton et al. 2011a,b). It has been hypothesized that these novel mtDNA-encoded proteins and other F- and M-specific mtDNA sequences could be responsible for the different modes of mtDNA transmission in bivalves, but this has still to be demonstrated. For example, the novel F genome-specific mt ORF, of significant length (>100 aa), located in the control region, was identified in five *Mytilus* species, thus suggesting its maintenance in the mytilid lineage (subfamily Mytilinae) for about 13 million years. Furthermore, this ORF seems to have a homologue in the F mt genome of *Musculista senhousia*, a DUI mytilid species in the subfamily Crenellinae. This results support its functional significance in marine mussels, and that novel mitochondrial genes are involved in key biological functions in bivalve species with DUI. The female-transmitted ORF protein is not only present in mitochondria but, more

surprisingly, it is also present on the nuclear membrane and in egg nucleoplasm in freshwater mussels (Breton et al. 2011a). These results established novel features for animal mitochondrial genomes: the presence of additional, lineage-specific, mtDNA-encoded proteins with functional significance and their involvement in extramitochondrial functions. These newly identified mt-ORFs in mussels are not the only mitochondrial genes suggested to have a functional significance in DUI. It was also proposed that the C-terminus coding extension of the Cox2 protein (Mcox2e), which is unique to freshwater mussel M genomes (Curole and Kocher 2002; Curole and Kocher 2005; Chakrabarti et al. 2006; Chakrabarti et al. 2007; Chapman et al. 2008), could represent an M-specific label for sperm mitochondria that determines their fate in the fertilized eggs, as observed in *Mytilus* (Cao et al. 2004; Cogswell et al. 2006).

1.6 – The analyzed species: development and reproductive biology

To understand the mitochondrial inheritance and to address the relationship between mitochondria and germ line formation, my PhD study was focused on the Manila clam *R. philippinarum* (Fig. 14). This DUI species belongs to the family Veneridae, a bivalve family found throughout the world. The Veneridae are better known as edible molluscs, and they are commonly called “clams”. The genus *Ruditapes* Chiamenti includes two species, *R. decussatus*, an Atlantic-Mediterranean species, and *R. philippinarum*, that is native to Japan with a wide distribution in the Indian and Pacific Oceans and subsequently introduced along the North American Pacific coast, Hawaii and more recently along the European coast of the Mediterranean. *R. philippinarum* is different from *R. decussatus* both for the shell and at anatomical level: the two siphons are joined together in the first species, while in the second they are separate (Cesari and Pellizzato 1990). The former is a DUI species, the latter is thought to be a SMI species.



Fig. 14 – *Ruditapes philippinarum* Adams and Reeve. (Images from http://www.a-m-a.it/public/veraci/vongola008_zoom.jpg; http://postfiles10.naver.net/20110502_265/kordipr_1304323139915w2Cbd_JPEG/%BC%AD%BD%C4.jpg?type=w2; <http://mislab.org/files/DSCF0244b.jpg>)

R. philippinarum is strictly gonochoric and its gonad forms every year at the beginning of the spawning season and right after degraded (Devauchelle 1990). During the non-reproductive season no ovary or testis can be seen and sex cannot be determined (Devauchelle 1990). Its reproductive tissue originates every reproductive season. The gonad includes a system of strongly branching acini connected by small ducts to an excretory duct directly connected to the urethra. Acini are made up of germinative epithelium supported by connective tissue forming a kind of packaging (Fig. 15). Gametogenesis is characterized by the appearance in the connective tissue of acini containing gametes (Fig. 15). Gonia localize at the periphery of the acinus, while mature gametes are free in the acinus lumen. There is no copulation and fertilization takes place externally.

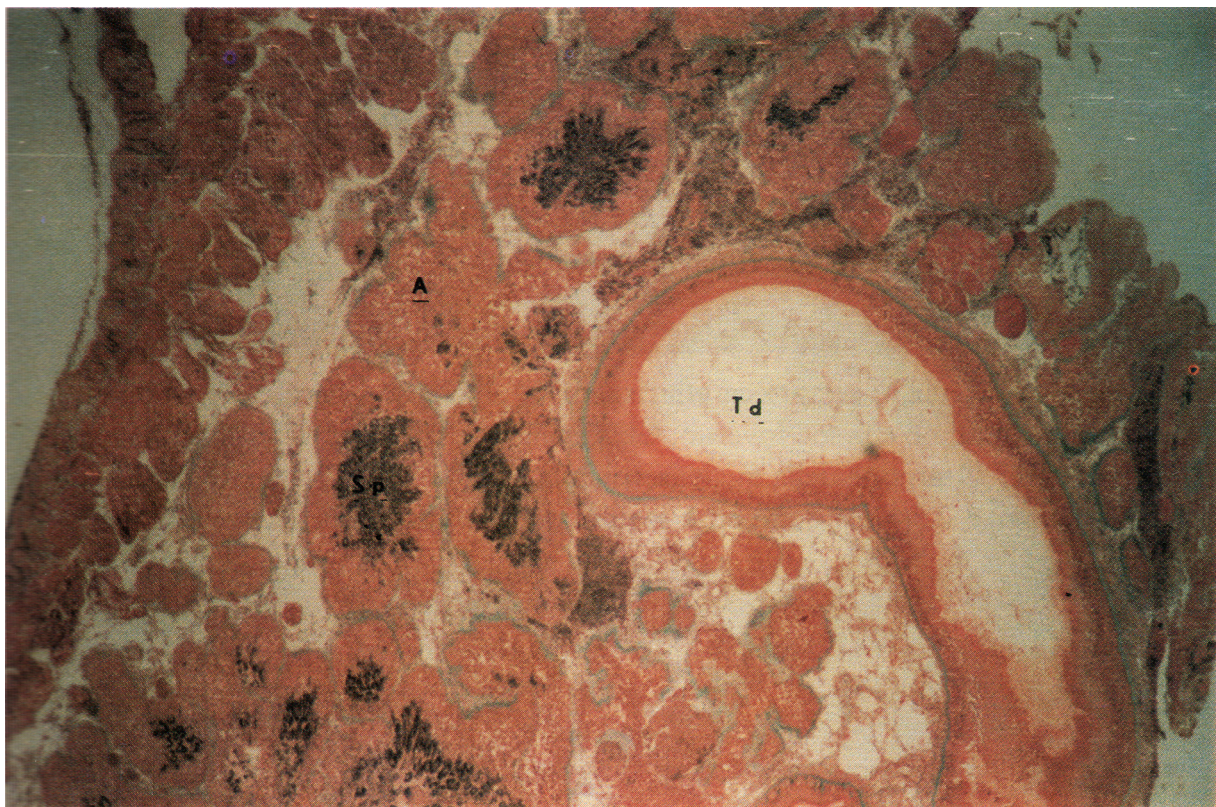


Fig. 15 – *R. philippinarum* testis morphology. During the reproductive season, acini form among connective tissue and intestinal loops. The overall morphology is similar in females, where acini are full of eggs. A - Acinus; Sp - Spermatozoa free in the acinus lumen; Td - digestive tract. (Image form Devauchelle 1990).

1.7 – Performed analyses

Exploiting the peculiar features of DUI, I first investigated the segregation patterns of spermatozoon mitochondria in *R. philippinarum* embryos using the mitochondrial-specific vital dye MitoTracker® Green FM.

Evidence was found that strictly regulated mitochondrial bottlenecks are present to assure sex-specific mtDNA segregation in PGCs of DUI species. A role of sperm mitochondria in testis formation in DUI species is in agreement with their retention in male embryos and segregation to primordial germ line. To understand whether sperm mitochondria could participate in germ line development of *R. philippinarum* I performed an immunostaining of a specific germ line determinant (Vasa) and compared its position to sperm mitochondria location. Cytoskeleton staining was performed to understand the movement of sperm mitochondria.

Moreover, in order to compare the DUI system with SMI animals, using Transmission Electron Microscopy I searched in *R. philippinarum* for typical structures related to germ line formation.

Finally, I analyzed the transcriptome of *R. philippinarum* searching for genes that showed an expression bias and that could have a role in sex determination and mitochondria inheritance. Then, I performed an *in situ* hybridization with Digoxigenin-labeled riboprobes on mature gonads to find the specific location of these nuclear transcripts, and of a putative new mitochondrial gene that could be involved in mitochondrial tagging and recognition.

2 – MATERIALS AND METHODS

2.1 – Sampling and spawning induction

R. philippinarum specimens were collected in Goro (Italy) during the reproductive season (July/August). Single clams were placed in beakers with artificial sea water (reverse osmosis water with Red Sea Coral Pro® aquariology sea salt added) changed every 12 h to remove any external contamination (*i.e.* sperm from possible former spawnings) (Fig. 16).

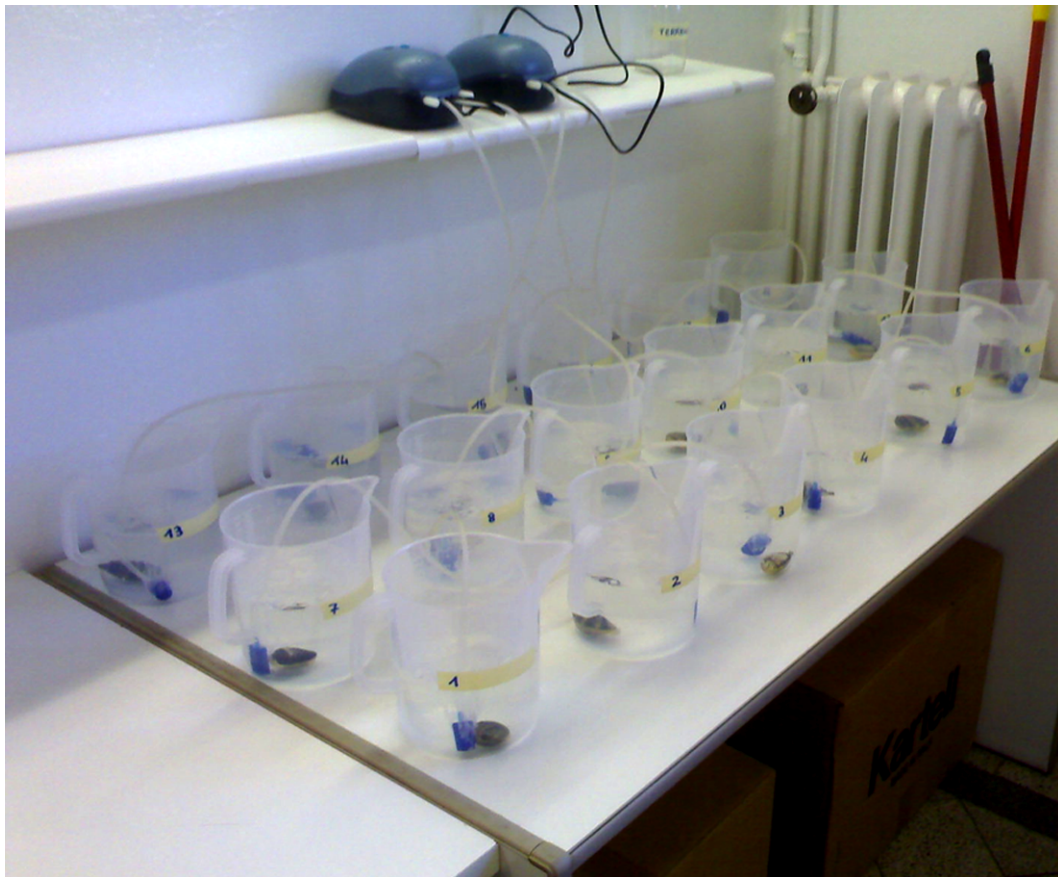


Fig. 16 – *R. philippinarum* specimen preparation.

After 24-36 h, I induced spawning with cycles of cold and warm water (22-29°C), every 30 min (Fig. 17).

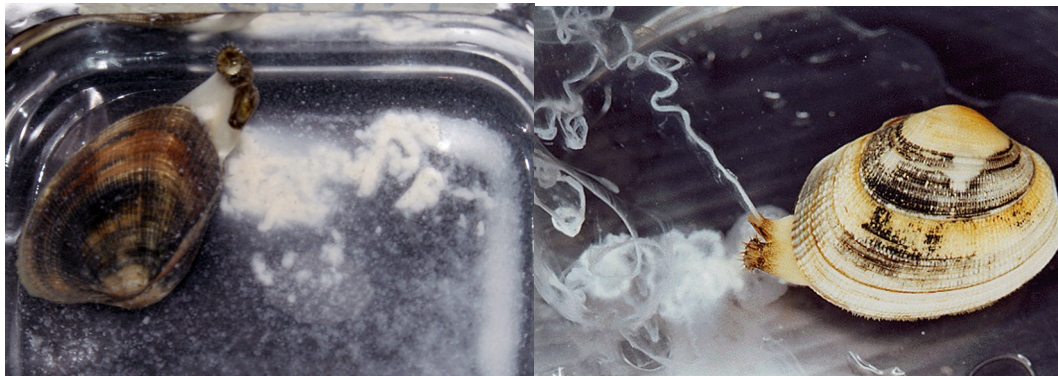


Fig. 17 – *R. philippinarum* spawning induction. (Bottom left) Spawning female. (Bottom right) Spawning male.

Spawned eggs and sperm were collected and embryo series were obtained by *in vitro* pair matings. For each experiment, only eggs from one female and sperm from one male were used for fertilization (*i.e.* single crosses). After fertilization, embryo development was visually checked with an optical microscope, and the stage noted. Samples were collected every 5 min in the first 60 min, and every 10 min afterwards, until 2 h after fertilization: 2-, 4-, 8-, 16- and 32-cell embryos were collected. The main reason for the 2 h limit was the sample

size of the *in vitro* fertilization: to allow fast collection, I kept developing embryos in a small quantity of artificial sea water. In my experience, under these conditions, overcrowding would easily lead to embryo death due to water poisoning by rotten unfertilized eggs, so I had to limit the sampling time.

2.2 – TEM sample preparation

Clams for gonad analysis were sampled in February (developing) and May (mature). Sample preparation for Transmission Electron Microscopy (TEM) analysis was performed following a standard protocol with some modification (see for example Erkan and Sousa 2002). Gonadic tissue was dissected using scalpels and immediately rinsed for primary fixation in 2% glutaraldehyde (in salt water: reverse osmosis water with Red Sea Coral Pro® salt added) for 10 min at 4°C. The samples were left for 2 h in new 2% glutaraldehyde, and then rinsed 5 times for 10 min in salt water. Secondary fixation was carried out in 1% osmium tetroxide in salt water for 1 h. After rinsing for 30 min in salt water, I proceeded with dehydration by acetone series (50-70-90-95-100%). 70% acetone solution was added with 1 g uranyl acetate every 100 ml (1% uranyl solution). To embed in resin, I mixed the same quantity of resins A-m and B (Fluka Durcupan ACM, A-m and B), and left the samples overnight in resin mix + acetone 100% (50:50). The next day, I transferred samples to pure resin mix for 1 h, then I changed with new resin mix for 1 h. Next, the samples were left 1 h in new resin mix added with catalyst (Fluka Durcupan ACM, C) (2 changes). Finally, samples were heated to 45°C for 24 h. Polymerization in embedding molds was completed after 3-4 days in oven at 60°C, followed by 1-2 days at 45 °C. A Reichert ultramicrotome was used to cut silver-gold ultrathin sections (60-90 nm) for TEM analysis. Sections were cut using diamond knives mounted on the ultramicrotome. Ultrathin sections were collected on 75 mesh, copper grids (coated by formvar) and stained: 20 min with 3% uranyl acetate (50 ml alcohol 50% + 1.5 g

uranyl acetate), then 15 min with lead citrate (0.125 g lead citrate + 49.5 ml distilled water + 0.5 ml NaOH 1 N), and then washed with distilled water. The sections were examined using a Philips CM100 (PW6021) TEM at 80kV. Pictures were recorded with a Kodak MEGAPLUS Camera, Model 1.6i, using AnalySIS® Software.

2.3 – SEM sample preparation

Sample were put directly in 2% glutaraldehyde in salt water (reverse osmosis water with Red Sea Coral Pro® salt added) for 10-15 min. Glutaraldehyde solution was changed and left for other 2 h. Samples were washed twice for 15 min in salt water and then dehydrated with an increasing quantity of ethylic alcohol (20-30-50-70-80-85-90-2x100%), trying to preserve blastomeres morphology (directly in absolute alcohol cause a bad shrink of the cells). A solution of hexamethyldisilazane:ethanol (50:50) was added and left for 30 min. After a wash with 200 µl of 100% hexamethyldisilazane, as soon as the embryos were sedimented (10-15 min), the 100% hexamethyldisilazane was changed (1 ml). Samples were allowed to evaporate overnight under an extractor fan. The day after, the liquid not evaporated was removed. Dried specimens were then mounted on brass stubs by means of a conducting tape and gold-coated in a BIO RAD SC502 sputter according to the firm specifications. Sample images were obtained with a JEOL–JSM 520 Scanning Electron Microscope (SEM) and digitally recorded.

2.4 – MitoTracker staining

The mitochondrial-specific vital dye MitoTracker® Green FM (Molecular Probes®) was dissolved in anhydrous dimethylsulfoxide (DMSO; Sigma Chemical®) to a concentration of 1 mM and added to the sperm suspension (final concentration 200 nM); the sperm were incubated for 20 min at room temperature in the dark. After checking by fluorescence

microscopy that the staining of sperm midpieces was successful, eggs were fertilized by dropping a small amount of the sperm suspension (about 500 μ l in 250 ml of water containing the eggs spawned by one female). The developing embryos were kept in the dark to prevent the decay of MitoTracker fluorescence. I put the sample on slides coated with 3-aminopropyltriethoxysilane (Sigma) and left the sample to deposit. Finally, I mounted directly in seawater. The visualization was performed by a Nikon Eclipse 90i fluorescence microscope using a FITC filter and picture were recorded by NIS-elements AR 3.0 software.

2.5 – SDS-PAGE and western blotting

Pieces of gonads and embryos were frozen in liquid nitrogen, stored at -80°C , and then processed by SDS-PAGE (Sodium Dodecyl Sulphate - PolyAcrylamide Gel Electrophoresis) and western blotting. Embryos of 2, 4 and 8 blastomeres were pooled for this analysis. Samples were homogenized in a buffer containing 10 mM Tris-HCl, pH 7.5, 1 mM ethylene glycol-bis(2-aminoethyl ether)-N,N,N',N'-tetraacetic acid (EGTA), 0.1% SDS in the presence of 2x protease inhibitor cocktail tablets (Complete Mini, Roche) and 1 mM phenylmethanesulfonylfluoride (PMSF), utilizing an Ultra Turrax T25 Janke & Kunkel IKA-labortechnik. Then samples were centrifuged at 10,000 rpm for 10 minutes at 4°C . The supernatant was stored at -80°C . Gonadic and embryonic extracts of *R. philippinarum* (10 μ g) were separated in 8.5% SDS polyacrylamide gels according to Laemmli (1970). For immunoblotting, proteins were transferred to Hybond-ECL membrane (Amersham International, Buckinghamshire, UK). Non-specific protein-binding sites were blocked with 5% dried skimmed milk (Bio-Rad Laboratories, Hercules, CA, USA), 3% Bovine Serum Albumin (BSA), and 0.1% Tween-20 (Sigma) in Tris-Buffered Saline [TBS: 1.7 g Trizma base, 5.6 g NaCl in 700ml in water] overnight at 4°C and subsequently washed with 0.1% Tween TBS. To recognize Vasa protein, I utilized an antiserum against chicken Vasa-

homolog produced in rabbit already in use in our laboratory (anti-Cvh; Tsunekawa et al. 2000). The membranes were treated as described in Maurizii et al. (2009). A bidimensional SDS-PAGE of gonadic extract was carried out as in GE Healthcare Handbook (80-6429-60AC).

2.6 – *vasa*-homolog

I analyzed the *vasa*-like gene of *R. philippinarum* found by whole transcriptome sequencing of gonads (Ghiselli et al. 2012). An ORF of 2,373 bp (base pairs) was identified, translated and aligned with Cvh (*Gallus gallus*, GenBank BAB12337.1) using T-COFFEE, version 8.99 (Notredame et al. 2000). Conserved domains were identified using InterProScan, version 4.8 (Hunter et al. 2009).

2.7 – Tissue processing and immunocytochemical analyses

2.7.1 – Embryos

Embryos were fixed in a solution containing 3.7% paraformaldehyde, 0.1% glutaraldehyde, and 1.5 μ M taxol in K-PIPES buffer [80 mM K Pipes; 1 mM $MgCl_2$; 5 mM EGTA; 0.2% Triton X-100] (pH 6.8) for 30 minutes at 37°C. After several washes in Tris-Buffered Saline solution [TBS: 155 mM NaCl, 10 mM Tris-HCl] (pH 7.4), embryos were put in methanol and stored at 4°C. After rehydration with TBS (pH 7.4), fixed embryos were put on slides coated with 3-Aminopropyltriethoxysilane (APES; Sigma), treated with 50 mM sodium borohydride in TBS for 60 minutes at RT and rinsed in TBS with several changes. Embryos for microtubule staining were digested with 0.01% Pronase E (Merck) in Phosphate-Buffered Saline solution (PBS) [128 mM NaCl, 2 mM KCl, 8 mM $Na_2HPO_4 \cdot 2H_2O$, 2 mM KH_2PO_4] (pH 7.2), for 6-7 minutes at RT. Permeabilization was performed adding TBS-Triton 1% to

all the samples and leaving over night at 4°C.

2.7.1.2 – *Vasa immunostaining*

Non-specific protein-binding sites were blocked with a buffer containing 10% Normal Goat Serum (NGS) and 1% BSA in TBS 0.1% Triton (pH 7.4). The primary antibody (anti-Cvh) was diluted 1: 2,000 with TBS containing 0.1% Triton, 10% Normal Goat Serum (NGS), and 1% BSA (pH 7.4) for 48 hours at 4°C. As secondary antibody I utilized a goat anti-rabbit polyclonal antibody, conjugated with N,N'-(dipropyl)-tetramethylindocarbocyanine (Cy3) (Zymed, Molecular Probes), diluted 1: 300 with TBS containing 0.1% Triton, 10% NGS, and 1% BSA (pH 7.4) for 30 hours at 4°C in the dark.

2.7.1.3 – *Microtubule immunostaining*

Embryos were incubated with a monoclonal anti- α -tubulin, clone DM 1A (Sigma), diluted 1: 1,800 with TBS-Triton 0.1% and 2% BSA (pH 7.4) for 48 hours at 4°C. Bound primary antibody was detected using Cy3-conjugate anti-mouse, produced in sheep (Sigma), diluted 1: 300 with TBS-Triton 0.1%, 2% BSA (pH 7.4), with about 40 hours of incubation at 4°C in the dark.

Nuclei of all samples were stained with 1 mM TO-PRO3 (Molecular Probes) diluted 1: 2,000 in PBS (pH 7.2) at RT in the dark. Samples were mounted in 2.5% 1,4-diazabicyclo[2.2.2]octane (DABCO; Sigma), 50 mM Tris (pH 8) and 90% glycerol, and stored at 4°C.

Controls were performed using embryos in which the first or the second antibody was omitted, and embryos treated only with normal serum. Imaging of embryos was recorded by a confocal laser scanning microscope (Leica confocal SP2 microscope), using Leica software.

2.7.2 – Gonads

Pieces of gonads were removed, fixed in a 3.7% paraformaldehyde and 0.1% glutaraldehyde solution in K-PIPES buffer (pH 7) for 3 hours and embedded in 7% agar. Sections of about 100 μm thickness were made using a Lancer Vibratome Series 1000 and post-fixed with increasing concentrations of methanol. Sections were rehydrated and then treated 1 hour and 15 minutes with sodium borohydride 70 mM in TBS (pH 7.4) at RT. After rinsing 1 hour and 15 minutes in TBS-Triton 0.1%, samples were permeabilized adding TBS-Triton 1% and left over night at 4°C. See *Vasa immunostaining* above for Vasa immunolocalization.

2.7.2.1 – Microfilament staining

Sections of gonads fixed in a 4% paraformaldehyde and 0.1% glutaraldehyde solution in K-PIPES buffer were incubated with FITC phalloidin (Invitrogen) to stain microfilaments. More in detail, sections were pre-incubated in PBS - 1% BSA (pH 7.2) for 30-40 min. Then they were put in a 0.32 μM phalloidin solution in PBS - 1% BSA (pH 7.2) for 45 min at room temperature in the dark. Next, samples were washed three times for 10 min each in PBS (pH 7.2), mounted in Prolong (Molecular Probes) and stored at 4°C.

2.8 – Analysis of transcripts with sex and family biases

During my last year of PhD, I spent six months at the University of Southern California, where I analyzed the gonad transcriptome of *R. philippinarum* obtained at the Nuzhdin Lab (Department of Biological Sciences – Molecular and Computational Biology section) through RNAseq (Mortazavi et al. 2008) on Illumina GAI platform. Two families (family = progeny from a single pair matings) were analyzed: Family 1, showing a female bias in the progeny (83% females), and Family 2, with a male-biased progeny (82% males) (see Ghiselli et al. 2012).

The transcription level was expressed in FPKM. FPKM of a region (gene, exon, segment of DNA, etc) is fragments mapped per 1000 bases per 1M reads mapped:

$$FPKM = \frac{\sum_{i=1}^N d_i}{\text{ReadLength}} \times \frac{1000}{N} \times \frac{1,000,000}{L}$$

where: d_i is the depth at position i that you need to sum across all N positions; ReadLength was of 76 bases; N is the total number of mappable fragments of the sample and L is the length of the transcript (in bp) (see also Supplementary Material in Mortazavi et al. 2008).

Searching for genes with sex/family bias (i.e. more expressed in one sex/family) that could be involved in reproduction and sex determination, I focused on those biased genes annotated in Reproduction and Ubiquitination Gene Ontology (GO) categories, and with BLASTX (Table 1; see Discussion for details). The protein inferred from these transcripts were analyzed using InterProScan, version 4.8 (Hunter et al. 2009) to find conserved functional domains. The same transcripts were also localized in tissues using *in situ* hybridization (see next paragraph).

2.9 – *In situ* hybridization

At the Neurobiology section (Department of Biological Sciences) of the University of Southern California I performed an *In Situ* Hybridization (ISH) analysis on *R. philippinarum* gonadic tissue. For this analysis, gonads from five specimens (3 males and 2 females) from Torrance (CA, USA) were used.

2.9.1 – Riboprobe construction

A probe against a novel mitochondrial ORF contained in the Male Unassigned Region 21 (MUR21) of M-type mtDNA was produced, together with three probes against nuclear

transcripts showing a sex and family bias and that could be involved in sex determination (Tables 1). These genes translate for proteins similar to: 1) the Proteasome subunit alpha 6 (here named PSA); 2) baculoviral IAP (inhibitor of apoptosis) repeat-containing 4 (named BIRING); 3) AN1-type zinc finger and ubiquitin domain-containing protein (named ANUBL1).

Table 1 – Transcripts target of *in situ* riboprobes.

Locus	Annotation	Length (bp)	Function	Probe name
M-mtDNA				
ORF-MUR21	Unassigned Region (UR)	519		ORF-21
Nu-DNA				
Ubiquitination-related genes				
3993	proteasome subunit alpha 6 (<i>psa6</i>)	881	Degradation	PSA
13574	baculoviral IAP repeat-containing 4 (<i>birc4</i>)	824	Anti-apoptosis	BIRING
1193	AN1 zinc finger + ubiquitin-like domain	2442	Ubiquitination	ANUBL1
Reproductive genes				
13574	baculoviral IAP repeat-containing 4 (<i>birc4</i>)	824	Anti-apoptosis	BIRING

M-mtDNA = Male mitochondrial genome; Nu-DNA = Nuclear genome.

For riboprobe construction, the Primer3 online program (<http://frodo.wi.mit.edu/>) was used to select optimal primer sequences that would result in a PCR product size of 400-600 base pairs (bp) and an annealing temperature of 60°C. The following primers were used to generate anti-sense *in situ* probes against the four genes.

M-type mitochondrial genome:

Novel gene: anti-sense probe, containing the entire ORF-21 sequence of 519 bp, was generated from the M-type mitochondrial whole genome sequence present in GenBank (AB065374):

- ORF-21, forward: 5' - GGTAGCACAAGGTTTCCAGAGTTTATGTGT - 3',
reverse: 5' - ACTTGTAACCCAGGGGTAAGAGGTCACA - 3' (product 603 bp).

Nuclear genes:

Ubiquitination genes:

- PSA, forward: 5' - AGAGCGAGGTATGAGGCAGCCA - 3', reverse: 5' - GTGGGTTTGCCTTAGTAACTGCACCA - 3' (product 400 bp; GenBank Accession Number of the whole gene sequence: JO114756).

Reproduction and Ubiquitination genes:

- BIRING, forward: 5' - ACGAATGGGGATGATCAGTCTAGCCA - 3', reverse: 5' - TGGTTCTGCGCATTCCATGCAGA - 3' (product 417 bp; GenBank Accession Number of the whole gene sequence: JO103463);
- ANUBL1, forward: 5' - GGCACGTGCTATGTCTGGACTGT - 3', reverse: 5' - TGGAAGCTTTGGGGCACTGACAA - 3' (product 454 bp; GenBank Accession Number of the whole gene sequence: JO102461).

In all cases, the T7 RNA polymerase binding sequences were added 5' to the anti-sense DNA sequence. RNA extraction was performed by TRIzol® from specimens used for the transcriptome library construction (Ghiselli et al. 2012). The target sequences were amplified by PCR from cDNAs obtained by SuperScript™ III First-Strand Synthesis System for RT-PCR (Invitrogen – life technologies).

Digoxigenin (DIG)-labeled riboprobes were obtained using the Roche in vitro transcription labeling protocol (Roche DIG RNA labeling kit).

2.9.2 – Tissue fixation and section preparation

ISH experiments were performed on 10-20 µm cryosectioned sections from clam mature gonads using standard techniques (see Schaeren-Wiemers and Gerfin-Moser 1993). In more detail, gonads were dissected and fixed in ice-cold 4% formaldehyde (FA) in 1x PBS (2-3 h at

4°C, shaking). Samples were transferred into 30% sucrose in 1x PBS overnight at 4°C, with shaking. Next, the sucrose was sucked off and TissueTek® OCT Compound (Sakura, USA) added, stirring with a clean plastic tip. Finally the samples were transferred to plastic molds filled with new OCT and freeze on dry ice. Blocks were stored at -80°C. Sections of 10-20 µm were cut on a cryostat and mounted on fisherbrand superfrost/plus slides (FisherScientific). Slides were stored at -80°C.

I processed and checked 63 slides of which 46 resulted to be useful for ISH analysis (sections containing gonadic tissues), for a total of 276 sections (6 sections x slide).

2.9.3 – Digestion, acetylation and permeabilization

The sections were fixed in ice-cold 4% FA for 10 min at RT. After three washes with 1x PBS for 3 min each, samples were digested in a Proteinase K solution [1 µg/ml in 50 mM Tris pH 8, and 5 mM EDTA in diethylpyrocarbonate (DEPC) treated water] for 5 min at RT. Samples were fixed again in 4% FA for 5 min at RT and washed three times with 1x PBS for 3 min each. Next I proceeded with acetylation in a 0.1 M Triethanolamine, 0.02 M HCl, 0.25% Acetic anhydride solution in DEPC water, for 10 min at RT with vigorous shaking. Samples were then permeabilized with 1x PBS 1% Triton for 30 min at RT and washed 3 times with 1x PBS for 5 min each.

2.9.4 – Hybridization

I placed on each slide 500 µl of hybridization buffer [50% formamide, 5x Saline-Sodium Citrate buffer (SSC); 5x Denharts; 2% Salmon sperm DNA; 0.8-1% Yeast tRNA in DEPC water] and I put them in a humidified chamber where they were incubated for 4 h at RT. Next, the hybridization buffer was replaced with 100 µl hybridization solution (hybridization buffer heated at 72°C for 15 min before adding the probe (200-400 ng/ml DIG RNA probe), which

was also heated at 72°C for 3 min and iced). After coverslipping the slides, I put them in a box with a piece of paper wet with a solution 5x SSC and 50% formamide, and they were incubated overnight at 72°C. The day after, slides were placed 5 min in 72°C 5x SSC. Next, they were transferred into 0.2x SSC at 72°C for 45 min, into new 0.2x SSC at 72°C for other 45 min, into new 0.2x SSC at RT for 5 min, and then transferred to Tris-Buffer Saline [TBS: 0.1 M Tris(-HCl), 0.15 M NaCl, in miliQ water] 5 min at RT (pH 7.5). To block non-specific binding, 500 µl of TBS containing 10% heat inactivate sheep serum (HISS) were placed on each slides for 2 h at RT. Next, the blocking solution was replaced with 300 µl of 1: 5,000 anti-digoxigenin antibody (Anti-Digoxigenin-AP, Fab fragments, Roche) diluted in TBS containing 3% HISS and slides were put in a humidified chamber at 4°C overnight. After washing with TBS for 4 h (30 min each), samples were equilibrated 5 min with solution A [0.1 M Tris, 0.1 M NaCl, 0.05 M MgCl₂, in miliQ water].

2.9.5 – Alkaline phosphatase color reaction

The solution A was replaced with 150 µl of solution B [153.3 µl solution A + 1.53 µl 10% Tween + 0.26 µl of Levamisole 500 mM + 0.53 µl of 5-bromo-4-chloro-3-indolyl phosphate (BCIP) 50 mg/ml + 0.53 µl of nitro blue tetrazolium (NBT) 100 mg/ml and vortex] and coverslipped. Slides were incubated at RT in the dark, until the color reaction was completed. Then the reaction was stopped with TE (10 mM Tris pH 8, 1 mM EDTA in miliQ water). Finally, samples were mounted with Dakocytomation glycerol and stored at RT.

Samples were analyzed with a Nikon Eclipse 80i microscope and images were captured using NIS-Elements D3.2 software, all with the same acquisition parameters. Images were not electronically processed to allow for accurate comparison.

3 – RESULTS

3.1 – Sperm morphology and localization of M mitochondria during embryo development

At maturity, spermatozoon midpiece normally carries four mitochondria in *R. philippinarum*. Out of a hundred spermatozoa from four males observed, only one contained five (Fig. 18). Also spermatozoa of the venerid *Pitar rudis* generally contain four midpiece-mitochondria, but a 10% with five was reported (Erkan and Sousa, 2002). In *R. philippinarum*, spermatozoon mitochondria measure 800-1000 nm in diameter, while in vitellogenic oocytes mitochondria can reach about 600 nm, but those bigger than 500 nm are rare. Mitochondrial dimensions obviously depend on the cell section level, and the highest value is the closest to reality. In any case, however, spermatozoon mitochondria are always larger than egg mitochondria. Egg diameter is about 75 μm , while early embryos measure 80-85 μm . The sperm-head is 3.5 μm long, excluding acrosome and midpiece.

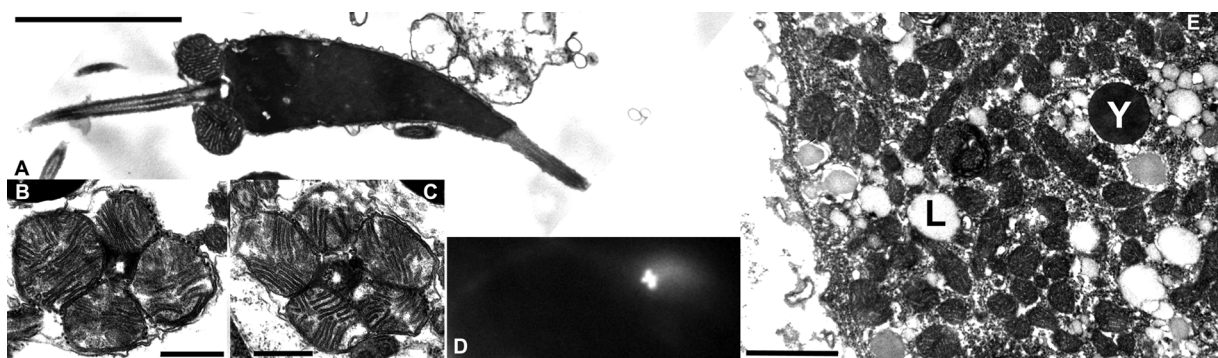


Fig. 18 – Gamete morphological analysis by TEM. (A) Whole spermatozoon (A: 2 μm bar). The midpiece of *R. philippinarum* spermatozoon normally carries four mitochondria (B), generally of 800-1000 nm in diameter; only once five mitochondria were found (C) (B, C: 500 nm bar). (D) Spermatozoon stained with MitoTracker Green FM: midpiece mitochondria showed strong fluorescence. (E) Oocyte during vitellogenesis: mitochondria usually measure less than 600 nm, but the highest values (more than 500 nm) are really rare (E: 1 μm bar). L – lipid droplet; Y – yolk granule.

In our experimental conditions, fertilized eggs started cleaving 45-50 min post fertilization (mpf), when the zygote divided into two cells (Fig. 19A, B; see figure caption for details). In this stage the two blastomeres are different in size (AB the smaller, CD the bigger; after Conklin 1897). The segmentation proceeds, reaching the veliger stage about 48 h post fertilization (hpf) (Figs 19 and 20).

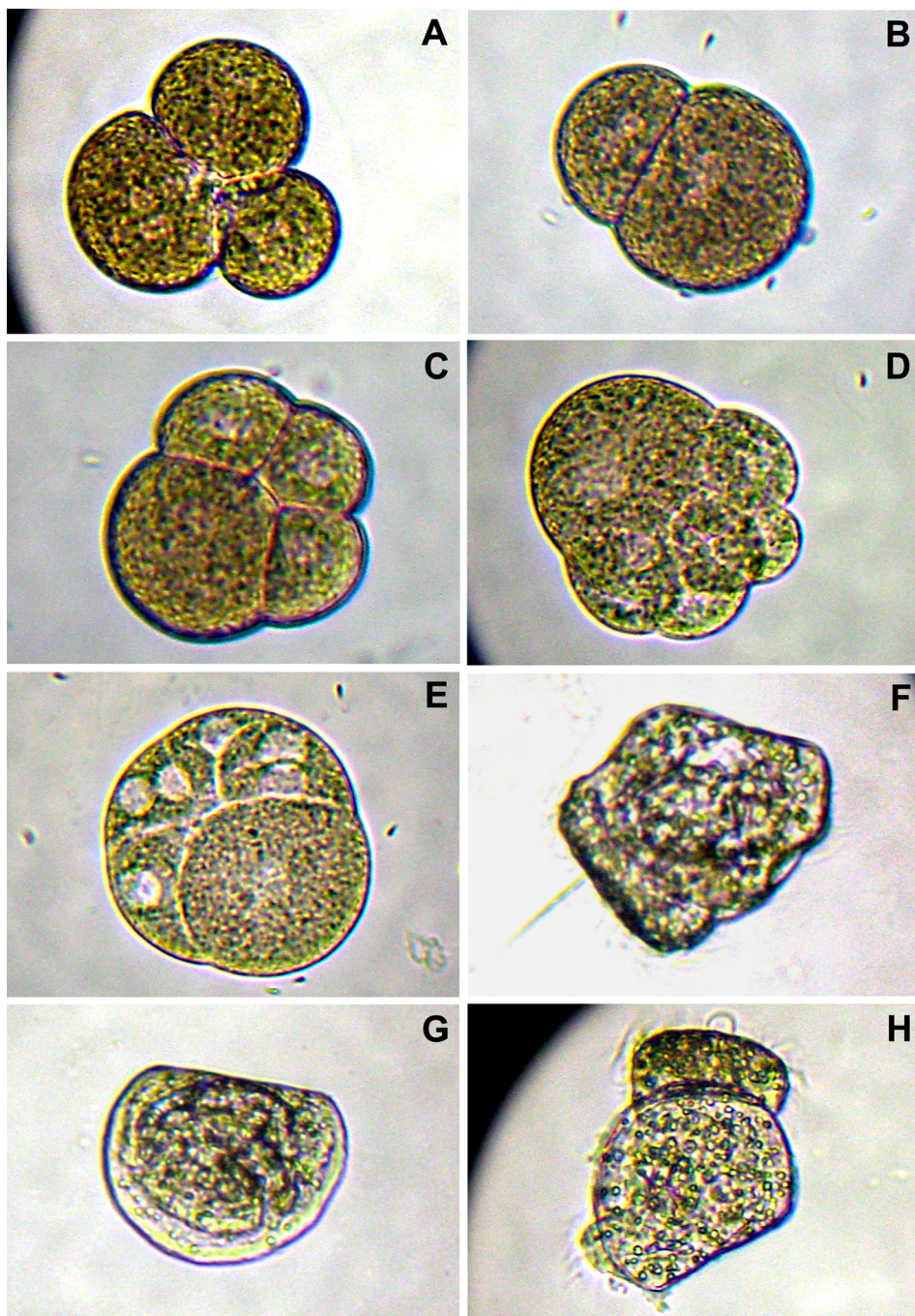
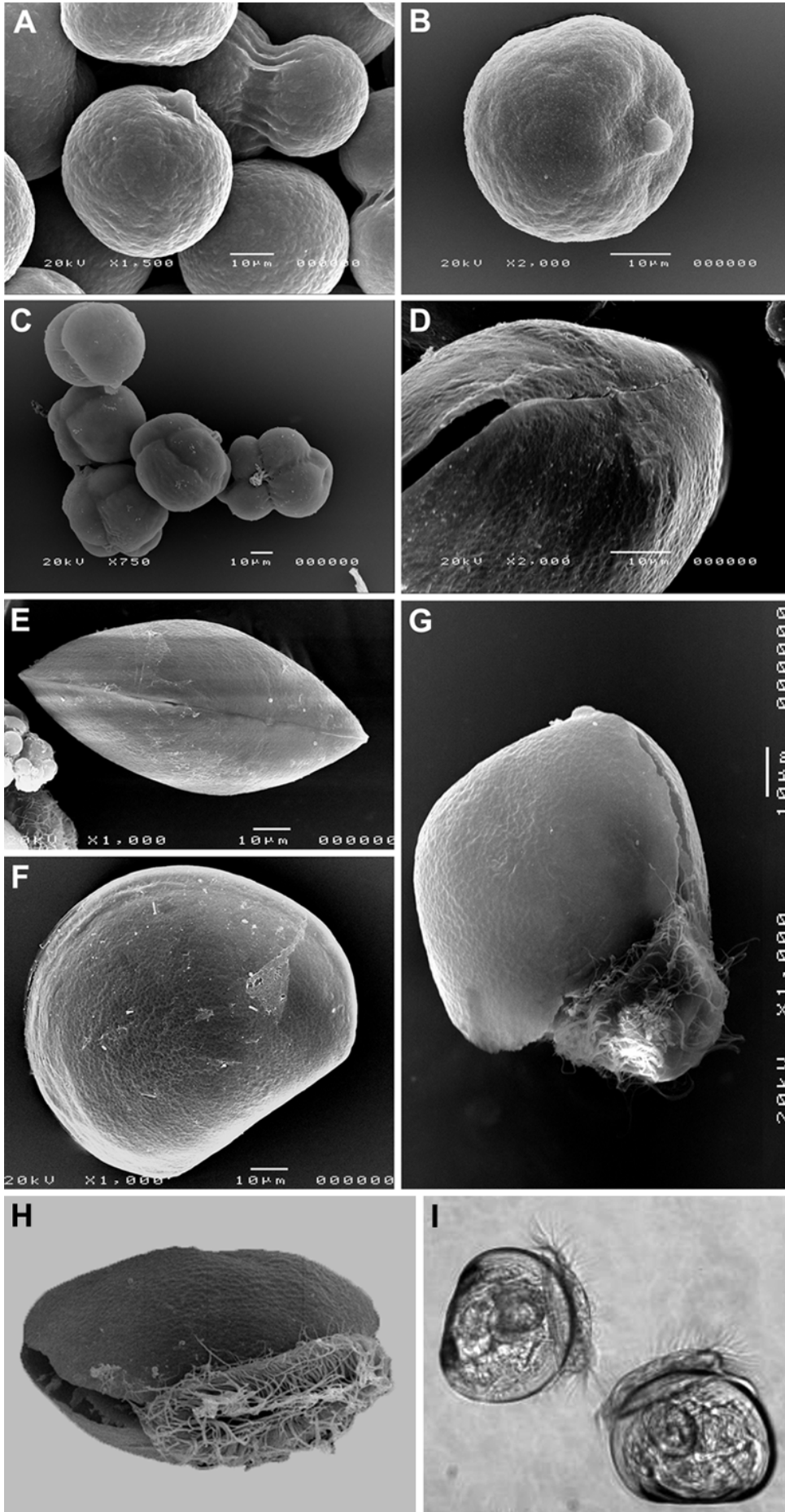


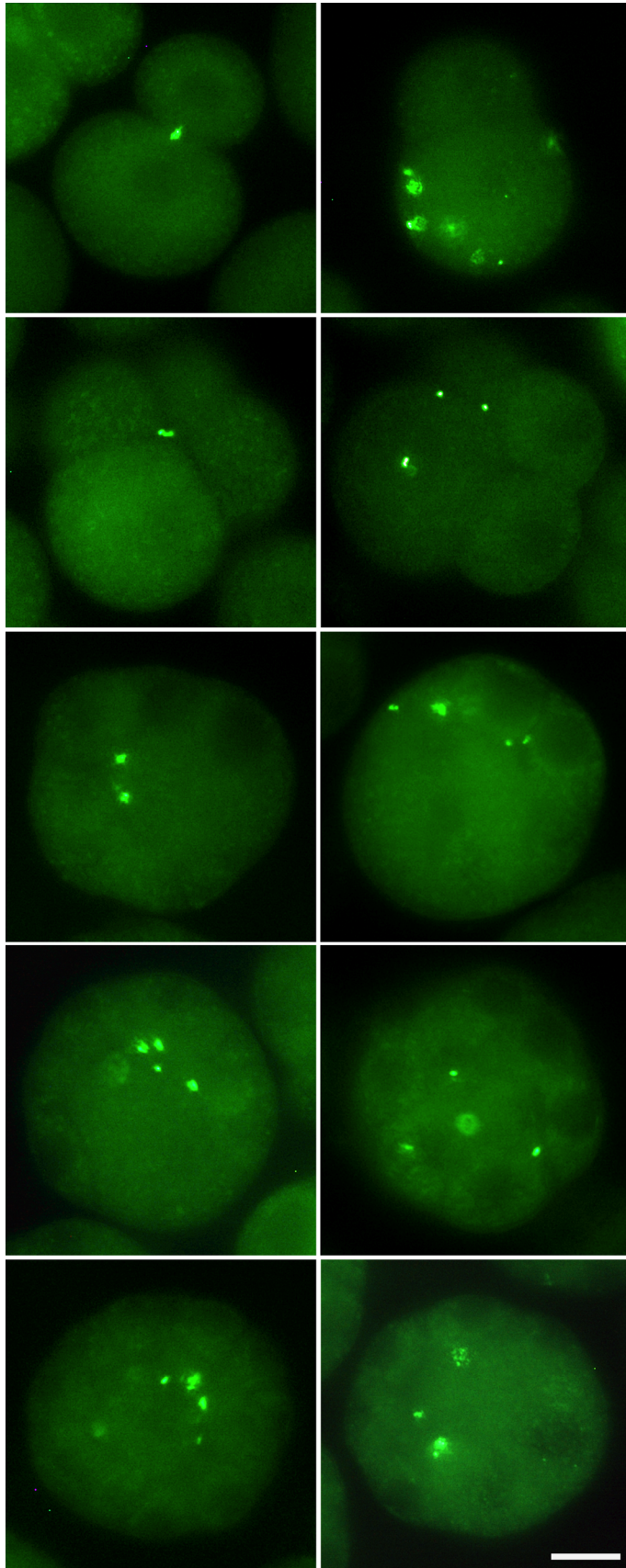
Fig. 19 – (Previous page) **Light microscopy of live *R. philippinarum* embryos during segmentation.** (A) Unequal cleavage is mediated by the formation of an anucleate vegetal protrusion, the polar lobe (PL). The first cleavage is equal, but the first polar lobe fuses with only one blastomere generating a smaller AB and a larger CD blastomere (B) (45-50 mpf). Only the CD blastomere has the capacity to form the polar lobe at the second cleavage. (C) The polar lobe fuses with only one of the daughter blastomeres forming a larger D and a smaller C blastomere (60 mpf). (D, E) 90 mpf: 8-blastomere embryo. (F) 15 hpf: Trocophore 75-90 μm . (G) 24 hpf: D-larva 90-100 μm . (H) 48 hpf: Veliger 100-160 μm .

Fig. 20 – (Next page) ***R. philippinarum* embryo development (SEM).** (A, B) Fertilized egg showing the polocyte, and a two-blastomere embryo on the background (A). (C) A group of four embryos with eight blastomeres. (D-F) D-larvae. (G, H) Veliger of *R. philippinarum*. (I) Light microscopy of live veligers of *Mytilus californianus*.



From the two-blastomere stage onwards, in embryos fertilized by sperm treated with MitoTracker®, I observed two distribution patterns of sperm mitochondria: in the “aggregated” pattern, sperm mitochondria formed a tight mass close to the cleavage furrow, while in the “dispersed” pattern, sperm mitochondria were scattered (Fig. 21). After 1 h embryos had four blastomeres, with one cell (D) bigger than the others. At this stage, in the aggregated pattern, sperm mitochondria were observed at the boundary among the four blastomeres (Fig. 21). At the 8-cell stage, 90 mpf, the aggregate of M-type mitochondria seemed to be less closely joined, when compared to the same stage in *Mytilus* (see Cao et al. 2004). After the 8-cell stage, even if the sperm mitochondria were still visible, their precise location could not be easily determined, because a clear identification of each blastomere was no longer possible. Evidence of duplication and/or degradation of sperm mitochondria was not observed during any of the analyzed stages, and a Real-Time qPCR confirmed that neither M- nor F-type mtDNAs underwent any significant increase or decrease in the first 2 h of development (Milani et al. 2012).

Fig. 21 – (Next page) **Distribution of spermatozoon mitochondria.** MitoTracker Green FM staining of sperm mitochondria allowed to follow with fluorescence microscopy their distribution in *R. philippinarum* embryos (2-, 4-, 8-, 16- and 32-blastomere stages). **Left column:** aggregated pattern. **Right column:** dispersed pattern. From the 8-blastomere stage onwards, the aggregated pattern seems to be less tight in the Manila clam than in *Mytilus*. A less stringent segregation mechanism could act in male embryos of *R. philippinarum*, accounting for the massive presence of M-mtDNA in somatic tissues of males. (20 µm bar).



Unfortunately, the staining of sperm mitochondria faded very quickly under the microscope light. Before the staining bleached, I managed to take pictures of embryos until the 32-blastomere stage to assess if in a given embryo spermatozoon mitochondria were aggregated or dispersed, but quantitative information about how many embryos showed the two different patterns was impossible to obtain.

3.2 – Gonad morphology

Female and male mature gonads of *R. philippinarum* consist of acini made of germinative epithelium supported by connective tissue (Devauchelle 1990). Different stages of gamete maturation within a single acinus can be seen (Devauchelle 1990; Fig. 22A and B). In female acini, oocytes are grouped at the periphery. During their maturation, oocytes become pedunculated and, shortly before spawning, lose their peduncles and fill the lumen of the acini (Devauchelle 1990 and Fig. 22A). Spermatogenesis occurs centripetally with mature spermatozoa free and mobile within the lumen of the acini (Devauchelle 1990 and Fig. 22B-D).

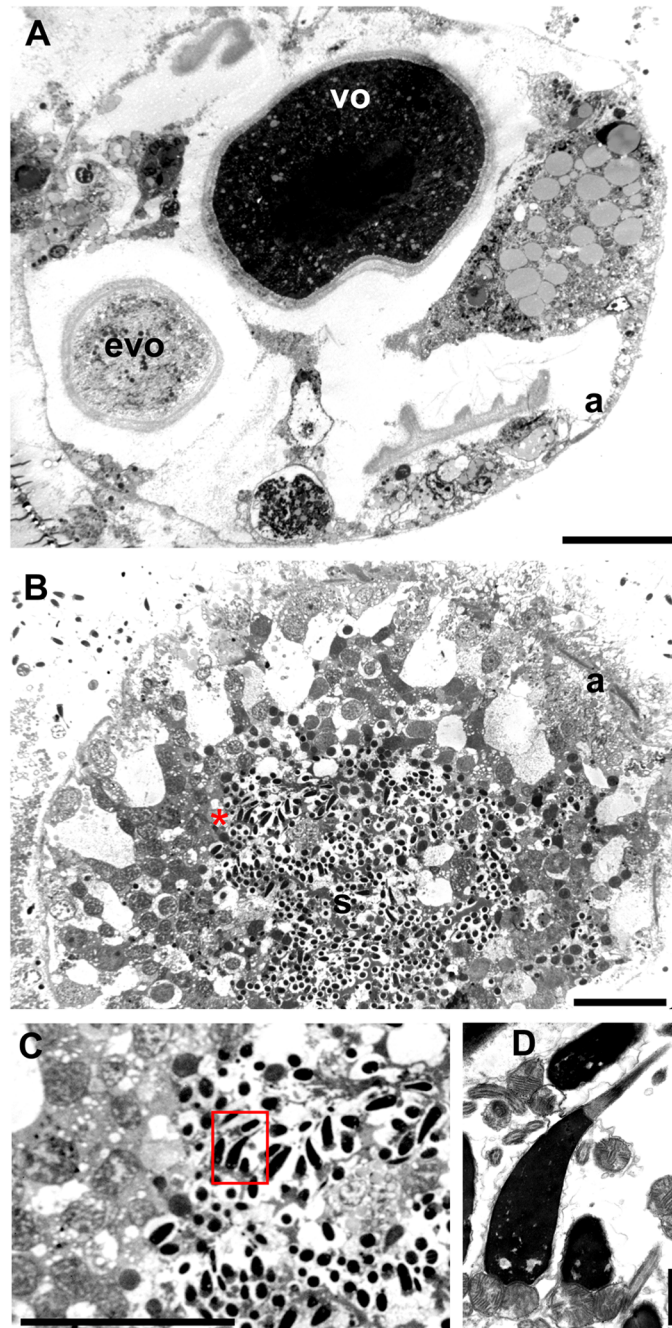


Fig. 22 – Morphological analysis of female and male gonads in *R. philippinarum* (TEM). (A) A female acinus, with oocytes at different stages of differentiation; evo – early vitellogenic oocyte; vo – vitellogenic oocyte; a – acinus wall (A: 20 μ m bar). (B) Portion of a male acinus in which spermatogenesis is developing centripetally, with mature spermatozoa (s) free within the acinus lumen (B: 20 μ m bar). (C) Magnification, from B, of the detail at the right side of the red asterisk, showing mature spermatozoa (C: 20 μ m bar). (D) The detail squared in C: a sperm head with acrosome and mitochondrial midpiece (D: 1 μ m bar).

As mentioned above, four mitochondria of about 1 μm in diameter form the midpiece of *R. philippinarum* spermatozoon, while egg mitochondria are quite smaller (about 0.6 μm in vitellogenic oocytes) (see Fig. 18). Ultrastructural analysis of developing gametes allowed the identification of both Balbiani body (Bb, Fig. 23) and Chromatoid body (Cb, Fig. 24), in early oocytes and early spermatids, respectively. Oogonia showed electrondense granules aggregating near two mitochondrial masses at opposite sides of the nucleus (Fig. 23A), where in early oocytes they formed the nuage of two identical Bbs (Fig. 23B and C). Each Bb was characterized by a dense nuage of about 1 μm and a mitochondrial mass of 10-28 organelles per section (Fig. 23B and C).

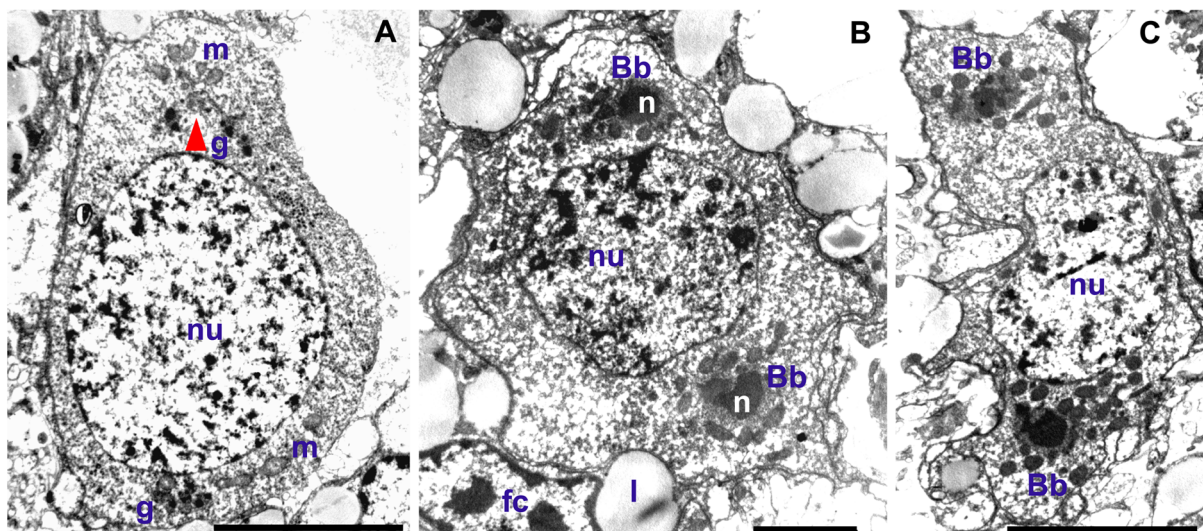


Fig. 23 – Ultrastructural analysis of the Balbiani body formation in *R. philippinarum* (TEM). (A) Oogonium showing electrondense granules (g) close to two mitochondrial masses (m) at opposite sides of the nucleus (nu) (A: 5 μm bar). (B, C) In early oocytes two identical Balbiani bodies (Bbs) are present, both containing a large and dense nuage (n) and a mitochondrial mass. fc – follicle cell; l – lipid droplet (B: 2 μm bar; C: 5 μm bar).

In early spermatids, the ultrastructural analysis allowed to identify a typical Chromatoid body (Cb) (Fig. 24), a bit longer than 1 μm , always located close to the nuclear membrane and surrounded by empty mitochondria (Fig. 24). A pore in the nuclear membrane could be seen

emitting material near the Cb (Fig. 24A-C). In the area among the nuclear pore, the empty mitochondria and the Cb, ribosomes of two different sizes were found on polyribosomes, with the small ones localized in a restricted zone (Fig. 24B and C).

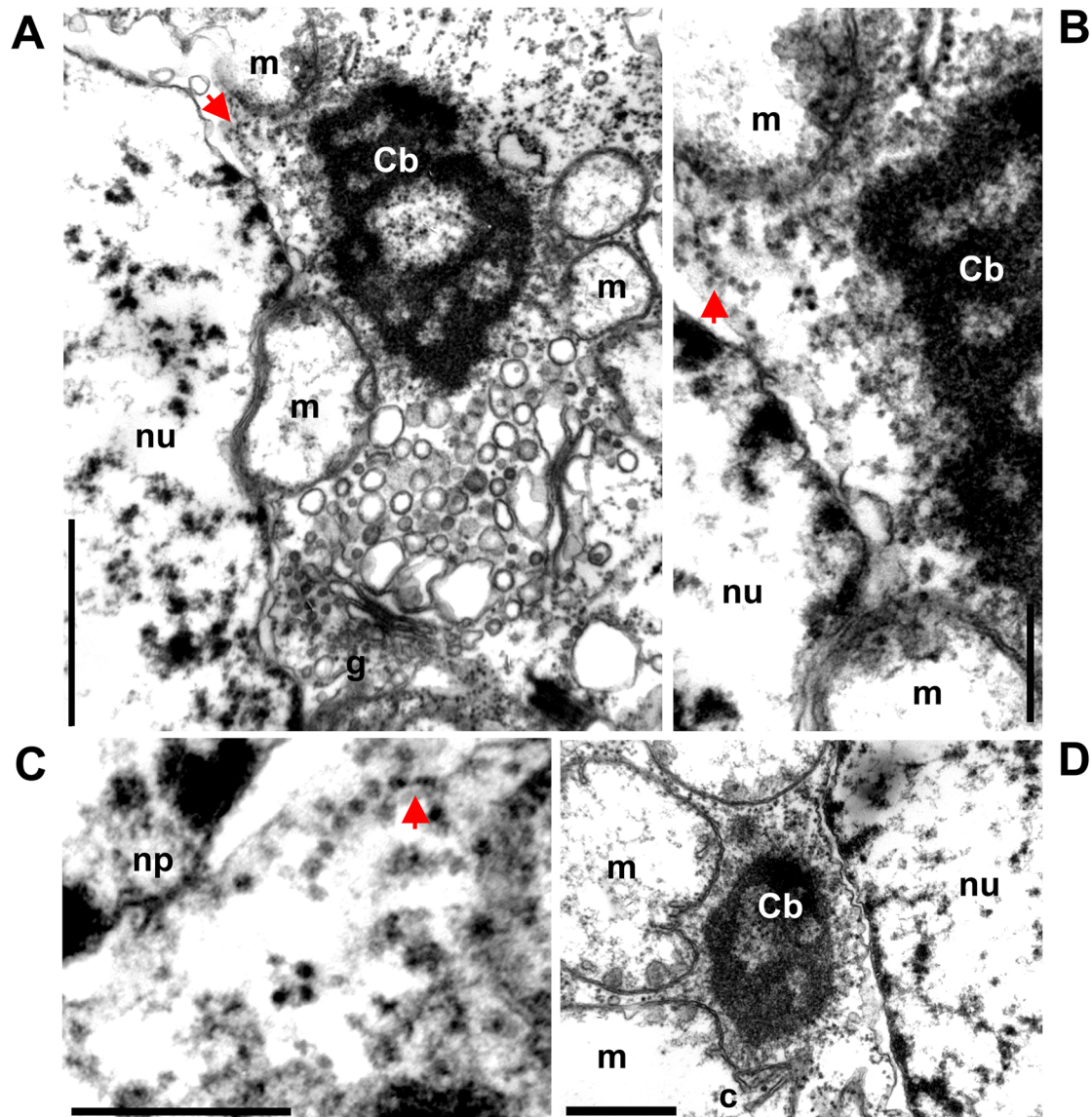


Fig. 24 – Ultrastructural analysis of the Chromatoid body formation in *R. philippinarum* (TEM). (A) Cytoplasmic area around the Chromatoid body (Cb) in an early spermatid (A: 1 μm bar); nu – nucleus; g – Golgi apparatus. (B) A detail from A showing the region among nucleus, mitochondria (m) and the Cb (B: 250 nm bar). (C) A detail of B: nuclear material outflows from a nuclear pore (np) and a polyribosome formed by ribosomes of two different sizes is visible, the smallest are indicated by an arrow (C: 250 nm bar). (D) The Cb is located close to the nuclear membrane and surrounded by empty mitochondria, some of which showing extruded cristae (c) (D: 500 nm bar). arrow – polyribosome.

3.3 – *R. philippinarum* vasa-homolog

The specificity of the anti-vasa Chicken antibody (anti-Cvh) was tested by performing mono and bidimensional western blots. In both gonad and embryo samples, monodimensional immunoblotting with anti-Cvh detected only one band of about 65 kDa as molecular mass (Fig. 25A). In gonadic extract, bidimensional analysis showed one big spot flanked by two smaller, all of about 65 kDa and isoelectric point (pI) around 5 (Fig. 25B).

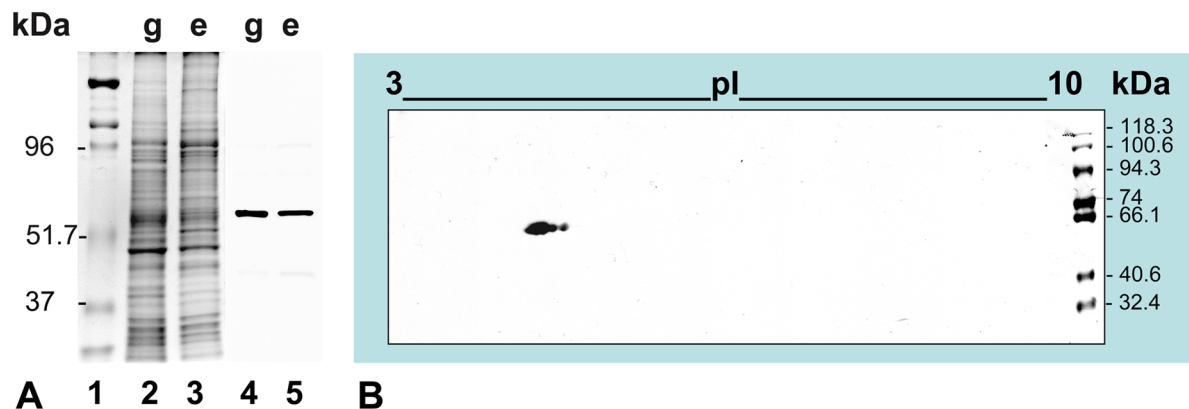


Fig. 25 – Specificity of the anti-Cvh antibody. (A) Monodimensional electrophoresis and immunoblotting of gonadic and embryonic extracts of *R. philippinarum*. Gel Coomassie stained (lanes 1-3). Lane 1: molecular mass standards with the value in kilodaltons (kDa) on the left. Lane 2: gonadic extract (g). Lane 3: embryonic extract (e). The antiserum against chicken Vasa-homolog (anti-Cvh) marks one protein band of about 65 kDa, both in gonadic and embryonic extracts (lanes 4, 5). (B) Bidimensional immunoblotting of gonadic extract with anti-Cvh. The antibody detects one big spot flanked by two smaller, all of about 65 kDa as molecular mass and with isoelectric point (pI) around 5.

I also analyzed *R. philippinarum* vasa homolog found by whole transcriptome sequencing of gonads (Ghiselli et al. 2012). I named it *vasph* (*vasa philippinarum* homolog). The inferred aminoacid sequence included 790 residues. T-COFFEE protein alignment with chicken Vasa-homolog showed a good CORE index (score = 95) (Notredame and Abergel 2003) (Fig. 26).

T-COFFEE, Version_8.99(Thu Feb 17 19:24:49 CET 2011 - Revision 594
 Cedric Notredame
 CPU TIME:0 sec.
 SCORE=95

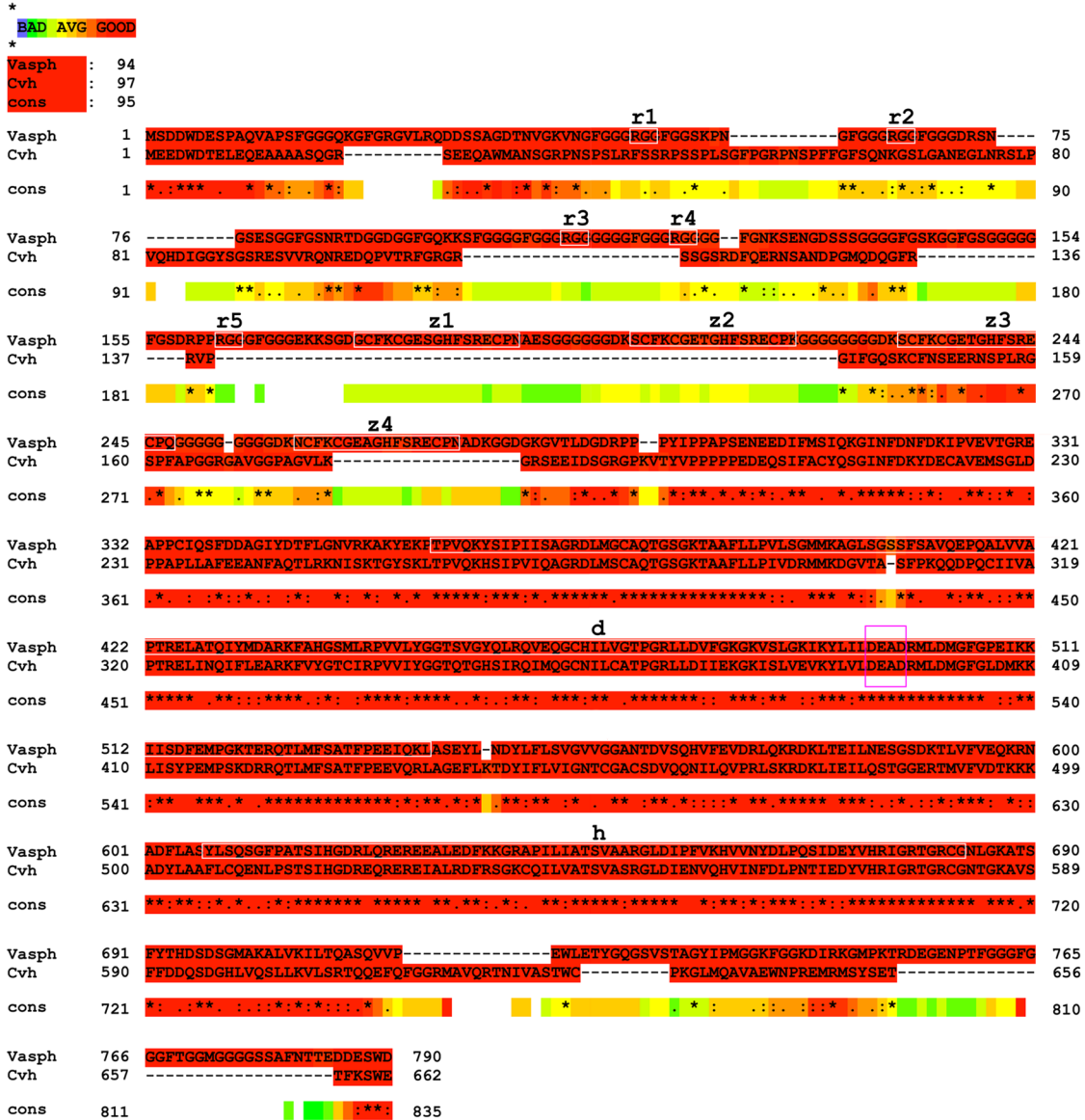


Fig. 26 – Vasa alignment. T-COFFEE alignment of Vasph (*Vasa philippinarum* homolog) and Cvh (chicken Vasa-homolog, *Gallus gallus*, GenBank BAB12337.1). Conserved domains are boxed in white and the DEAD motif in pink (see also Fig. 27). cons = consensus.

Using InterProScan, four CCHC-type zinc fingers (GO:0008270, location: 176-192; 204-220; 231-247; 259-275), a DEAD-box RNA helicase (GO:0008026, location: 361-540), and a C-terminal helicase (GO:0004386, location: 607-683) were found (Fig. 27). In addition, in the

predicted protein sequence five RNA-binding RGG motifs were included in the N-terminal region (Fig. 27).

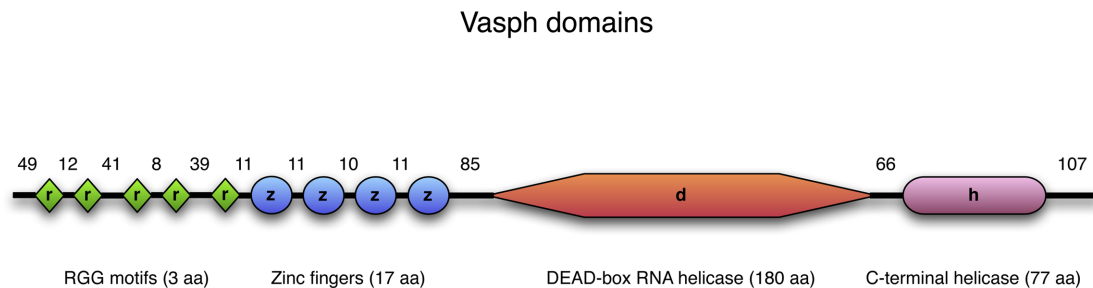


Fig. 27 – Vasph domains. Vasa conserved domains found in Vasph inferred sequence by InterProScan (version 4.8). There are four CCHC-type zinc fingers (17 aminoacids, aa, each), a DEAD-box RNA helicase (180 aa), and a C-terminal helicase (77 aa). In addition, five RNA-binding RGG motifs are included in the N-terminal region. The number of aminoacids of the regions between the domains are reported above the scheme.

Once verified anti-Cvh specificity, I analyzed Vasph expression in gonads and early embryos of *R. philippinarum*. At the beginning of the reproductive season, when gonads start forming, I found small groups of cells that were anti-Cvh labeled (Fig. 28A and B). These Vasph-stained cells were detected in the connective tissue among unlabeled intestinal loops (Fig. 28A), which is the normal position for bivalve gonad formation (Devauchelle 1990). In a following stage of gonad differentiation, Vasph-labeled cells formed an empty space in the middle of the aggregate, becoming the wall of incipient acini with a lumen at the center (Fig. 28C-F). Finally, in mature gonads acini appeared full of gametes (Fig. 28G-H). In a female acinus (Fig. 28G), oocytes showed a diffused cytoplasmic immunolocalization of Vasph. A small aggregation of granules was evident in the cytoplasm of the biggest oocyte (Fig. 28G). In male acini, a diffused staining was found in spermatogenic cells along the acinus wall (Fig. 28H).

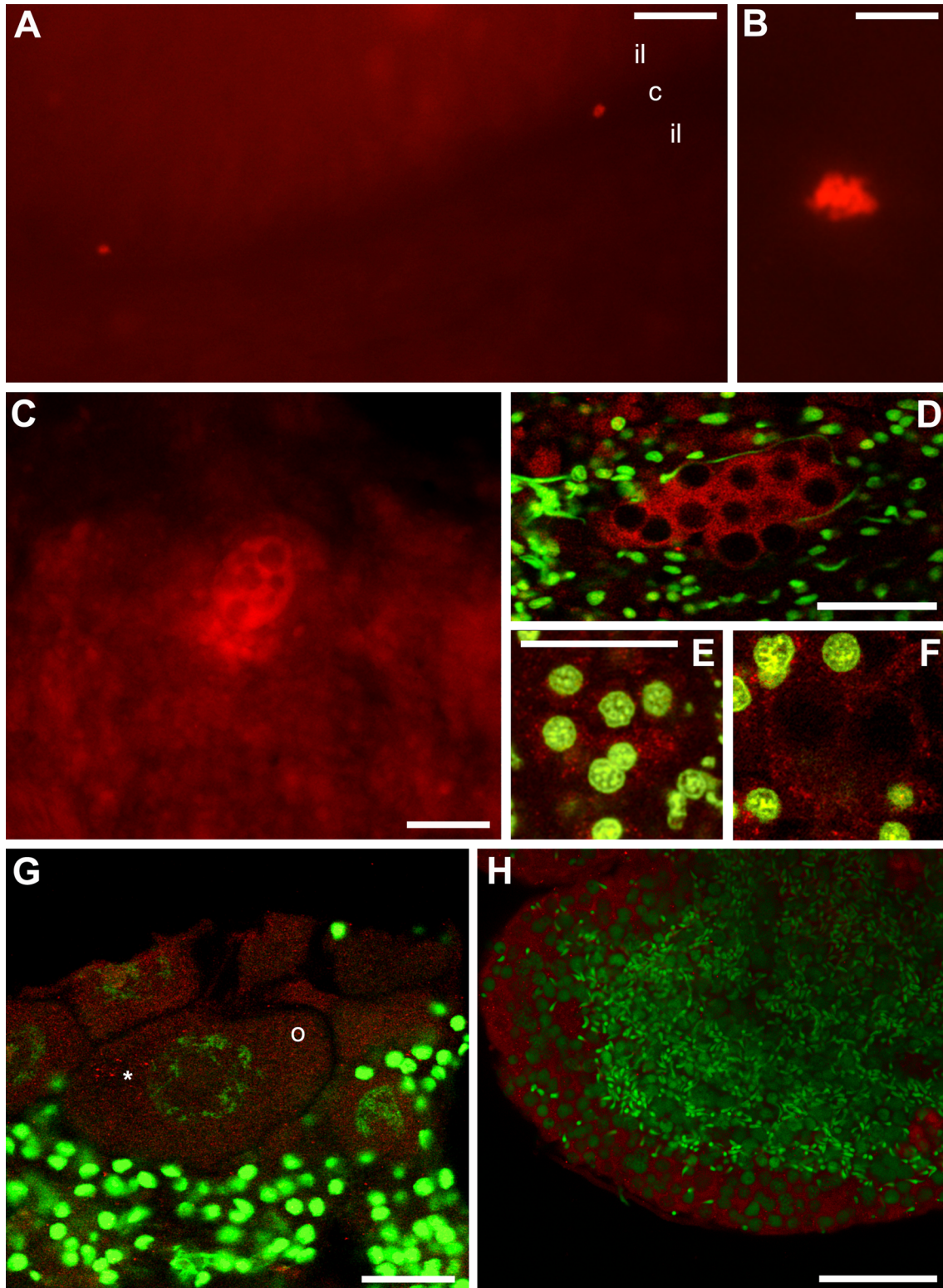


Fig. 28 – Vasph immunolocalization with anti-Cvh during *R. philippinarum* gonad differentiation. (A-C) Fluorescence microscope analysis on sections of a gonad at the beginning of its differentiation. (A) Two small spots result labeled in the connective tissue (c) between two intestinal loops (il), that are not labeled (A: 250 μ m bar). (B) In a magnification of A the staining of the early gonad is better visible (B: 50 μ m bar). (C) A following stage of gonadic development, in which the germ cells, strongly stained, start forming acini with some

big cavities in the middle (C: 50 μm bar). **(D-F)** Confocal analysis on sections of a more differentiated gonad. Anti-Cvh (red) and TO-PRO-3 iodide staining DNA (green). **(D)** Incipient acini with some Vasph stained cells visible on a line around the cavities; the numerous cells of the surrounding connective tissue are not labeled (D: 50 μm bar). **(E, F)** Two images at various depths of the same sample of D. **(E)** Germ cells with big nuclei and a strong Vasph-staining are visible (E: 24 μm bar). **(F)** In a deeper region of the gonadic tissue observed in E, labeled germ cells are located around a still empty acinus lumen (same magnification of E). **(G, H)** Confocal analysis on sections of female and male mature gonads. **(G)** Oocytes strictly packed in an elongated acinus show a diffuse cytoplasmic immunolocalization of Vasph. In the biggest oocyte (o), some strongly labeled granules are seen in a region of the cytoplasm (asterisk) (G: 30 μm bar). **(H)** Male acinus full of spermatozoa: a diffused staining is present only in the spermatogenic cells located near the acinus wall (H: 50 μm bar).

In spawned eggs, Vasph-staining showed granules dispersed in the cytoplasm, with no evident pattern of aggregation (Fig. 29A). On the contrary, in 2-blastomere embryos Vasph immunostaining showed a more strongly stained zone along the cleavage furrow, both with confocal (Fig. 29B) and fluorescence (Fig. 29C) microscope. Some bigger labeled spots were aggregated where the midbody formed (Fig. 29B-E). Control embryos did not show any labeling (Fig. 29F).

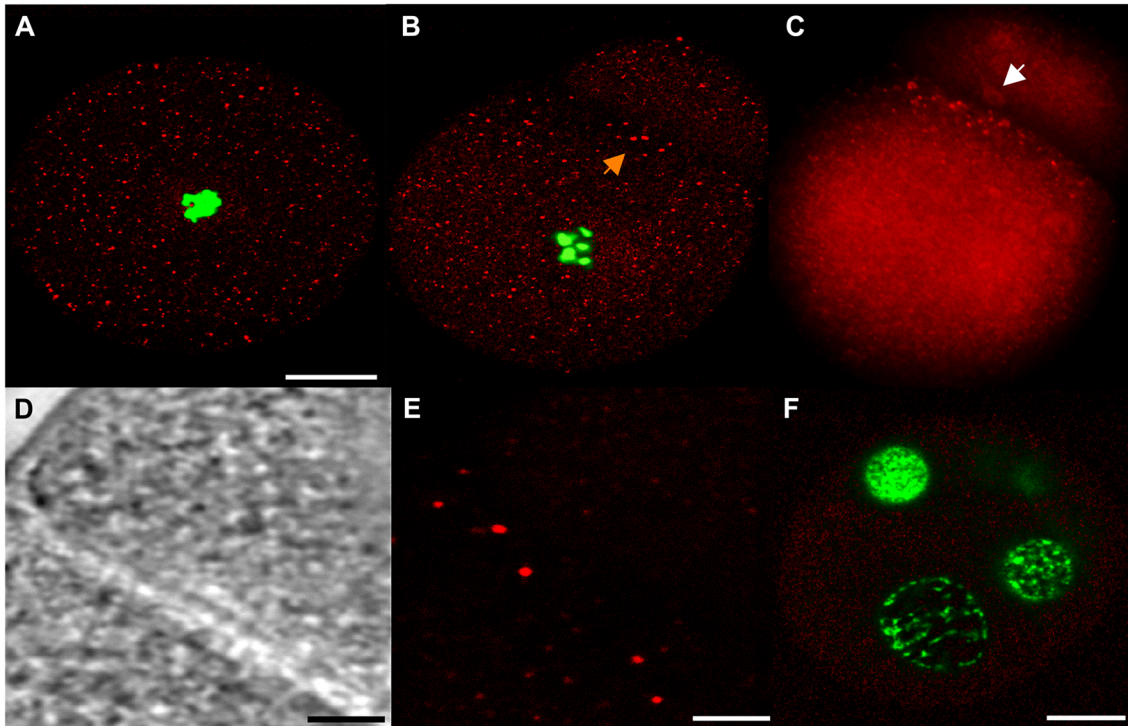


Fig. 29 – Vasph immunolocalization with anti-Cvh in *R. philippinarum* embryos. (A) Stained egg at confocal microscope showing small granules equally dispersed in the cytoplasm (A: 20 μ m bar). (B) Confocal microscope analysis of a 2-blastomere embryo: some small stained spots are dispersed in the cytoplasm, but an aggregation of bigger granules with a stronger labeling is localized close to the cleavage furrow (arrow). Anti-Cvh and TO-PRO-3 iodide staining DNA are represented by red and green, respectively. (C) The same embryo under fluorescence microscope; a trace of the midbody can be perceived (white arrow) (B, C: same magnification of A). (D, E) The same detail of the cleavage shown in B, with transmitted light (D) and confocal microscope (E) (D, E: 4 μ m bar). (F) Confocal microscope analysis of a 4-blastomere embryo, in which only secondary antibody was used. No staining is visible (F: 20 μ m bar).

3.4 – Distribution of microtubules and spermatozoon mitochondria in early embryos

In early embryos, microtubule staining with anti- α -tubulin antibody showed a higher density of short microtubules along the blastomere cortex and longer microtubules between cortex and nuclei, underlining the structural function of microtubular cytoskeleton in positioning the nucleus at the center of the cell (Fig. 30). Furthermore, microtubule staining showed a well-defined midbody located in the middle of the cleavage furrow of 2-blastomere embryos (Fig. 30D and E). In the same area the four mitochondria from spermatozoon were aggregated in male embryos, as shown by MitoTracker staining (Fig. 30A; see also Fig. 21).

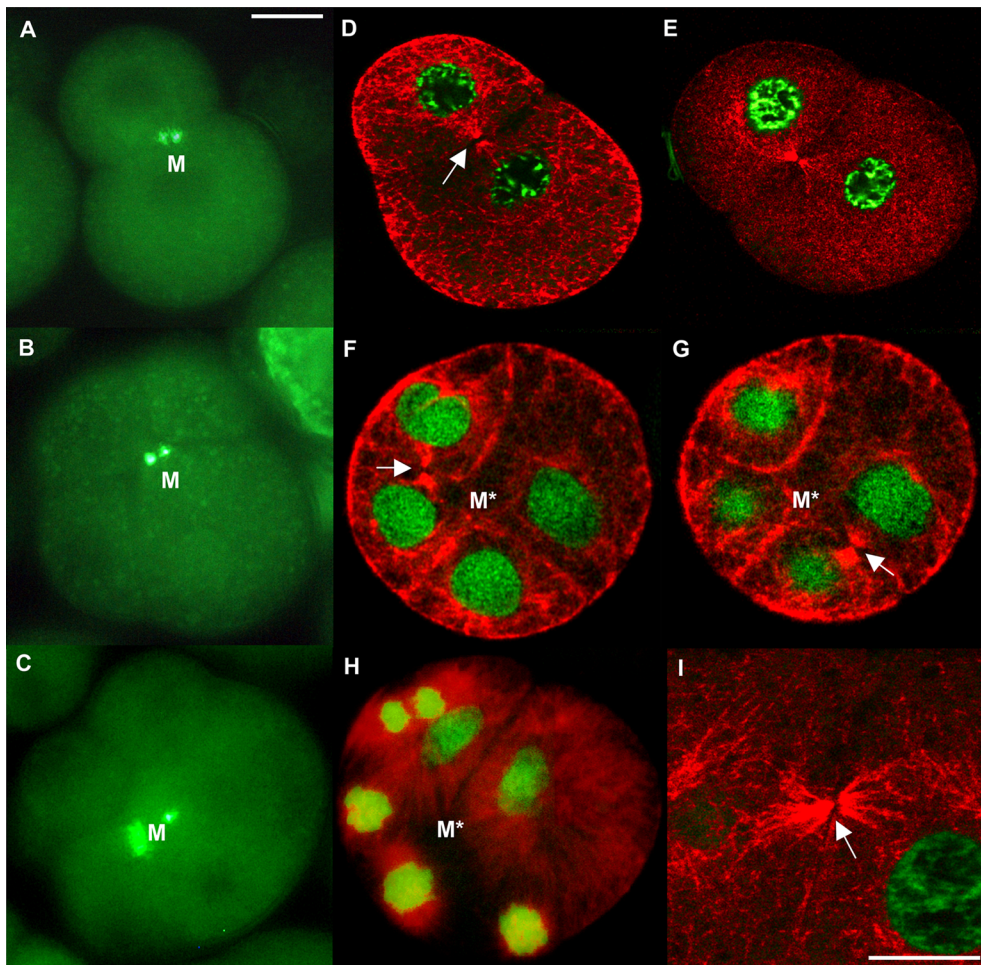


Fig. 30 – Distribution patterns of spermatozoon mitochondria and microtubules in *R. philippinarum* male early embryos. (A-C) Fluorescence microscope analysis. The staining with MitoTracker Green shows an aggregation of spermatozoon mitochondria (M, in light green) in 2- (A), 4- (B) and 8- (C) blastomere male embryos. (D-I) Confocal microscope analysis. (D, E) Microtubule immunolocalization in 2-blastomere male embryos. Anti- α -tubulin (red) and TO-PRO-3 iodide staining DNA (green). A well defined midbody (white arrow) is localized in the middle of the first cleavage furrow, corresponding to the area in which the four spermatozoon mitochondria aggregate in male embryos. (F, G) Microtubule immunolocalization in 4-blastomere male embryos. The two images are acquired at various depths within the same embryo: the two new spindles to form the 4-blastomere embryo are positioned in tangential directions, far from the region (M*) where the four M-type mitochondria localize (white arrows indicate the midbodies), as clearly shown also in 8-blastomere embryos (H) (A-H: bar 20 μm). (I) Detail of a midbody (white arrow) (I: bar 15 μm).

In 4-blastomere embryos the new spindles (marked by the two midbodies in Fig. 30F and G) formed in tangential directions, around the region where the four M-type mitochondria were located, that was on the animal-vegetal (a-v) axis (Fig. 30B, and scheme in Fig. 31). The same could be seen in 8-blastomere embryos (Fig. 30C and H).

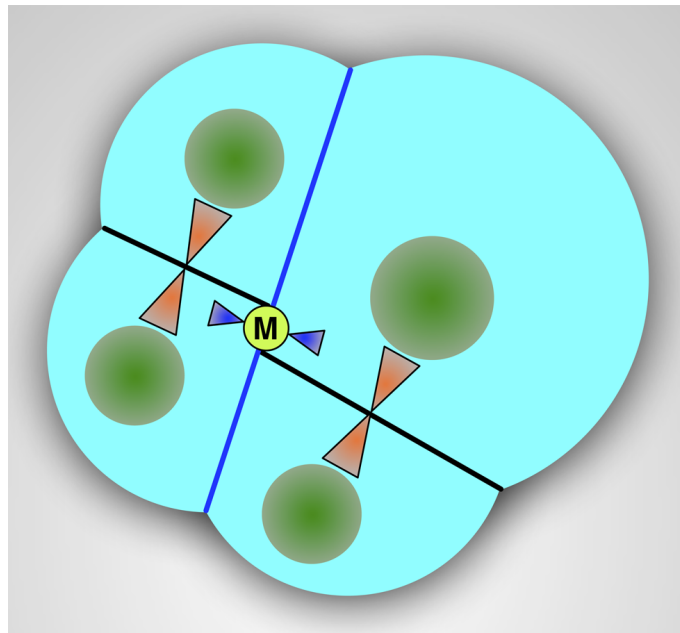


Fig. 31 – Segregation scheme of spermatozoon mitochondria in DUI male embryos. The scheme shows the position of the two midbodies (orange triangles) in a developing 4-blastomere embryo. The plane of the first cleavage is shown with a blue line, and the first midbody, by this time disassembled, is in blue. During the following divisions the same architecture is maintained, with the new spindles (orange) in tangential directions, far from the animal-vegetal axis on which spermatozoon mitochondria (M) were arranged (light green circle). Nuclei in dark green.

Finally, in some 2-blastomere embryos, TEM observations clearly showed a midbody associated to mitochondria of about 1 μm (Fig. 32), which were most likely the M ones. Moreover, in some sections, a centriole appeared to still link spermatozoon mitochondria (Fig. 32B). At the cleavage level, there was always an abundance of F-type mitochondria,

clearly recognizable by their smaller size, some of which fusing with the cleavage membrane (Fig. 32B).

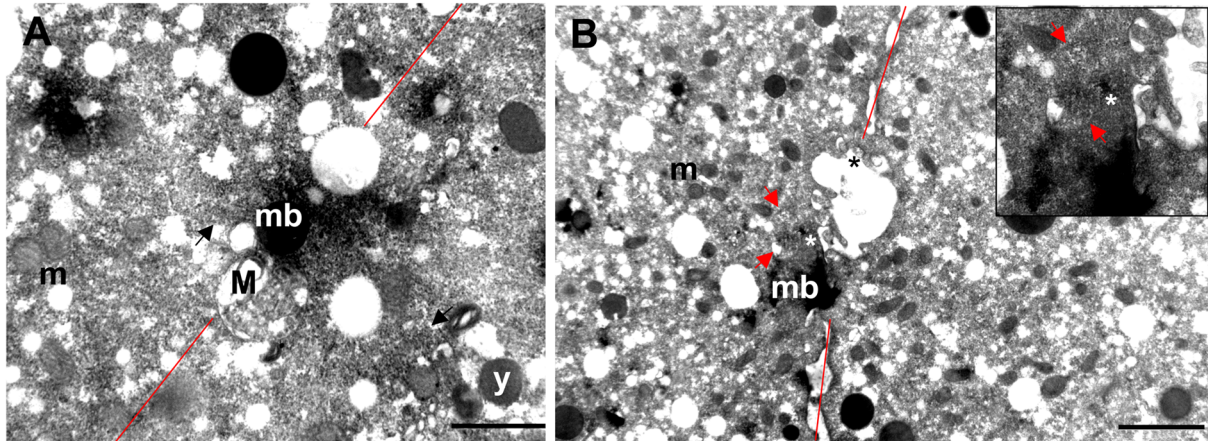


Fig. 32 – Ultrastructural analysis of *R. philippinarum* male early embryos. (A, B) 2-blastomere embryos showing a midbody (mb). The cleavage plane is marked with a red line. (A) One spermatozoon mitochondrion of about 1 μm (M) is positioned near the midbody; black arrows indicate microtubules; m – egg mitochondria; y – yolk (A: bar 1 μm). (B) The egg mitochondria (m), abundant at the cleavage level, are recognizable by the smaller size; some are fusing with the cleavage membrane (black asterisk). Spermatozoon mitochondria (red arrows) are visible near the midbody (mb); a centriole (white asterisk) appears to still link the sperm mitochondria (detail in the inset) (B: bar 2 μm).

3.5 – Mitochondrial genes and ORF-MUR21 expression

In the M mtDNA of *R. philippinarum* (Fig. 33) I found an Open Reading Frame (ORF) in the Male Unassigned Region 21 (MUR21; Figs 33 and 34).

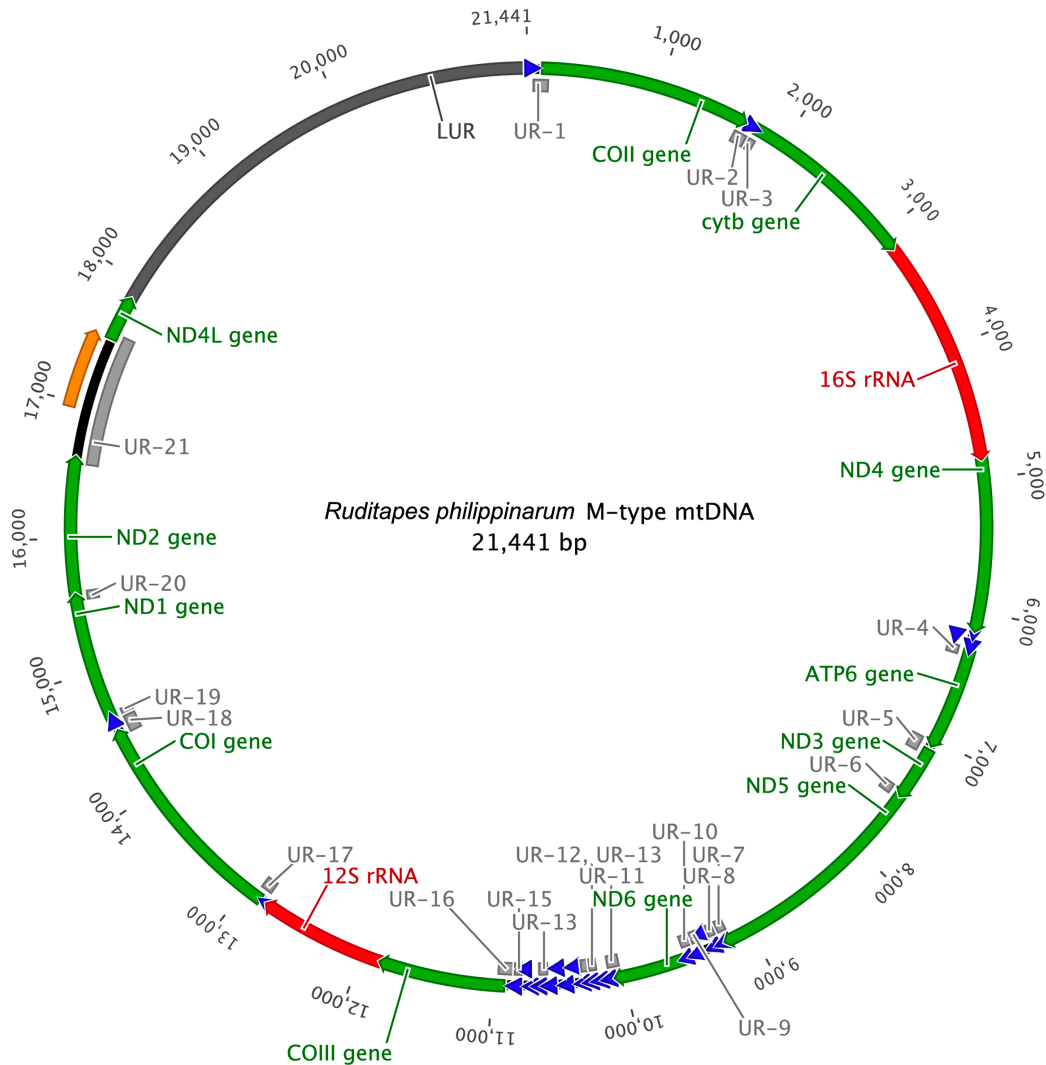


Fig. 33 – *R. philippinarum* M-type mitochondrial DNA. Scheme of the whole mt genome, reporting coding genes (in green), rRNA (in red), Unassigned Regions (URs, in light gray), Large Unassigned Region (LUR, in dark gray), tRNA (blue triangles). ORF-21 in orange.

The ORF-21 nucleotide sequence includes 519 bp (Fig. 34), and the translated protein is of 172 amino acids (aa) (Fig. 35). The sequences of the seven males analyzed only show synonymous mutations (Fig. 34).

CLUSTAL W (1.83) multiple sequence alignment

```

Rp-m1_MUR21 AAGCTATAGGGATTAGGAATACTTCTTATAAGCGGTTAATTTTCTTAAGTAGTTTTTTGTTTTTATTGGTGAGTAGTAATGGTATGTTTGTAAAAAGA 100
Rp-m2_MUR21 AAGCTATAGGGATTAGGAATACTTCTTATAAGCGGTTAATTTTCTTAAGTAGTTTTTTGTTTTTATTGGTGAGTAGTAATGGTATGTTTGTAAAAAGA 100
Rp-m3_MUR21 AAGCTATAGGGATTAGGAATACTTCTTATAAGCGGTTAATTTTCTTAAGTAGTTTTTTGTTTTTATTGGTGAGTAGTAATGGTATGTTTGTAAAAAGA 100
Rp-m4_MUR21 AAGCTATAGGGATTAGGAATACTTCTTATAAGCGGTTAATTTTCTTAAGTAGTTTTTTGTTTTTATTGGTGAGTAGTAATGGTATGTTTGTAAAAAGA 100
Rp-m5_MUR21 AAGCTATAGGGATTAGGAATACTTCTTATAAGCGGTTAATTTTCTTAAGTAGTTTTTTGTTTTTATTGGTGAGTAGTAATGGTATGTTTGTAAAAAGA 100
Rp-m6_MUR21 AAGCTATAGGGATTAGGAATACTTCTTATAAGCGGTTAATTTTCTTAAGTAGTTTTTTGTTTTTATTGGTGAGTAGTAATGGTATGTTTGTAAAAAGA 100
Rp-m7_MUR21 AAGCTATAGGGATTAGGAATACTTCTTATAAGCGGTTAATTTTCTTAAGTAGTTTTTTGTTTTTATTGGTGAGTAGTAATGGTATGTTTGTAAAAAGA 100
*****

Rp-m1_MUR21 TTCTGTAAGGCGAGGTATTAGAAATTTTGGCGGGATTTTGGTTATGTTTAAATTCGCATAAACTTTTTTACAAAAATATGATAGTAATTTAAGTTTT 200
Rp-m2_MUR21 TTCTGTAAGGCGAGGTATTAGAAATTTTGGCGGGATTTTGGTTATGTTTAAATTCGCATAAACTTTTTTACAAAAATATGATAGTAATTTAAGTTTT 200
Rp-m3_MUR21 TTCTGTAAGGCGAGGTATTAGAAATTTTGGCGGGATTTTGGTTATGTTTAAATTCGCATAAACTTTTTTACAAAAATATGATAGTAATTTAAGTTTT 200
Rp-m4_MUR21 TTCTGTAAGGCGAGGTATTAGAAATTTTGGCGGGATTTTGGTTATGTTTAAATTCGCATAAACTTTTTTACAAAAATATGATAGTAATTTAAGTTTT 200
Rp-m5_MUR21 TTCTGTAAGGCGAGGTATTAGAAATTTTGGCGGGATTTTGGTTATGTTTAAATTCGCATAAACTTTTTTACAAAAATATGATAGTAATTTAAGTTTT 200
Rp-m6_MUR21 TTCTGTAAGGCGAGGTATTAGAAATTTTGGCGGGATTTTGGTTATGTTTAAATTCGCATAAACTTTTTTACAAAAATATGATAGTAATTTAAGTTTT 200
Rp-m7_MUR21 TTCTGTAAGGCGAGGTATTAGAAATTTTGGCGGGATTTTGGTTATGTTTAAATTCGCATAAACTTTTTTACAAAAATATGATAGTAATTTAAGTTTT 200
*****

Rp-m1_MUR21 TTCTGTTAAATGGTGAATAATAATAATAATTTCTTAAAGCAATATAGTAAATAGAGAAAATTTATAGGTCAAAAATAGGGATTATTTTAAATGTGTT 300
Rp-m2_MUR21 TTCTGTTAAATGGTGAATAATAATAATAATTTCTTAAAGCAATATAGTAAATAGAGAAAATTTATAGGTCAAAAATAGGGATTATTTTAAATGTGTT 300
Rp-m3_MUR21 TTCTGTTAAATGGTGAATAATAATAATAATTTCTTAAAGCAATATAGTAAATAGAGAAAATTTATAGGTCAAAAATAGGGATTATTTTAAATGTGTT 300
Rp-m4_MUR21 TTCTGTTAAATGGTGAATAATAATAATAATTTCTTAAAGCAATATAGTAAATAGAGAAAATTTATAGGTCAAAAATAGGGATTATTTTAAATGTGTT 300
Rp-m5_MUR21 TTCTGTTAAATGGTGAATAATAATAATAATTTCTTAAAGCAATATAGTAAATAGAGAAAATTTATAGGTCAAAAATAGGGATTATTTTAAATGTGTT 300
Rp-m6_MUR21 TTCTGTTAAATGGTGAATAATAATAATAATTTCTTAAAGCAATATAGTAAATAGAGAAAATTTATAGGTCAAAAATAGGGATTATTTTAAATGTGTT 300
Rp-m7_MUR21 TTCTGTTAAATGGTGAATAATAATAATAATTTCTTAAAGCAATATAGTAAATAGAGAAAATTTATAGGTCAAAAATAGGGATTATTTTAAATGTGTT 300
*****

Rp-m1_MUR21 TATTTTTAGCCTCTTACACGCTTGTATTATAAAGGTTAGTATAGTAAACAGGTAGCACAAAGGTTCCAGAGTTTATGTTTACCTTAGTTTATAGTAATC 400
Rp-m2_MUR21 TATTTTTAGCCTCTTACACGCTTGTATTATAAAGGTTAGTATAGTAAACAGGTAGCACAAAGGTTCCAGAGTTTATGTTTACCTTAGTTTATAGTAATC 400
Rp-m3_MUR21 TATTTTTAGCCTCTTACACGCTTGTATTATAAAGGTTAGTATAGTAAACAGGTAGCACAAAGGTTCCAGAGTTTATGTTTACCTTAGTTTATAGTAATC 400
Rp-m4_MUR21 TATTTTTAGCCTCTTACACGCTTGTATTATAAAGGTTAGTATAGTAAACAGGTAGCACAAAGGTTCCAGAGTTTATGTTTACCTTAGTTTATAGTAATC 400
Rp-m5_MUR21 TATTTTTAGCCTCTTACACGCTTGTATTATAAAGGTTAGTATAGTAAACAGGTAGCACAAAGGTTCCAGAGTTTATGTTTACCTTAGTTTATAGTAATC 400
Rp-m6_MUR21 TATTTTTAGCCTCTTACACGCTTGTATTATAAAGGTTAGTATAGTAAACAGGTAGCACAAAGGTTCCAGAGTTTATGTTTACCTTAGTTTATAGTAATC 400
Rp-m7_MUR21 TATTTTTAGCCTCTTACACGCTTGTATTATAAAGGTTAGTATAGTAAACAGGTAGCACAAAGGTTCCAGAGTTTATGTTTACCTTAGTTTATAGTAATC 400
*****

Rp-m1_MUR21 ATGTGAGTGCAGTTCGCTTTATTTGCTTTTTATGCTAGGATCTAAGTTGTCAGATTTCTATCTTTGATGTTTTTTTTCTTGGGTTGAATCTTTAG 500
Rp-m2_MUR21 ATGTGAGTGCAGTTCGCTTTATTTGCTTTTTATGCTAGGATCTAAGTTGTCAGATTTCTATCTTTGATGTTTTTTTTCTTGGGTTGAATCTTTAG 500
Rp-m3_MUR21 ATGTGAGTGCAGTTCGCTTTATTTGCTTTTTATGCTAGGATCTAAGTTGTCAGATTTCTATCTTTGATGTTTTTTTTCTTGGGTTGAATCTTTAG 500
Rp-m4_MUR21 ATGTGAGTGCAGTTCGCTTTATTTGCTTTTTATGCTAGGATCTAAGTTGTCAGATTTCTATCTTTGATGTTTTTTTTCTTGGGTTGAATCTTTAG 500
Rp-m5_MUR21 ATGTGAGTGCAGTTCGCTTTATTTGCTTTTTATGCTAGGATCTAAGTTGTCAGATTTCTATCTTTGATGTTTTTTTTCTTGGGTTGAATCTTTAG 500
Rp-m6_MUR21 ATGTGAGTGCAGTTCGCTTTATTTGCTTTTTATGCTAGGATCTAAGTTGTCAGATTTCTATCTTTGATGTTTTTTTTCTTGGGTTGAATCTTTAG 500
Rp-m7_MUR21 ATGTGAGTGCAGTTCGCTTTATTTGCTTTTTATGCTAGGATCTAAGTTGTCAGATTTCTATCTTTGATGTTTTTTTTCTTGGGTTGAATCTTTAG 500
*****

Rp-m1_MUR21 TAACTCTGTTTCTTAAGGAGTTTTTTCCGGTAATATTACCGTGGTTAGTTACACTTCAAAGTTTTTGGTTAATAATTTTTTTCTGTGAAAGGAAA 600
Rp-m2_MUR21 TAACTCTGTTTCTTAAGGAGTTTTTTCCGGTAATATTACCGTGGTTAGTTACACTTCAAAGTTTTTGGTTAATAATTTTTTTCTGTGAAAGGAAA 600
Rp-m3_MUR21 TAACTCTGTTTCTTAAGGAGTTTTTTCCGGTAATATTACCGTGGTTAGTTACACTTCAAAGTTTTTGGTTAATAATTTTTTTCTGTGAAAGGAAA 600
Rp-m4_MUR21 TAACTCTGTTTCTTAAGGAGTTTTTTCCGGTAATATTACCGTGGTTAGTTACACTTCAAAGTTTTTGGTTAATAATTTTTTTCTGTGAAAGGAAA 600
Rp-m5_MUR21 TAACTCTGTTTCTTAAGGAGTTTTTTCCGGTAATATTACCGTGGTTAGTTACACTTCAAAGTTTTTGGTTAATAATTTTTTTCTGTGAAAGGAAA 600
Rp-m6_MUR21 TAACTCTGTTTCTTAAGGAGTTTTTTCCGGTAATATTACCGTGGTTAGTTACACTTCAAAGTTTTTGGTTAATAATTTTTTTCTGTGAAAGGAAA 600
Rp-m7_MUR21 TAACTCTGTTTCTTAAGGAGTTTTTTCCGGTAATATTACCGTGGTTAGTTACACTTCAAAGTTTTTGGTTAATAATTTTTTTCTGTGAAAGGAAA 600
*****

Rp-m1_MUR21 CCCATGTGAGTTTACTGAAACGAGTAGACCATTGCCGTCGTCATCGTCATCFCFTTCTGTTCCFCFTTCTGTTAAACCCCAAAACAAAGTTTATTCGGCT 700
Rp-m2_MUR21 CCCATGTGAGTTTACTGAAACGAGTAGACCATTGCCGTCGTCATCGTCATCFCFTTCTGTTCCFCFTTCTGTTAAACCCCAAAACAAAGTTTATTCGGCT 700
Rp-m3_MUR21 CCCATGTGAGTTTACTGAAACGAGTAGACCATTGCCGTCGTCATCGTCATCFCFTTCTGTTCCFCFTTCTGTTAAACCCCAAAACAAAGTTTATTCGGCT 700
Rp-m4_MUR21 CCCATGTGAGTTTACTGAAACGAGTAGACCATTGCCGTCGTCATCGTCATCFCFTTCTGTTCCFCFTTCTGTTAAACCCCAAAACAAAGTTTATTCGGCT 700
Rp-m5_MUR21 CCCATGTGAGTTTACTGAAACGAGTAGACCATTGCCGTCGTCATCGTCATCFCFTTCTGTTCCFCFTTCTGTTAAACCCCAAAACAAAGTTTATTCGGCT 700
Rp-m6_MUR21 CCCATGTGAGTTTACTGAAACGAGTAGACCATTGCCGTCGTCATCGTCATCFCFTTCTGTTCCFCFTTCTGTTAAACCCCAAAACAAAGTTTATTCGGCT 700
Rp-m7_MUR21 CCCATGTGAGTTTACTGAAACGAGTAGACCATTGCCGTCGTCATCGTCATCFCFTTCTGTTCCFCFTTCTGTTAAACCCCAAAACAAAGTTTATTCGGCT 700
*****

Rp-m1_MUR21 CCAATTTATTTAGTGGGAGAAAAGAGATTTTGACTTCTAATGAGATTAAGAAAAGAAAATTTGTTATTTAAAGTAATTTGCTTAGATAGAAAAGGAGA 800
Rp-m2_MUR21 CCAATTTATTTAGTGGGAGAAAAGAGATTTTGACTTCTAATGAGATTAAGAAAAGAAAATTTGTTATTTAAAGTAATTTGCTTAGATAGAAAAGGAGA 800
Rp-m3_MUR21 CCAATTTATTTAGTGGGAGAAAAGAGATTTTGACTTCTAATGAGATTAAGAAAAGAAAATTTGTTATTTAAAGTAATTTGCTTAGATAGAAAAGGAGA 800
Rp-m4_MUR21 CCAATTTATTTAGTGGGAGAAAAGAGATTTTGACTTCTAATGAGATTAAGAAAAGAAAATTTGTTATTTAAAGTAATTTGCTTAGATAGAAAAGGAGA 800
Rp-m5_MUR21 CCAATTTATTTAGTGGGAGAAAAGAGATTTTGACTTCTAATGAGATTAAGAAAAGAAAATTTGTTATTTAAAGTAATTTGCTTAGATAGAAAAGGAGA 800
Rp-m6_MUR21 CCAATTTATTTAGTGGGAGAAAAGAGATTTTGACTTCTAATGAGATTAAGAAAAGAAAATTTGTTATTTAAAGTAATTTGCTTAGATAGAAAAGGAGA 800
Rp-m7_MUR21 CCAATTTATTTAGTGGGAGAAAAGAGATTTTGACTTCTAATGAGATTAAGAAAAGAAAATTTGTTATTTAAAGTAATTTGCTTAGATAGAAAAGGAGA 800
*****

Rp-m1_MUR21 ACCAGAATTTTAAAGTTATATTTGCTACTTTTGGGAAAAGTAGACTTACCCTGTGAGAAATCCCTCAAAGTTGTAACCTTTTGTATTTGCAATGGA 900
Rp-m2_MUR21 ACCAGAATTTTAAAGTTATATTTGCTACTTTTGGGAAAAGTAGACTTACCCTGTGAGAAATCCCTCAAAGTTGTAACCTTTTGTATTTGCAATGGA 900
Rp-m3_MUR21 ACCAGAATTTTAAAGTTATATTTGCTACTTTTGGGAAAAGTAGACTTACCCTGTGAGAAATCCCTCAAAGTTGTAACCTTTTGTATTTGCAATGGA 900
Rp-m4_MUR21 ACCAGAATTTTAAAGTTATATTTGCTACTTTTGGGAAAAGTAGACTTACCCTGTGAGAAATCCCTCAAAGTTGTAACCTTTTGTATTTGCAATGGA 900
Rp-m5_MUR21 ACCAGAATTTTAAAGTTATATTTGCTACTTTTGGGAAAAGTAGACTTACCCTGTGAGAAATCCCTCAAAGTTGTAACCTTTTGTATTTGCAATGGA 900
Rp-m6_MUR21 ACCAGAATTTTAAAGTTATATTTGCTACTTTTGGGAAAAGTAGACTTACCCTGTGAGAAATCCCTCAAAGTTGTAACCTTTTGTATTTGCAATGGA 900
Rp-m7_MUR21 ACCAGAATTTTAAAGTTATATTTGCTACTTTTGGGAAAAGTAGACTTACCCTGTGAGAAATCCCTCAAAGTTGTAACCTTTTGTATTTGCAATGGA 900
*****

Rp-m1_MUR21 TGATCCCTGACTCAAACCTAGTGTAATATGTGACCTCTTACCCTGGTTTACAAGTAAATC 959
Rp-m2_MUR21 TGATCCCTGACTCAAACCTAGTGTAATATGTGACCTCTTACCCTGGTTTACAAGTAAATC 959
Rp-m3_MUR21 TGATCCCTGACTCAAACCTAGTGTAATATGTGACCTCTTACCCTGGTTTACAAGTAAATC 959
Rp-m4_MUR21 TGATCCCTGACTCAAACCTAGTGTAATATGTGACCTCTTACCCTGGTTTACAAGTAAATC 959
Rp-m5_MUR21 TGATCCCTGACTCAAACCTAGTGTAATATGTGACCTCTTACCCTGGTTTACAAGTAAATC 959
Rp-m6_MUR21 TGATCCCTGACTCAAACCTAGTGTAATATGTGACCTCTTACCCTGGTTTACAAGTAAATC 959
Rp-m7_MUR21 TGATCCCTGACTCAAACCTAGTGTAATATGTGACCTCTTACCCTGGTTTACAAGTAAATC 959
*****

```

Fig. 34 – MUR21 nucleotide alignment. Sequences of the seven males analyzed. Boxes indicate mutations (red boxes synonymous mutations in the ORF). The orange line borders the ORF sequence.

```

CLUSTAL W (1.83) multiple sequence alignment

Rp-m1_ORF-MUR21  MWVAVAFILSFIASDLSCQISIFDVFFSWVESLVTTLFLKEFFSGNIYVVS  50
Rp-m2_ORF-MUR21  MWVAVAFILSFIASDLSCQISIFDVFFSWVESLVTTLFLKEFFSGNIYVVS  50
Rp-m3_ORF-MUR21  MWVAVAFILSFIASDLSCQISIFDVFFSWVESLVTTLFLKEFFSGNIYVVS  50
Rp-m4_ORF-MUR21  MWVAVAFILSFIASDLSCQISIFDVFFSWVESLVTTLFLKEFFSGNIYVVS  50
Rp-m5_ORF-MUR21  MWVAVAFILSFIASDLSCQISIFDVFFSWVESLVTTLFLKEFFSGNIYVVS  50
Rp-m6_ORF-MUR21  MWVAVAFILSFIASDLSCQISIFDVFFSWVESLVTTLFLKEFFSGNIYVVS  50
Rp-m7_ORF-MUR21  MWVAVAFILSFIASDLSCQISIFDVFFSWVESLVTTLFLKEFFSGNIYVVS  50
*****

Rp-m1_ORF-MUR21  YTFKVFWLMIFFSVKGNPCEFTETSSPLPSSSSSSSSVPSSSKPPKQVYSA  100
Rp-m2_ORF-MUR21  YTFKVFWLMIFFSVKGNPCEFTETSSPLPSSSSSSSSVPSSSKPPKQVYSA  100
Rp-m3_ORF-MUR21  YTFKVFWLMIFFSVKGNPCEFTETSSPLPSSSSSSSSVPSSSKPPKQVYSA  100
Rp-m4_ORF-MUR21  YTFKVFWLMIFFSVKGNPCEFTETSSPLPSSSSSSSSVPSSSKPPKQVYSA  100
Rp-m5_ORF-MUR21  YTFKVFWLMIFFSVKGNPCEFTETSSPLPSSSSSSSSVPSSSKPPKQVYSA  100
Rp-m6_ORF-MUR21  YTFKVFWLMIFFSVKGNPCEFTETSSPLPSSSSSSSSVPSSSKPPKQVYSA  100
Rp-m7_ORF-MUR21  YTFKVFWLMIFFSVKGNPCEFTETSSPLPSSSSSSSSVPSSSKPPKQVYSA  100
*****

Rp-m1_ORF-MUR21  PIIISGSKEDFDYLSLSKENLLFKVIVLDSKENQNFKSYIVYFWEKVDL  150
Rp-m2_ORF-MUR21  PIIISGSKEDFDYLSLSKENLLFKVIVLDSKENQNFKSYIVYFWEKVDL  150
Rp-m3_ORF-MUR21  PIIISGSKEDFDYLSLSKENLLFKVIVLDSKENQNFKSYIVYFWEKVDL  150
Rp-m4_ORF-MUR21  PIIISGSKEDFDYLSLSKENLLFKVIVLDSKENQNFKSYIVYFWEKVDL  150
Rp-m5_ORF-MUR21  PIIISGSKEDFDYLSLSKENLLFKVIVLDSKENQNFKSYIVYFWEKVDL  150
Rp-m6_ORF-MUR21  PIIISGSKEDFDYLSLSKENLLFKVIVLDSKENQNFKSYIVYFWEKVDL  150
Rp-m7_ORF-MUR21  PIIISGSKEDFDYLSLSKENLLFKVIVLDSKENQNFKSYIVYFWEKVDL  150
*****

Rp-m1_ORF-MUR21  PCENPSKVVTVLIIAMDDPDSN  172
Rp-m2_ORF-MUR21  PCENPSKVVTVLIIAMDDPDSN  172
Rp-m3_ORF-MUR21  PCENPSKVVTVLIIAMDDPDSN  172
Rp-m4_ORF-MUR21  PCENPSKVVTVLIIAMDDPDSN  172
Rp-m5_ORF-MUR21  PCENPSKVVTVLIIAMDDPDSN  172
Rp-m6_ORF-MUR21  PCENPSKVVTVLIIAMDDPDSN  172
Rp-m7_ORF-MUR21  PCENPSKVVTVLIIAMDDPDSN  172
*****

```

Fig. 35 – ORF-MUR21 putative protein alignment. All the seven aminoacidic sequences are identical.

The analysis of the M-type mtDNA expression showed that five mitochondrial coding genes (*cytb*, *nd4*, *nd5*, *nd2*, *nd4L*) have a similar expression level to ORF-21 (Table 2; Fig. 36). p-values < 0.001 were considered significant.

Table 2 – Expression of coding genes of *R. philippinarum* M-type mtDNA compared with the ORF-21 expression in males.

Name	Min	Max	Length	Mean Exp.	Diff. Exp. with ORF-21
<i>cox2</i>	122	1,669	1,548	6293.24	>
<i>cytb</i>	1,794	3,116	1,323	3187.51	ns
<i>nd4</i>	4,836	6,119	1,284	2147.92	ns
<i>atp6</i>	6,306	7,043	738	4382.51	>
<i>nd3</i>	7,111	7,470	360	4410.91	>
<i>nd5</i>	7,505	9,193	1,689	2061.84	ns
<i>nd6</i>	9,561	10,052	492	4501.08	>
<i>cox3</i>	10,936	11,829	894	6132.99	>
<i>cox1</i>	12,888	14,495	1,608	5910.16	>
<i>nd1</i>	14,643	15,560	918	4563.95	>
<i>nd2</i>	15,579	16,595	1,017	1406.53	ns
<i>nd4L</i>	17,555	17,842	288	2779.47	ns
ORF-21	16,996	17,514	519	2015.66	na

Min = starting nucleotide position; Max = last nucleotide position; Mean Exp. = Mean Expression = FPKM means; Diff. Exp. with ORF-21 = Difference in Expression with ORF-21; > = significantly higher expression ($p < 0.001$; significance calculated with the Wilcoxon rank-sum test); ns = not significant; na = not available.

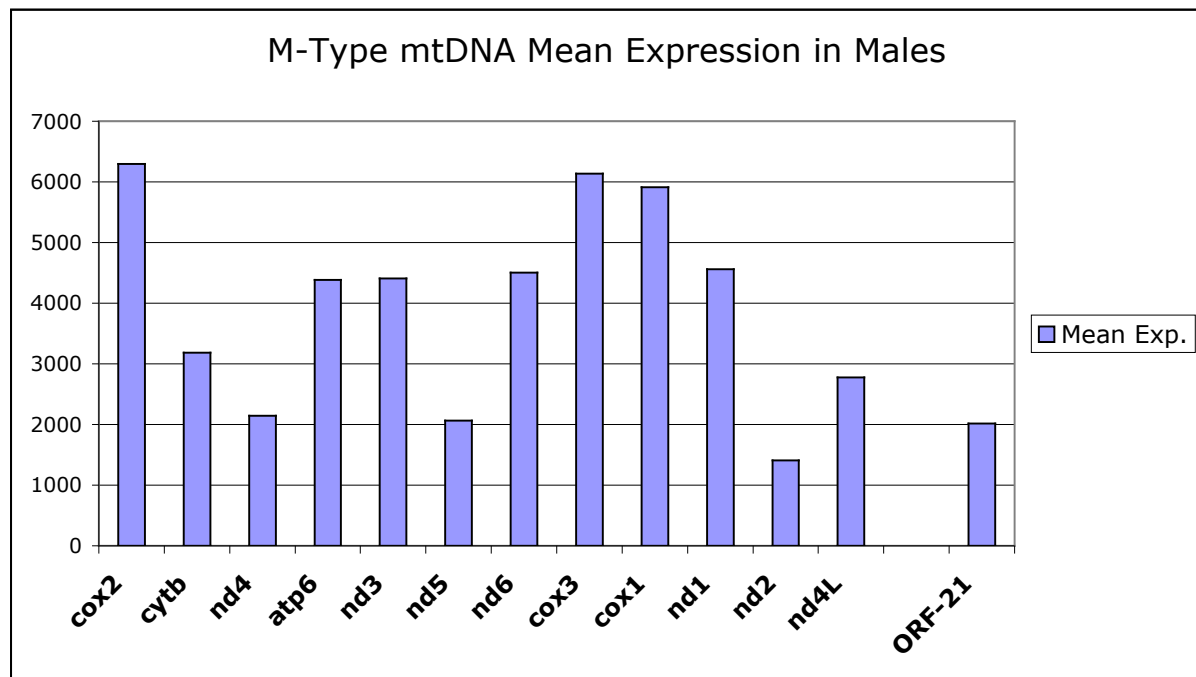


Fig. 36 – Expression of coding genes of *R. philippinarum* M-type mtDNA.

3.6 – Functional domains of inferred proteins

The comparison of transcriptomes between a family producing predominantly females (Family 1) and a family producing predominantly males (Family 2) identified nuclear genes with sex and family biases involved in reproduction and ubiquitination, which are candidate genes for the regulation of sex-specific aspects of DUI system. In this study I analyzed these biased genes and ORF-21, first of all using InterProScan on inferred proteins to find functional domains, and then by *in situ* hybridization to localize them in tissues.

In the ORF-21 inferred protein InterProScan found a signal peptide (location: 1-18) and two transmembrane regions in the N-terminal region (location: 5-27, 41-61) (Fig. 37).

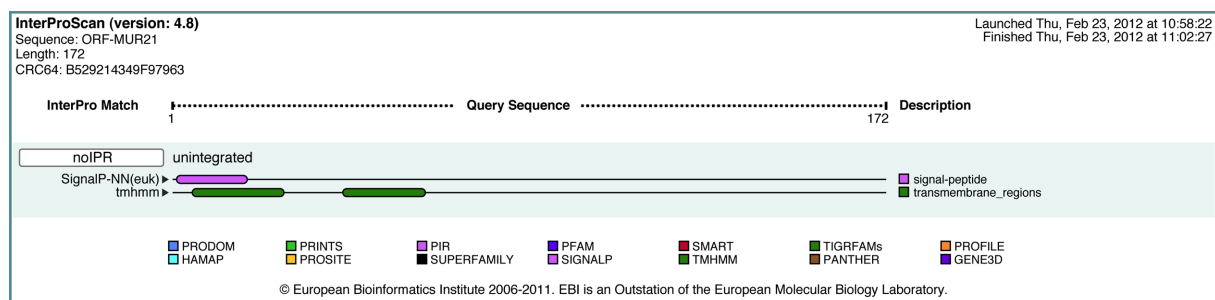


Fig. 37 – Conserved functional domains of ORF-21 inferred protein. In the ORF-21 inferred protein InterProScan found a signal peptide and two transmembrane regions.

In PSA, a Proteasome Subunit Alpha conserved site (Proteasome_A_N, location: 30-52) and a subunit alpha/beta (Proteasome, location: 55-240) were found (Fig. 38). In BIRING inferred protein InterProScan found a Baculoviral inhibition of apoptosis protein repeat (BIR, location: 29-93) and a Zinc finger, RING-type (ZF_RING_2, location: 222-257) (Fig. 39), and I named it BIRING because it is a “BIR + RING containing protein”. In the ANUBL1 inferred protein an ubiquitin domain (GO:0005515, location: 7-73) and a Zinc finger zf-AN1 (GO:0008270, location: 590-630) were found (Fig. 40). For this reason it was recognized as a “AN1 zinc

finger + Ubiquitin-Like domain fusion protein”, and therefore named ANUBL1 (<http://www.proteinatlas.org/ENSG00000172671/gene>).

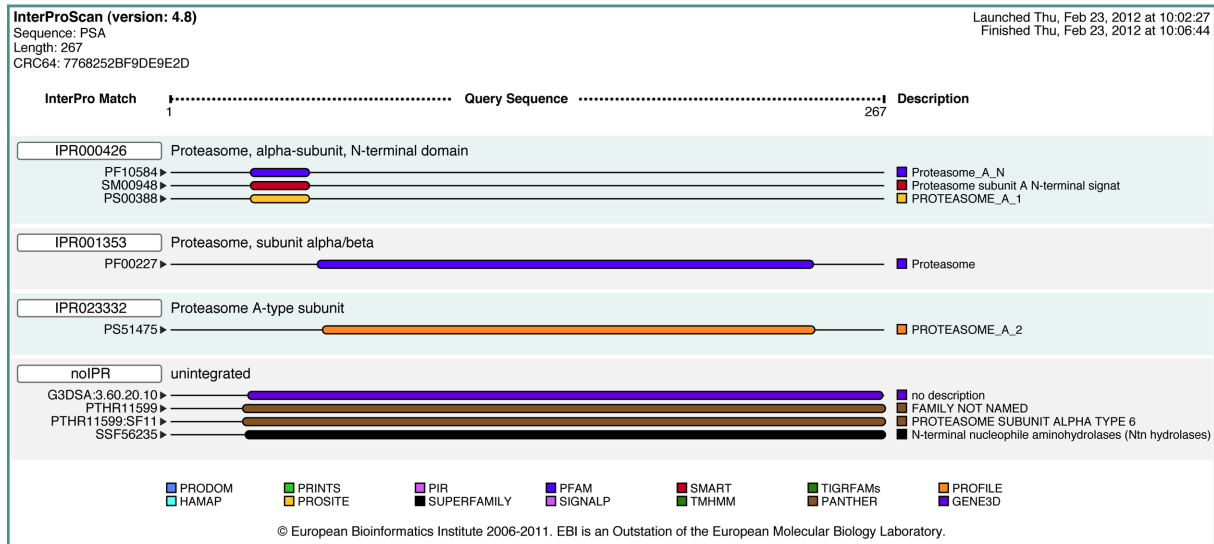


Fig. 38 – Conserved functional domains of PSA inferred protein. Using InterProScan, a proteasome alpha-subunit conserved site was found (Proteasome_A_N, location: 30-52), and a proteasome subunit alpha/beta (Proteasome, location: 55-240).

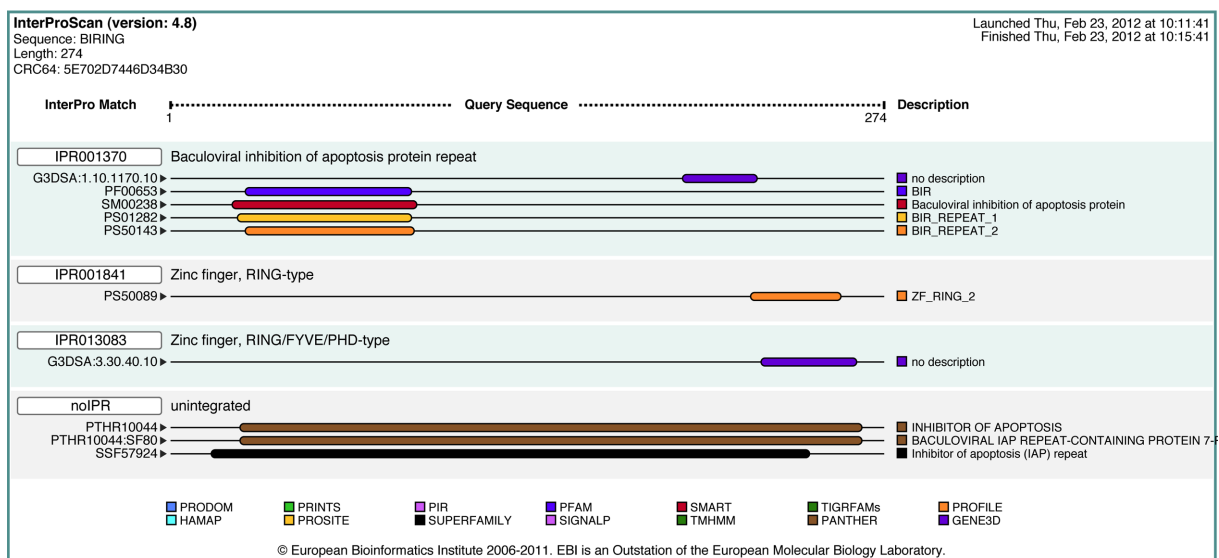


Fig. 39 – Conserved functional domains of BIRING inferred protein. InterProScan found a Baculoviral inhibition of apoptosis protein repeat (BIR, location: 29-93) and a Zinc finger, RING-type (ZF_RING_2, location: 222-257).

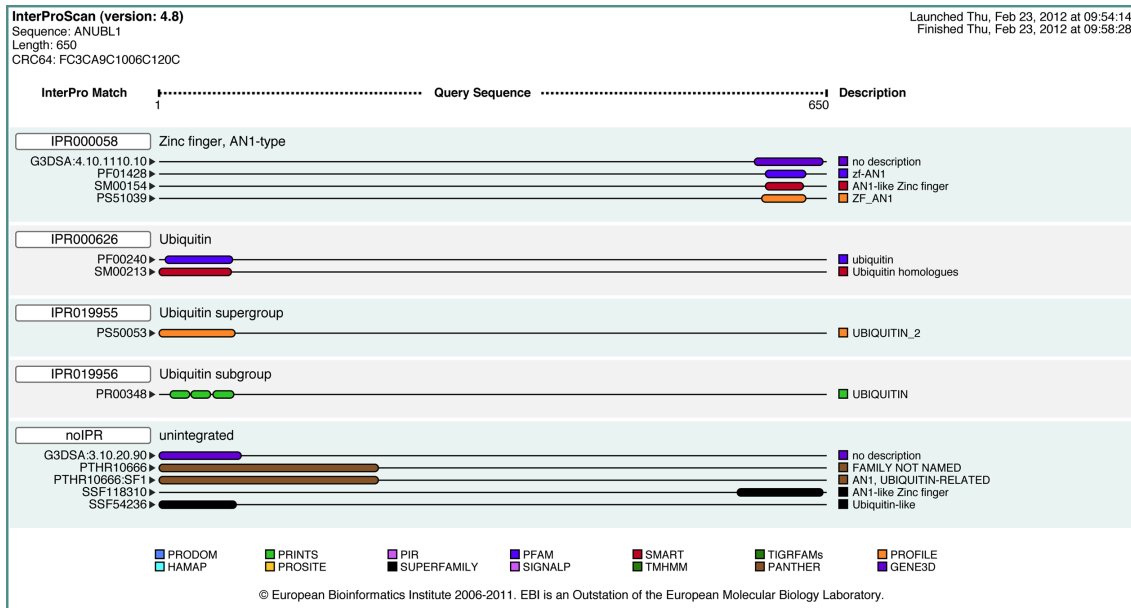


Fig. 40 – Conserved functional domains of ANUBL1 inferred protein. InterProScan found an ubiquitin domain (GO:0005515, location: 7-73) and a Zinc finger zf-AN1 (GO:0008270, location: 590-630).

3.7 – *In situ* hybridization

A scheme of gonad and surrounding tissues is reported in Fig. 41. All the probes labeled both the acinus and its lumen, indicating a positive reaction with both spermatogenic cells and mature sperm (Figs 42-45). In female acini, the labeling was restricted to eggs in the acinus lumen (Figs 43-45). ORF-21 did not stain female tissues, as expected being a specific M-type mtDNA feature. More in detail, ORF-21 showed the highest staining intensity (Fig. 42), with the staining appearing after few hours from the beginning of the color reaction. PSA (Fig. 43) and ANUBL1 (Fig. 45) probes showed the highest intensity in eggs. BIRING stained equally male and female gametes (Fig. 44). ANUBL1 staining in quite similar in acinus and mature spermatozoa (Fig. 45). Interestingly, ORF-21 and PSA only appeared to have a high staining along the acinus wall (Figs 42 and 43). The intensity of the staining evaluated by sight (as in Gogusev et al. 1997; Table 3) is in agreement with the transcription level, indicated in Table 4 by FPKM values.

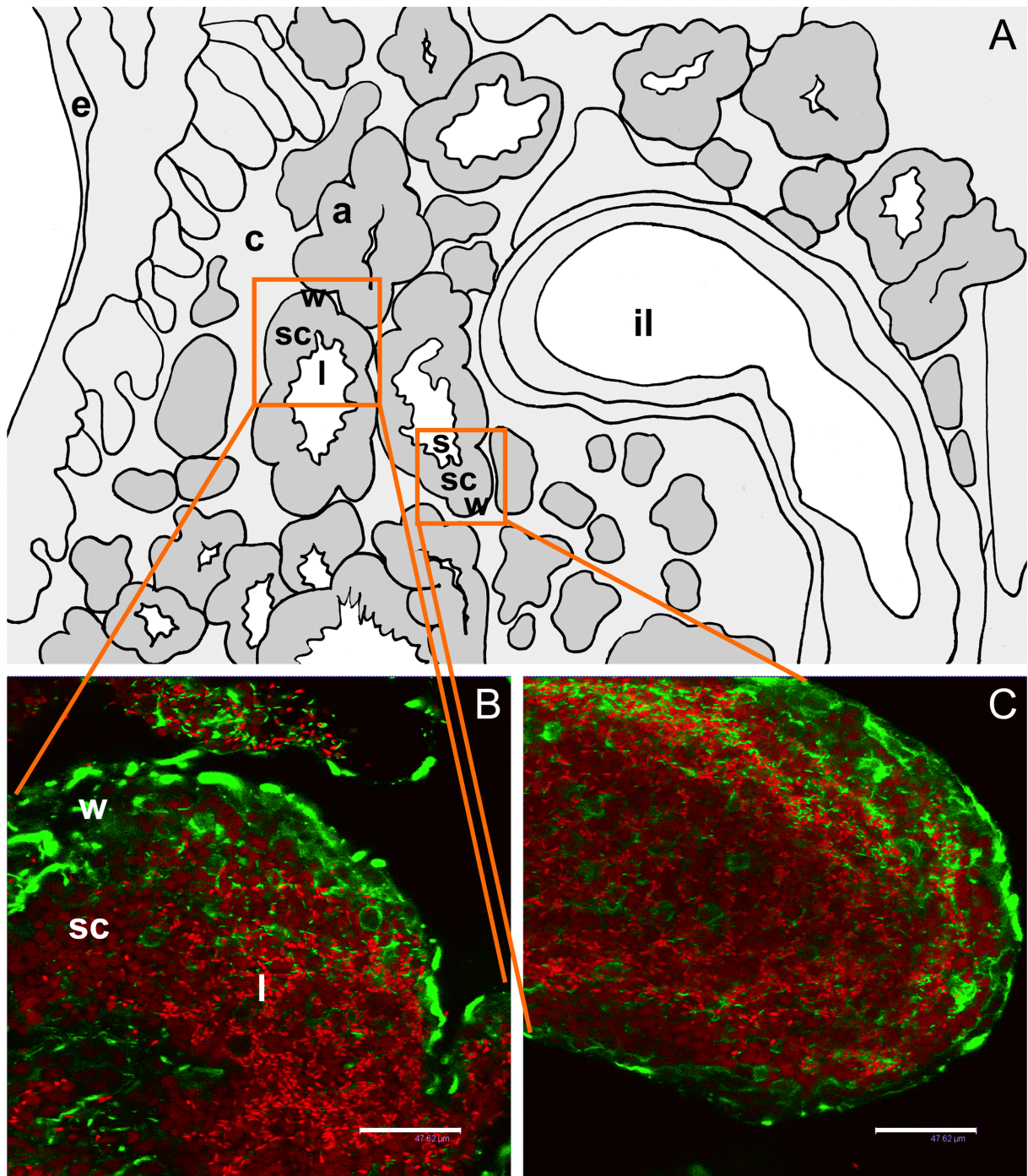


Fig. 41 – Morphology and localization of gonadic tissue. (A) Scheme of a male gonad and surrounding tissues. The gonadic tissue develops intimately wrapped with connective tissue (c) and intestine loops (il). The gonadic unit is the acinus (a), formed by a wall of germ cells (w), spermatogenic cells (sc), centripetally from the wall, and mature spermatozoa free in the acinus lumen (l). (B, C) Details of an acinus at confocal microscope. Phalloidin staining (in green) strongly labels microfilaments present in the acinus wall. Nuclei are in red (TO-PRO3): spermatogenic cells have a deep red large nucleus, spermatozoa show a light red and pointed nucleus (sperm head). (Bars = 47.62 μm).

Table 3 – Means of FPKM (fragments per kilobase of exon per million fragments mapped) of analyzed transcripts.

	Males Fam1	Males Fam2	Females Fam1	Females Fam2	Bias
ORF-21	2586.12	1445.20	na	na	Male mtDNA specific
<i>psa</i>	108.55	206.93	98.38	217.87	Family 2
<i>biring</i>	10.96	59.95	5.57	8.53	Males and Family 2
<i>anubl1</i>	221.10	169.07	4.79	6.49	Males

na = not available.

Table 4 – Transcript staining in *R. philippinarum* gonadic tissue. The staining intensity was evaluated by sight (as in Gogusev et al. 1997).

Probe	Staining localization	Time of maximum staining	Staining intensity
ORF-21	M acinus wall	Few hours	high +
	M spermatogenic cells	Few hours	high +
	sperm (acinus lumen)	Few hours	high +
	eggs	na	na
PSA	M acinus wall	2 days	high
	M spermatogenic cells	2 days	medium
	sperm (acinus lumen)	2 days	medium
	eggs	2 days	high
BIRING	M acinus wall	2 days	na
	M spermatogenic cells	2 days	medium
	sperm (acinus lumen)	2 days	medium
	eggs	2 days	low
ANUBL1	M acinus wall	2 days	na
	M spermatogenic cells	2 days	high
	sperm (acinus lumen)	2 days	high +
	eggs	2 days	medium

na = not available.

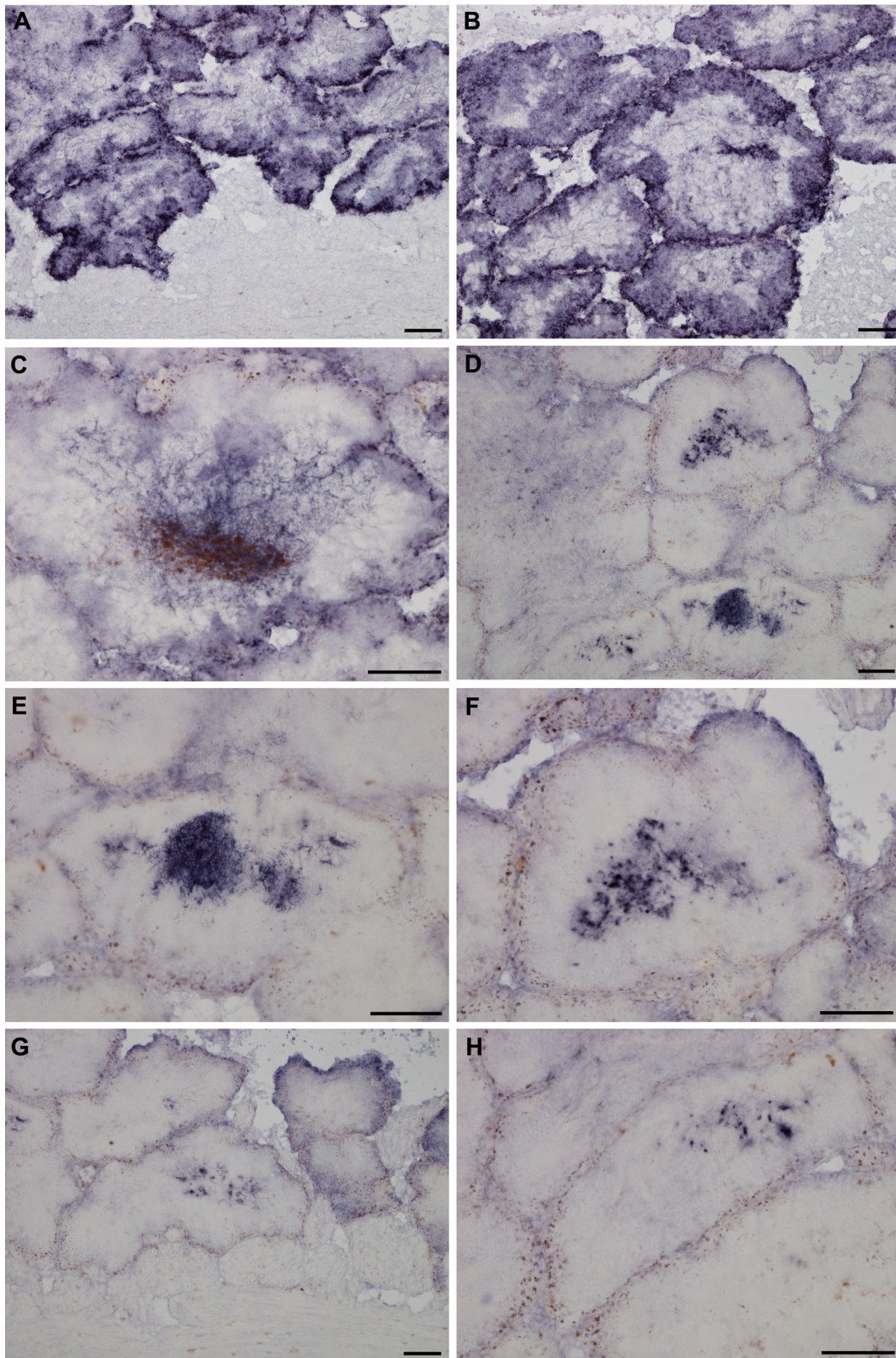


Fig. 42 – ORF-21 expression in male gonad and surrounding tissues. ORF-21 probe showed the highest color reaction (see also Tables 3 and 4), with the staining appearing in few hours. No labeling is present in eggs. The probe labeled both the acinus (**A, B**) and its lumen (**C-H**), indicating a positive reaction with both spermatogenic cells and mature sperm. Also the collector tubes, full of sperm, appeared stained (**C**). Interestingly, ORF-21 and PSA only appeared to have an high staining along the acinus wall (**A, B**) (Bars = 100 μ m).

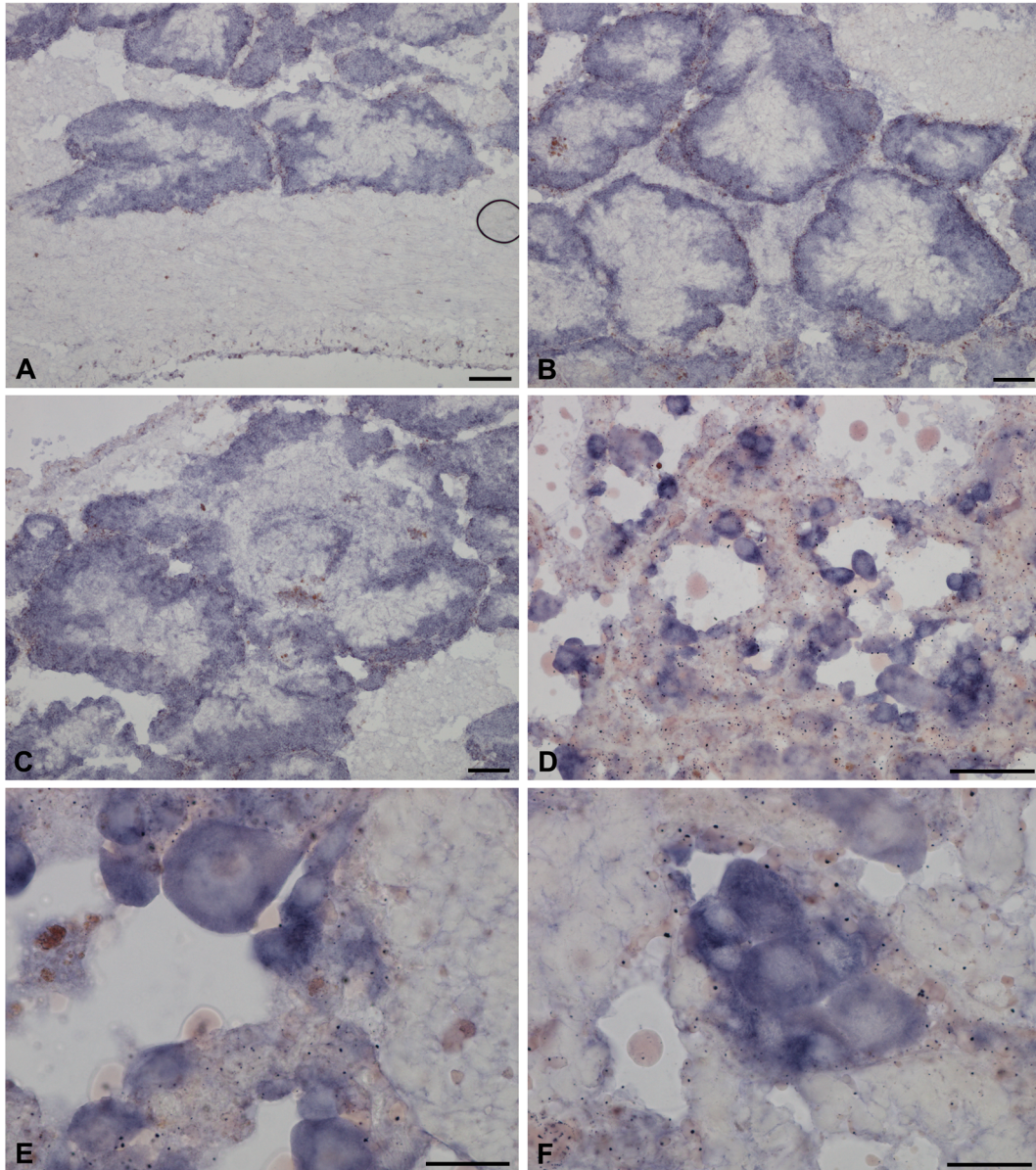


Fig. 43 – *psa* expression in gonad and surrounding tissues. (A-C) Male gonad: a medium staining was visible in male acini and mature spermatozoa visible in the lumen (C). Interestingly, PSA and ORF-21 only appeared to have an high staining along the acinus wall (B). (D-F) Female gonad: PSA probe showed the highest intensity in eggs, in both developing and mature eggs (see also Tables 3 and 4). (A-D: bars = 100 μm ; E, F: bars = 50 μm).

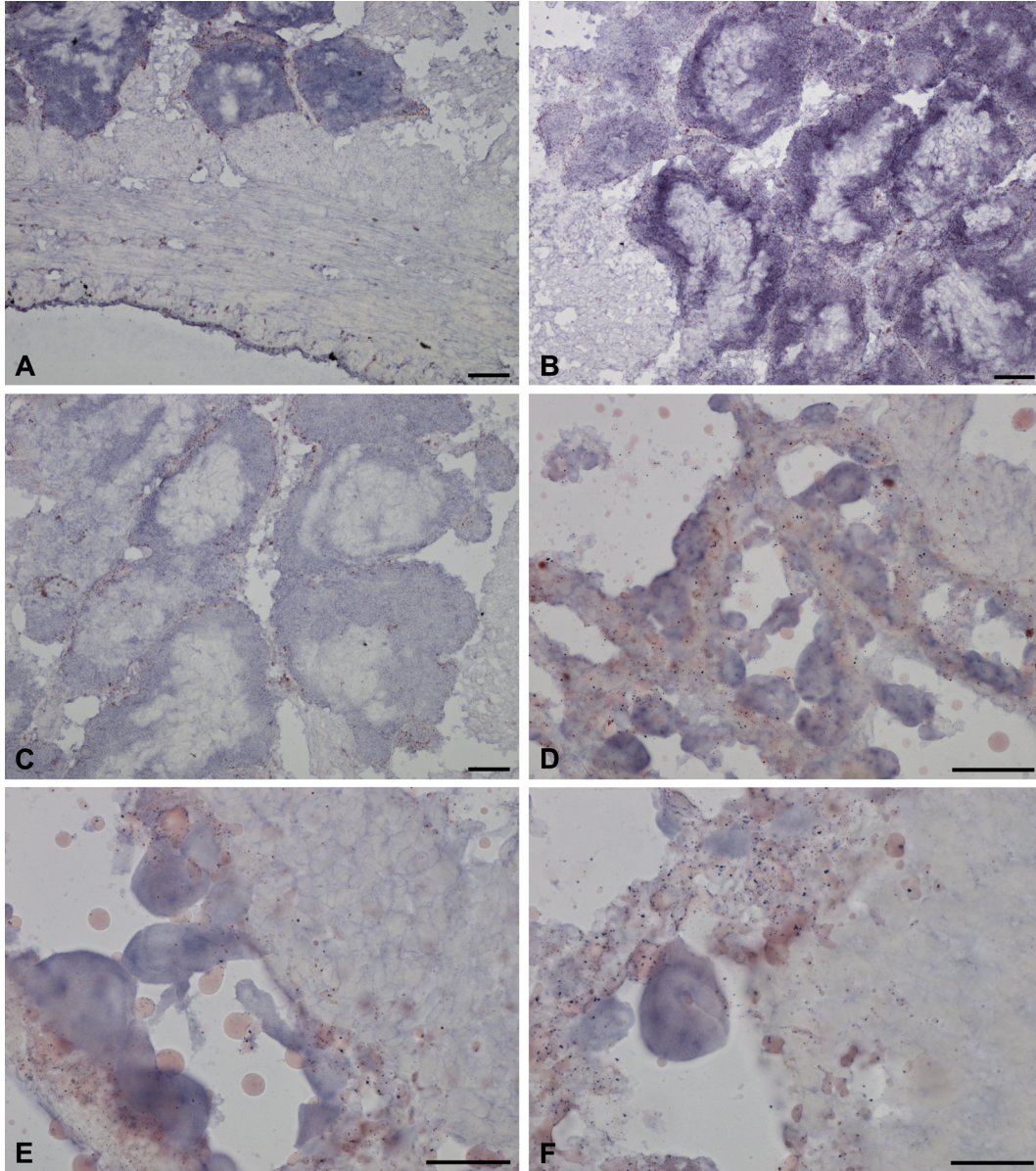


Fig. 44 – *biring* expression in gonad and surrounding tissues. (A-C) Male gonad: BIRING probe reacted in the acinus, where appeared to be higher than in mature spermatozoa, weakly visible in the lumen (C). (D-F) A medium staining was visible in both developing and mature eggs. (See also Tables 3 and 4) (A-D: bars = 100 μ m; E, F: bars = 50 μ m).

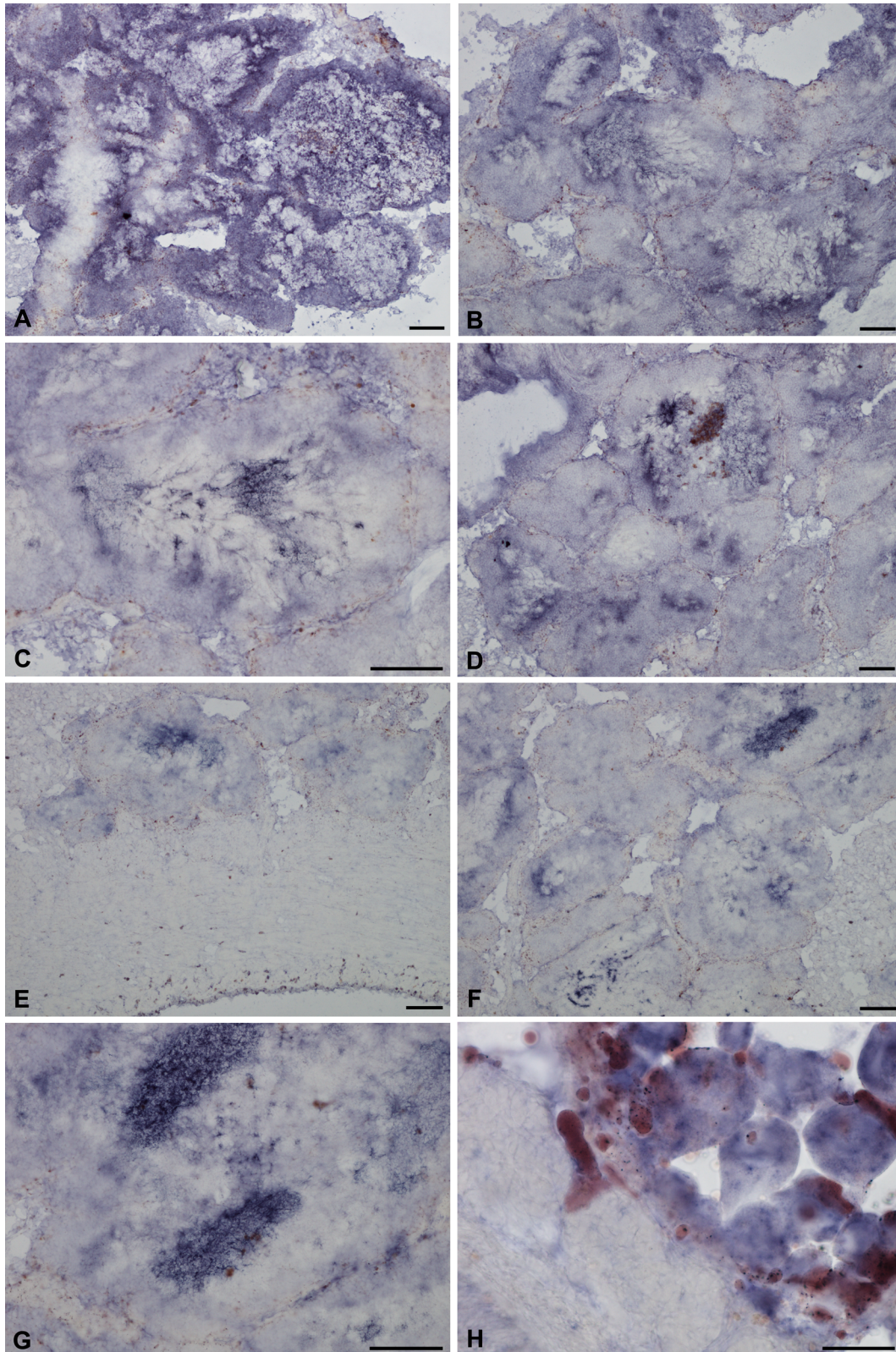


Fig. 45 – *anubl1* expression in gonad and surrounding tissues. (A-G) Male gonad: ANUBL1 reaction showed the highest staining intensity together with ORF-21 (see also Tables 3 and 4). ANUBL1 staining in mature spermatozoa appeared to be higher than in the acinus. **(H) Female gonad:** a medium staining was visible in eggs. (A-G: bars = 100 μ m; H: bars = 50 μ m).

4 – DISCUSSION

4.1 – Patterns of spermatozoon mitochondria distribution in early embryos of *R. philippinarum*

In the Manila clam, as in most animals, sperm mitochondria penetrate the egg cytoplasm at fertilization (see Longo 1987), and M mitochondria are far rarer than F mitochondria in the zygote. Since *R. philippinarum* has DUI, different mechanisms of mitochondrial replication and/or degradation must operate during development to produce eggs homoplasmic for F-type mtDNA, and sperm homoplasmic for the M-type.

In order to trace the movement of M-type mitochondria in embryos, *R. philippinarum* eggs were fertilized with sperm stained with MitoTracker Green FM. In both 2- and 4-cell stages, sperm mitochondria were randomly dispersed among blastomeres in some embryos, while they were aggregated in some others (Fig. 21). I considered a pattern to be “aggregated” when sperm mitochondria were located along the cleavage plane dividing AB and CD blastomeres in 2-cell stage, and in a region among the four blastomeres at the 4-cell stage (following Cogswell et al. 2006). The observed mitochondrial distribution is fully in line with what was found in *Mytilus*, in which the following four points have been demonstrated: 1) the existence of the two above mentioned patterns; 2) the pattern is mother-dependend (*i.e.* the pattern produced is independent from the father); 3) the aggregate pattern occurs in male embryos and the dispersed in female embryos; and 4) this is a nuclearly inherited property (Cao et al. 2004; Obata and Komaru 2005; Cogswell et al. 2006; Kenchington et al. 2009). Authors do not agree whether paternal mtDNA and maleness are causally linked or not; *i.e.* whether male mitochondria would trigger or not mussel gonad to develop into testis (see a detailed discussion in Kenchington et al. 2009).

I can here fully confirm the existence of the above mentioned two patterns in *R. philippinarum* (point 1). Although I could not provide a quantitative approach because of problems with MitoTracker staining persistence, this is the first evidence that aggregated and dispersed patterns of sperm mitochondria in developing embryos do exist also in a DUI species outside the *Mytilus* complex. This observation strongly links these patterns with DUI, even more considering that no aggregation of sperm mitochondria near the cleavage between blastomeres was observed in *Crassostrea gigas*, a bivalve with SMI (Obata et al. 2008).

In *R. philippinarum*, mesoderm tissues of adult males contain both M and F -type mitochondria (Passamonti and Scali 2001; Ghiselli et al. 2011). Thus, the observed segregation pattern (Fig. 21) should be considered as a mesoderm “enrichment” mechanism of M mitochondria in the developing male embryos.

4.2 – Mitochondrial inheritance and mitochondrial bottleneck in *R. philippinarum*

Oocytes of many organisms (amphibians, fishes, insects, planarians, chaetognaths, nematodes, and mammals) possess a cytoplasmic region, called “germ plasm” or “pole plasm”, that segregates in the germ line and it is necessary for its specification (Kloc et al. 2004). It usually contains the Balbiani body (Bb), consisting in an electron-dense material (nuage) rich in ribonucleoproteins and mitochondria. Some of these mitochondria aggregate with germ line determinants during oogenesis (reviewed in Kloc et al. 2004).

In DUI species, it is conceivable that in male Primordial Germ Cells (PGCs) M mitochondria have to overcome or prevent the replication of F mitochondria coming from the Bb, so that they can replace them. The mechanisms allowing M mitochondria to displace the F-type in the male germ line of DUI species are still unknown. A replicative advantage of M mitochondria was proposed by Cogswell et al. (2006). Another possible mechanism is the complete prevention of F-type mtDNA replication and/or its degradation. Both hypotheses

still have to be investigated. Also, the strong (often predominant) presence of M mtDNA in male somatic tissues of *R. philippinarum* raises some concerns on the accuracy of this active segregation mechanisms in male embryos. In fact, while in mytilids this system seems to be quite precise, given the rare presence of M mtDNA outside the gonad, a leakage of M-type is evidently very frequent in *R. philippinarum*.

According to Shoubridge and Wai (2007), there is some genetic evidence that segregation of mtDNA sequence variants is a stochastic process occurring during PGC formation, since they observed no strong selection against oocytes carrying pathogenic mutations. On the contrary, according to other authors, the mitochondrial bottleneck could actually act as a selection mechanism (see Introduction and Boldogh and Pon 2006; Zhou et al. 2010; Kogo et al. 2011). What I observed is that there must be an efficient mechanism for selection of mitochondria in *R. philippinarum* since, despite the leakage during M-type active segregation in males, and the sporadic malfunctioning of M-type selective elimination in females, both sperm and eggs are strictly homoplasmic for their sex-specific mtDNAs. It is a matter of conjecture whether this mechanism is restricted to DUI species only, or whether it is rather a variation of a more common mechanism that usually segregates mitochondria to germ line.

Given the above mentioned observations, three main selection processes must operate on sperm-derived mitochondria to grant (in males) or prevent (in females) their invasion of germ line, and therefore their transmission to the next generation. In chronological order, the first process (which I refer to here as DUI Checkpoint #1, see Fig. 48) is the active segregation of sperm mitochondria that starts from the very first embryo division, as observed in male embryos of *M. edulis* (Cao et al. 2004; Cogswell et al. 2006), *M. galloprovincialis* (Obata and Komaru 2005), and *R. philippinarum* (Milani et al. 2011, 2012). The aggregated pattern of M mitochondria was observed in male embryos of *Mytilus* until the D-larva stage (Cao et al. 2004), and until the 32-cell stage in *R. philippinarum*, although in this case the aggregation

was less tight from the 8-cell embryo onwards (Milani et al. 2012). The massive presence of M mtDNA in the somatic tissues of *R. philippinarum* males suggests that M-type mitochondrial leakage does happen frequently during embryo cleavage; as a consequence, M mtDNAs are commonly present in other tissues of mesodermic derivation, like the adductor muscle, and even in tissues of ectodermic derivation, like the mantle (Ghiselli et al. 2011). Therefore, checkpoint #1 appears to be more relaxed in *R. philippinarum* than in mytilids and more analyses are needed to understand exactly how this happens.

A second mechanism (DUI Checkpoint #2 in Fig. 48) operates in females, and it works exactly as it does in species with Strictly Maternal Inheritance (SMI). In mammals, the sperm-derived mitochondria are selectively degraded and this process depends on ubiquitination (Sutovsky et al. 1999): the sperm mitochondria are labeled with ubiquitin during spermatogenesis, and are degraded shortly after fertilization. In DUI species, a similar process is blocked in males and occurs later in females (not before the D-larva stage: Cao et al. 2004; Cogswell et al. 2006). The finding of M-type mtDNA in females shows that this mechanism is not always error-free. Another theory is that the M-type could be only diluted in females, without being degraded (Milani et al. 2012).

Our analysis showed that both DUI Checkpoint #1 and Checkpoint #2 are not perfect in *R. philippinarum*. As a consequence, the strict mtDNA homoplasmy observed in sperm and eggs may require the presence of a third selection mechanism, which I refer to as Checkpoint #3 (Fig. 48). This mechanism would act as a filter for germ line mitochondria and it may operate when PGCs establish themselves (i.e. whenever PGCs separate from somatic cells). This Checkpoint #3 should be considered as the “mitochondrial bottleneck” for DUI species. Given the supposed origin of DUI from SMI, Checkpoint #3 is probably established with a molecular machinery similar to that of SMI.

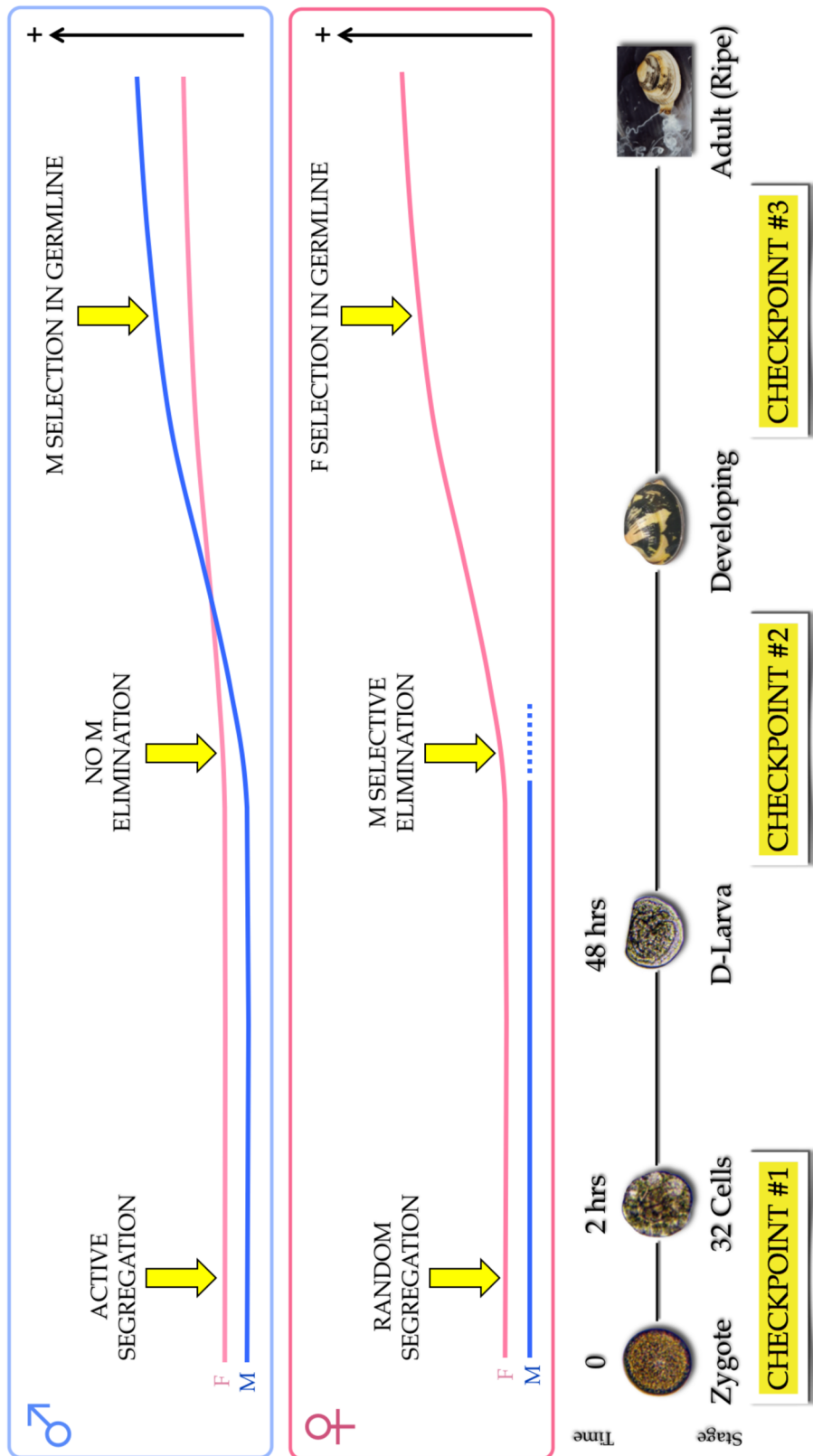


Fig. 48 – Proposed model for germ line mitochondria selection under DUI. The yellow arrows indicate the three Checkpoints. The curves represent a schematic visualization of the mtDNA copy number variation during development. (Image from Ghiselli et al. 2011).

Summarizing, the evidence that gametes are strictly homoplasmic indicates that the selection of sex-specific mitochondria (*i.e.* Checkpoint #3) is downstream in *R. philippinarum*, maybe at the PGCs establishment (Ghiselli et al. 2011). The fact that males show high levels of M-mtDNA in their somatic tissues (Passamonti and Scali 2001; Ghiselli et al. 2011) suggests that the leakage of M-type mitochondria happens more frequently in clams than in mussels, and in an early stage during *R. philippinarum* embryo cleavage, leading to a more relaxed functioning of the Checkpoint #1. Indeed, from the 8-blastomere stage onwards, aggregated pattern seems to be less tight in the Manila clam than in *Mytilus* (see Fig. 21 and compare to Fig. 4 in Cao et al. 2004), in which a closer association among M mitochondria appears until the D-larva stage. It is tempting to speculate that a less stringent segregation mechanism is acting in male embryos of *R. philippinarum*, accounting for the massive presence of M-mtDNA in somatic tissues of males.

4.3 – Mitochondrial DNA replication in *R. philippinarum* early embryo development

The Real-Time qPCR analysis on developing embryos (Milani et al. 2012) showed that the elimination of sperm mitochondria (*i.e.* Checkpoint #2) does not occur in early embryo stages: actually, 2 h after fertilization (32-blastomere stage), no significant reduction of the M-mtDNA was detected. This finding is in line with those in *Mytilus edulis*: by staining sperm mitochondria with MitoTracker, Cao et al. (2004) observed that M mitochondria persist until the trochophore stage even in embryos with the dispersed pattern (females); moreover, Sutherland et al. (1998) found that the process of elimination must occur after 18 h and be complete between 24 and 48 h post fertilization. The vast majority of *R. philippinarum* adult females did not show detectable traces of M-mtDNA in their tissues (see Ghiselli et al. 2011, for details), so that M mitochondria must be either eliminated or strongly diluted between larval and adult stages.

Indeed, given the overall qPCR results, I cannot support or discard the existence of a degradation mechanism of M mitochondria at a later developmental stage of females, similar to the ubiquitin-mediated one found in mammals (Sutovsky et al. 1999). The mechanism observed by Sutovsky et al. (1999) acts very early after fertilization, while in our case, if an ubiquitin-mediated process is present, it must occur later during embryo development. Even using a very sensitive technical approach such as Real-Time qPCR, the absence of detectable M-mtDNA in most adult females might be either the effect of an active degradation (as hypothesized in Checkpoint #2), or M-mtDNA duplication inhibition, followed by a massive dilution during female development. The qPCR analysis also showed that there is no significant variation in F-mtDNA content at least until 2 h after fertilization (32-blastomere stage).

The overall results suggest that in DUI, neither male nor female mitochondria undergo DNA replication boosts in the earliest embryo development. The lack of replication of mitochondria and their genomes during the first stages of embryonic development is in agreement to what has been observed in many other non-DUI animals, in which mitochondrial biogenesis is arrested in early embryogenesis: the total amount of mtDNA per embryo does not change until gastrulation in fishes (Wang and Yan 1992), before the pluteus stage in sea urchin (Matsumoto et al. 1974), before the swimming tadpole stage in frogs (Chase and Dawid 1972), or before larval stage in nematodes (Tsang and Lemire 2002). The mtDNA copy number is also constant until implantation in mouse (Piko and Taylor 1987).

Given that in *R. philippinarum* male mitochondria do not duplicate their DNA during early embryo stages, the ones contributing to male germ cell precursors are simply apportioned from those present in the fertilizing spermatozoon.

When germ line forms, only some sperm mitochondria enter it, eventually invading the gonad, while some others end up in other embryonic compartments. This was shown by

previous Real-Time analyses on *R. philippinarum* tissues (Ghiselli et al. 2011), and by the observation of the loosely aggregated pattern after the 8-blastomere stage (see Fig. 21; Milani et al. 2012). Moreover, spermatozoon has only four large mitochondria carrying a few dozens mtDNAs each (see Ghiselli et al. 2011). For these reasons, I can speculate that the M mtDNA bottleneck is narrow in the germ line of male Manila clams.

All that considered, mtDNA replication has to occur on a later stage, probably after germ line formation, to account for both M-type mitochondrial invasion of male germ line and F-type amplification in females. In any case, both the bottlenecks must be strictly regulated, because gametes are homoplasmic in *R. philippinarum* (Ghiselli et al. 2011). More analyses are needed to understand the dynamics of this basic cellular process.

4.4 – Unusual and conserved features of germ cells in DUI organisms

Germ line formation is a central topic to understand development. Recent researches (Reunov et al. 2000; Amikura et al. 2001; Isaeva and Reunov 2001; Amikura et al. 2005) indicate that mitochondria play a key role in several steps of this process. This is the reason why I decided to approach the issue by using a DUI experimental system, i.e. *R. philippinarum*, whose features provide a unique point of view for understanding the influence of mitochondria on germ line development. Because of this, I searched for typical structures involved in germ line specification.

In *R. philippinarum* oogonia, TEM analysis showed electrondense granules that aggregate close to two mitochondrial masses at the opposite sides of the nucleus (Fig. 23A). In oocytes these structures form two identical Bbs (Fig. 23B and C) similar to those described in other animals. The presence of two distinct Bbs is indeed an unusual feature; actually, as far as I know, *R. philippinarum* is the first species showing two Bbs in each oocyte, both containing a nuage clearly recognizable with TEM. This feature might be tentatively interpreted as a

remnant of an archaic hermaphroditic condition (Davison 2006). In fact, hermaphrodite bivalves present an ovotestis with two separated parts: one producing eggs, the other producing sperm. Moreover, the presence of DUI in bivalves has been related to the maintenance of gonochorism (Breton et al. 2011a). However, more data relating the presence of two Bbs to hermaphroditism in *Bivalvia* are needed to support this hypothesis.

The Chromatoid body (Cb) observed in *R. philippinarum* early spermatids (Fig. 24) is morphologically identical to those described in mouse (Reunov 2006; Kotaja and Sassone-Corsi 2007) and rat (Söderström and Parvinen 1976; Russell and Frank 1978; Parvinen 2005). It is always located close to the nuclear membrane and surrounded by empty mitochondria, some showing extruded cristae (Fig. 24D). This may indicate their involvement in *R. philippinarum* Cb formation, as also observed in sea urchins (Reunov et al. 2000). In the same cytoplasmic area, ribosomes of two different sizes forming polyribosomes were found (Fig. 24A-C), as reported in *Drosophila* (Amikura et al. 2001). Amikura et al. (2005) demonstrated, by inhibition of prokaryotic-type translation, that the small ribosomes are of mitochondrial origin. The structural similarity between the Manila clam and model organisms suggests that these mitochondrial ribosomes could play a similar role in the germ line development of this bivalve. In *R. philippinarum* spermatids, also the nucleus contributes to Cb formation, since material outflow from pores of the nuclear membrane can be seen in proximity of Cb (Fig. 24A-C), as documented in rats (Söderström and Parvinen 1976) and amphibians (Peruquetti et al. 2011).

4.5 – Vasp and germ line formation

Vasa is an evolutionary conserved component of the germ plasm (Hay et al. 1988a,b; Lasko and Ashburner 1988; Komiya et al. 1994; Williamson and Lehmann 1996; Nakao 1999;

Castrillon et al. 2000; Knaut et al. 2000; Kobayashi et al. 2000; Kuznicki et al. 2000; Raz 2000; Mochizuki et al. 2001; Gustafson and Wessel 2010).

To detect Vasa expression, I used an antibody against chicken Vasa (anti-Cvh) (Tsunekawa et al. 2000), since a specific antibody for Vasa of *R. philippinarum* was not available. This antibody reacted in monodimensional immunoblotting of gonadic and embryonic extracts with a band of about 65 kDa (Fig. 25A) that with bidimensional immunoblotting is resolved in three spots (Fig. 25B), probably isoforms of the same protein, with mass and isoelectric point in the range of the known Vasa-homologs (Gustafson and Wessel 2010). Further, I compared the sequence of *R. philippinarum* Vasa (Vasph) to chicken Vasa. The detection of one protein by western blot, the high CORE index of the alignment of Vasph and chicken Vasa-homolog (score = 95) (Fig. 26) and the identification in Vasph of Vasa conserved domains by InterProScan (Fig. 27) support the specific staining of the antibody used, even more considering the specific labeling observed in gametogenetic cells, while no staining was found in other tissues (intestine and connective) (Fig. 28). Thus, Vasa appears to be a specific marker of germ cells in *R. philippinarum*, as in other animals (see: Hay et al. 1988a,b; Lasko and Ashburner 1988; Komiya et al. 1994; Nakao 1999; Castrillon et al. 2000; Kobayashi et al. 2000; Mochizuki et al. 2001; Gustafson and Wessel 2010). Up to now, only the distribution of *vasa* mRNAs was analyzed in molluscs (Fabioux et al. 2004a; Fabioux et al. 2004b; Kakoi et al. 2008; Swartz et al. 2008; Kranz et al. 2010; Obata et al. 2010), and this is the first study about immunolocalization of Vasa protein.

Clam gonad is not permanent and the mechanism of its reformation every mating season is not fully documented. I showed that the wall of the acini is formed by Vasa labeled cells, which can be interpreted as undifferentiated germ cells. This cell aggregation defines a central empty area (Fig. 28C-F), the acinus lumen, which in mature gonads is full of gametes (Fig. 28G and H).

I also used Vasa to localize germ plasm both in eggs and in early embryos of *R. philippinarum*. In eggs labeled with anti-Cvh, a spotted staining dispersed in the cytoplasm was found, while a more strongly labeled zone was visible along the cleavage furrow in 2-blastomere embryos (Fig. 29). This finding is in line with what found in embryos of other animals, in which Vasa localized in the middle portion of the first cleavage furrow (Tsunekawa et al. 2000).

This early Vasa segregation supports a preformation mechanism for germ line determination in *R. philippinarum*. In animals, germ cells can be specified by maternally inherited determinants (preformation) and by inductive signals from surrounding tissues during development (epigenesis) (Extavour and Akam 2003). Among bivalves, in *Crassostrea gigas* (Fabioux et al. 2004b) and *Sphaerium striatinum* (Woods 1931) *vasa* mRNA is restricted to a defined zone during the first embryo stages suggesting a specification by preformation. The early segregation of Vasa in *R. philippinarum* suggests that maternal factors already present in the eggs could be involved in PGCs formation, supporting the hypothesis that maternal nuclear genes act as germ line determining factors (see also Ghiselli et al. 2012).

4.6 – Spermatozoon mitochondria and male germ line formation

As discussed above, both nuclear and mitochondrial factors play a role in nuage formation in both SMI and DUI species. However, a few questions remain open in DUI species. How do sperm mitochondria enter male germ line? How do they displace maternal mitochondria in germ cells?

In *M. galloprovincialis* sperm mitochondria and nucleus remain at the entry point of eggs treated with colchicines (Obata and Komaru 2005), suggesting a role of microtubules in the movements of sperm mitochondria soon after fertilization. In *R. philippinarum* embryos, the microtubule immunostaining showed a well-defined midbody in the middle of the first

cleavage furrow, corresponding to the area in which the aggregate of spermatozoon mitochondria localizes (Fig. 30).

It is well known that, when the cleavage furrow ingresses compressing the spindle midzone, it creates an intercellular bridge containing a midbody at the center (Paweletz 2001; Skop et al. 2004; Eggert et al. 2006). Thus, the midbody is a structure of tightly packed microtubules and associated proteins derived from the constriction of the central spindle (Eggert et al. 2006). Although no clear function has been ascribed to the midbody yet, it contains proteins indispensable for cytokinesis, asymmetric cell division, and chromosome segregation (Skop et al. 2004; Eggert et al. 2006; Cai et al. 2010).

The midbody might be also involved in the trafficking of important signaling molecules along the microtubules and in the segregation of material for germ line development. Indeed, the germ plasm is segregated into germ cells by dynein- and kinesin-dependent transport on centrosome-nucleated microtubules (Becalska and Gavis 2010; Lerit and Gavis 2011), and the disruption of some midbody proteins causes a failure in progeny production (Gönczy et al. 2000; Piano et al. 2000; Maeda et al. 2001; Skop et al. 2004). In this way, in many animals, germ line determinants aggregate in the middle of the first cleavage furrow (Kloc et al. 1998; Tsunekawa et al. 2000), where in DUI male embryos the aggregate of spermatozoon mitochondria localizes.

In this context, spermatozoon mitochondria in DUI species may be recognized by specific motor proteins that would carry them to the central spindle, where the cleavage furrow of the 2-cell stage forms.

In *R. philippinarum*, the midbody also appears to have a role in positioning M-type mitochondria in a stable zygote area on the a-v axis, avoiding a complete dispersal in the blastomeres: in spiral segmentation, after the first division, this central zone is no more directly involved in the following cleavages, which take place around it (Tyler and Kimber

2006), so that the mitochondrial aggregation can be maintained in place. As clearly shown in 4-blastomere embryos of *R. philippinarum*, the new spindles form in tangential directions, far from the region on the a-v axis where the aggregate of M-type mitochondria is located (Figs 30 and 31). Although microtubules emanate from the spindle poles during early anaphase, the microtubules of the central spindle eventually lose their connections with poles (Glotzer 2009), and any material localized in the midzone can be easily maintained in position.

TEM observations on sections of *R. philippinarum* 2-blastomere embryos showed F-type mitochondria at the division plane, some fused with the cleavage membrane (Fig. 32), supporting their involvement in its building, as already proposed (Bieliavsky and Geuskens 1990; Skop et al. 2004, and references therein). Moreover, the same sections showed a midbody in proximity of one or more mitochondria of about 1 μm in diameter (Fig. 32). These should be interpreted as spermatozoon mitochondria, since no organelle of a comparable size was found in unfertilized oocytes. Further support to this is the observation that, in some sections, a complete spermatozoon midpiece was detected with a centriole still linking the spermatozoon mitochondria (Fig. 32B).

Therefore, on the basis of my observations, sperm mitochondria appear to be not detached from the distal centriole of the midpiece during the first embryo cleavage of *R. philippinarum* male embryos, therefore allowing their simple transport to the midzone by microtubule nucleation. In mammals, the sperm mitochondrial sheath appears to be associated with microtubule-based structures to secure the destruction of sperm mitochondria in a specific compartment of the embryo (Sutovsky et al. 1996). In DUI species a similar mechanism could be responsible for the transportation of male mitochondria towards PGCs.

During the development of DUI male embryos, spermatozoon mitochondria must be recognized by egg factors to be actively transferred by microtubules together with germ plasm

in the PGCs, where they become dominant and replace Bb mitochondria during germ line formation.

4.7 – “MtRPH-21”: a mitochondrial tag for sex-specific mitochondrial transmission?

Novel genes in the male mitochondrial genome of DUI species were proposed to be responsible for the maintenance/degradation of sperm mitochondria during embryo development (Breton et al. 2009; Breton et al. 2011a,b). Lineage-specific mtDNA-encoded proteins are already known to play a role in key biological functions and important adaptive processes (Monchois et al. 2001; Chase 2007; Khalturin et al. 2008; Khalturin et al. 2009). Interestingly, the two novel mtDNA-encoded proteins found in DUI mussels were shown to be mt genome-specific (for F or M genomes) (Breton et al. 2009; Breton et al. 2011a,b). It has been hypothesized that they could be responsible for the different modes of mtDNA transmission in DUI bivalves, and several observations support their functional significance in freshwater mussels (Breton et al. 2009, 2011a).

In the M mtDNA of *R. philippinarum* (Fig. 33) I found an Open Reading Frame (ORF) in the Male Unassigned Region 21 (MUR21) (Figs 33 and 34). Interestingly, its transcription level is comparable to that of some mitochondrial coding genes (Table 2; Fig. 36).

The ORF-21 nucleotide sequence shows only synonymous mutations (Fig. 34), therefore translating always the same putative protein of 172 aa (called MtRPH-21) (Fig. 35). MtRPH-21 shows no homology with any other known protein. The only clue about its possible function is the presence of two transmembrane regions in the first half of the protein (Fig. 37), which is an extremely interesting feature, if we consider that a predicted transmembrane helix is constantly present in the same position (at the N-terminus) of all DUI mussels new ORF proteins found so far (Breton et al. 2009, 2011a,b). Moreover, *in situ* hybridization showed a

specific transcription in spermatogenic cells, and the staining was never present in the surrounding tissues (Fig. 42). This supports a role of MtRPH-21 in sperm formation.

The overall observations could suggest a role of MtRPH-21 as mitochondrial tag, therefore involved in the discrimination of the two mitochondrial types, and possibly influencing their processing inside the embryo.

Since M-type mitochondrial DNA is present in almost all male somatic tissues analyzed (Ghiselli et al. 2011), but ORF-21 is only expressed in testes, two mechanisms are conceivable to gain such specific expression pattern: *i)* M mtDNA transcription may be wholly silenced outside the gonad; *ii)* a specific silencing or degradation of the ORF-21 mRNA is present in the male somatic cells. The M-type functioning only in spermatogenic cells was formerly sustained by Obata et al. (2011), that proposed different M- and F-type tissue-specific transcriptional regulation in *Mytilus*. No data are available for *R. philippinarum* and more experiments are planned on the issue. Nevertheless, it would be important to clarify this point, for example by performing an expression analysis of mitochondrial genes in somatic tissues that will clearly show if the F-type is really the only mtDNA transcribed in the soma.

In my *in situ* hybridization analyses, ORF-21 labeling is equally strong in all sperm developing stages, supporting its similar expression during male gamete formation (Fig. 42). Interestingly, ORF-21 mRNA appeared to have a high staining along the acinus wall (Fig. 42). This suggests that its transcription starts at the beginning of gamete formation in the germ cells localized at the acinus wall area.

In conclusion, I feel confident to suggest a possible function in gamete formation and maybe in mitochondrial tagging for this putative novel protein. Of course, further experiments are needed to confirm that this specific novel protein is translated in *R. philippinarum*, as it was proved for a novel protein in unionids (Breton et al. 2011a).

4.8 – Sex-determining factors: characterization and localization

As already mentioned, sex determination in bivalves is not yet known. In DUI species, the peculiar segregation pattern of spermatozoon mitochondria was correlated with the existence of sex-biased lineages. This led to the hypothesis that male mitochondria could have an active role in the masculinization of the gonad through a series of specific signals between the nucleus and mitochondria (Kenchington et al. 2002).

A *de novo* annotation of 17,186 transcripts from *R. philippinarum* was recently obtained in collaboration with the University of Southern California (Ghiselli et al. 2012), and the comparison of the transcriptomes of male and female gonads allowed the identification of 1,575 genes with a strong sex-specific expression (i.e. genes that could be involved in sex determination; see Ghiselli et al. 2012).

Comparing the transcriptomes of a *R. philippinarum* family producing predominantly females (Family 1) with a family producing predominantly males (Family 2), BLAST2GO and BLASTX identified genes with sex and family biases involved in reproduction and ubiquitination (Reproduction GO:0000003; Ubiquitination GO:0016567), which are candidate genes for the regulation of sex-specific aspects of DUI system.

Reproductive genes can be obviously related to sex and sex-determination, while ubiquitination is more known for its role in protein degradation. However, ubiquitination also regulates gene expression: ubiquitin proteolysis can control transcription through degradation of specific transcription factors (Salghetti et al. 2001) and can be involved in mRNA processing (Muratani et al. 2005). Additionally, ubiquitination, through gene expression regulation, plays a role in sex determination (*Drosophila*: Bayrer et al. 2005; *C. elegans*: Hodgkin 1987; Hansen and Pilgrim 1999; Starostina et al. 2007; Kulkarni and Smith 2008), sex transition (i.e. gonadal transformation from ovary to testis in proterogynic species) and testis maturation (teleost fishes: Fujiwara et al. 1994; Sun et al. 2008; *Caenorhabditis*

elegans: Shimada et al. 2006), and in human male germ-cell development (Ginalski et al. 2004).

The best documented relationship between ubiquitination and sex determination comes from *C. elegans*, in which manipulation of ubiquitination activity at different developmental stages revealed its involvement in sperm fertility and sex-specific development (Hodgkin 1987; Hansen and Pilgrim 1999; Starostina et al. 2007; Kulkarni and Smith 2008).

In this study, I analyzed the localization of transcripts with specific biases by *in situ* hybridization; in particular, I chose those protein coding genes that in other animals are involved in reproduction and ubiquitination (Tables 1 and 3): PSA, BIRING, and ANUBL1 (see the following sections for a detailed discussion of each gene). Their inferred proteins show complete domains in common with proteins with a known function, supporting their functional conservation (Figs 38-40).

In situ hybridization was performed to confirm the specific localization of these transcripts. In fact, the sampling of a pure gonadic tissue is not possible in venerids because it develops intimately wrapped with connective tissue and intestine loops. For this reason a proof of the specific expression of these genes in gonads needed a visual confirmation.

The finding that all the tested probes labeled gametogenetic cells only, while the surrounding tissues were not stained (Figs 42-45), proves their specific transcription in developing gametes. Moreover, the intensity of the *in situ* hybridization staining (Table 4) reflects the transcription level, indicated in Table 3 by RNA-Seq FPKM values (Ghiselli et al. 2012). For example, the mitochondrial ORF-21 has a much higher expression level (FPKM from 1445.20 to 2586.12) than the most expressed nuclear gene considered for this analysis (221.10 for *anubl1*). Similarly, the ORF-21 labeling showed the highest intensity and the color reaction happened faster (few hours for ORF-21 and two days for the nuclear riboprobes).

4.8.1 – The proteasomal machinery: PSA

The proteasome is a complex multisubunit protease known to be implicated in male sexual differentiation (Shimada et al. 2006). The presence of a proteasome subunit (*psa*) among Family 2-biased genes of *R. philippinarum* indicates a different utilization of this gene in the two lineages and consequently its possible involvement in the development of the progeny towards males. PSA probe showed the highest intensity in eggs (Fig. 43), and this makes it a candidate factor for preformation in eggs that will develop into males.

In Diz et al. (2009) the proteome of eggs from two *M. edulis* lines (families), which differ in the sex ratio of the progeny (line M, 91% males; line F, 100% females), was analyzed by two-dimensional electrophoresis. They hypothesized that proteins showing differences between the lines might potentially be involved in the DUI mechanism, and their expression might have some causal link with sex determination. The differential molecular tag of mitochondria derived from eggs and sperm and the interaction of these labels with recognition factors were suggested to determine mitochondrial fate (Zouros 2000; Burzynski et al. 2003; Cao et al. 2004; Breton et al. 2006, 2007; Theologidis et al. 2007; Venetis et al. 2007; Cao et al. 2009). I want to highlight that one of the spots found by Diz et al. (2009), and showing the greatest differential expression between lines (≥ 1.5 -fold difference; see Table IV in Diz et al. 2009), was identified by mass spectrometry to be the Proteasome subunit β type 6 precursor.

Considering that the proteasome subunit α transcript was more expressed in *R. philippinarum* male-biased family, and that the same bias was shown in *M. edulis* by the subunit β of the same molecular machinery (20S core of the proteasome; see Fig. 49), I think that the proteasome function in the DUI molecular machinery should be further investigated.

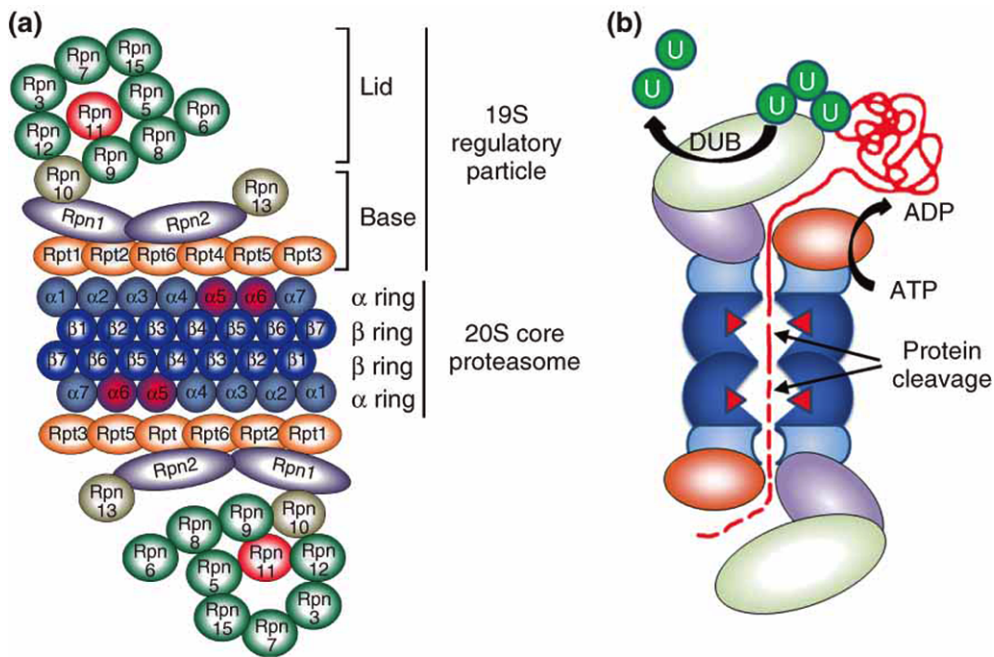


Fig. 49 – Proteasome complex structure. (Image from Brooks 2010).

4.8.2 – Inhibitors of Apoptosis Protein: BIRING

In both reproduction and ubiquitination categories, *biring* shows a strong sex-family interaction in *R. philippinarum*: it is male- and Family 2-biased (Ghiselli et al. 2012). This gene was recognized as a member of the IAP family (Inhibitors of Apoptosis Protein) (Salvesen and Duckett 2002). As their name implies, IAPs confer protection from death-inducing stimuli (Deveraux and Reed 1999), but, intriguingly, several members of the family appear to have distinct functions unrelated to apoptosis (Verhagen et al. 2001).

The existence of a baculovirus IAP repeat (a ~70-residue zinc-binding domain, named BIR) in a protein constitutes membership of the IAP family (Hinds et al. 1999; Miller 1999; Sun et al. 1999). Zinc-finger proteins include DNA-binding domains and have a wide variety of functions, most of which encompass some form of transcriptional activation or repression (Kaplan and Calame 1997; Koebernick and Pieler 2002; Schmitz et al. 2004). BIRs are essential for the anti-apoptotic properties of the IAPs (Duckett et al. 1998).

The baculoviral IAP (the first described) and several cellular IAPs contain also a second type

of zinc-binding motif known as RING domain, invariably found at the extreme carboxyl terminus of the protein (Fig. 50). In BIRING inferred protein, a BIR and a RING domains were found by InterProScan at the N-terminus and C-terminus respectively (hence the name BIRING).

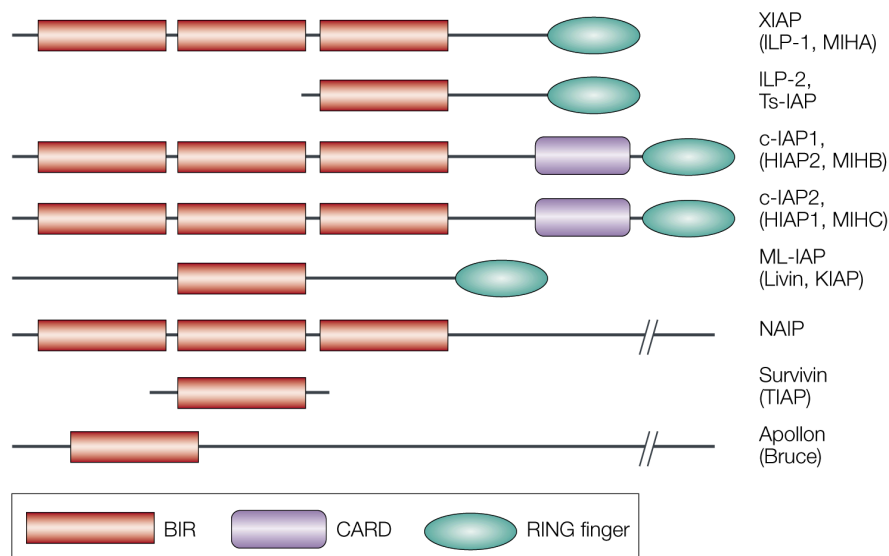


Fig. 50 – Mammalian IAPs/BIRPs. Alternative designations are shown in parentheses. The X-linked IAP (XIAP) is the best-characterized member of this family. BIR, baculovirus IAP repeat; CARD, caspase-recruitment domain; ILP, IAP-like protein; MIHA, mammalian IAP homologue A; NAIP, neuronal apoptosis inhibitory protein. (Image from Salvesen and Duckett 2002).

Emerging data indicate that RING-containing proteins can catalyze the degradation of both themselves and selected target proteins through ubiquitination. Joazeiro and Weissman (2000) showed that RINGs have a key role in the targeted degradation of proteins by the ubiquitin–proteasome system. This process involves the sequential covalent addition of Ubiquitin, a 76-residue protein, onto specific lysine residues on the target protein (Pickart 2000; Weissman 2001).

Ubiquitination does not always result in targeted degradation: in some situations, ubiquitination can modify the biological activity or subcellular localization of a protein (Hicke 2001). This is most often seen with the addition of a single ubiquitin moiety (monoubiquitination), whereas the sequential formation of oligomeric ubiquitin chains (polyubiquitination) usually directs the target protein for degradation by the 26S proteasome (Salvesen and Duckett 2002).

Interestingly, single BIR-containing Proteins (BIRPs) have important roles in mitosis, particularly in microtubule organization. Studies of these genes in *C. elegans*, yeast, mouse and humans identified integral roles of certain IAPs/BIRPs in cytokinesis and in mitotic-spindle formation (Li et al. 1998; Fraser et al. 1999; Uren et al. 1999; Speliotes et al. 2000; Uren et al. 2000; Silke and Vaux 2001; Li et al. 2002; Rajagopalan and Balasubramanian 2002). BIRPs possibly have a role in localizing proteins involved in numerous mitotic processes to the spindle midzone (Salvesen and Duckett 2002).

In the light of the hypothesized role of the midbody for the correct displacement of spermatozoon mitochondria in DUI early embryos, I think the IAP family deserves a punctual examination. The fact that *biring* is more highly transcribed in males of the male-biased family might support its role in the heredity of sperm mitochondria in DUI species. *In situ* hybridization showed that BIRING probe stained equally male and female gametes (Fig. 44), but, as for the other proteins analyzed in this study, a verification through protein detection is still needed. A role of BIRING in mitochondrial targeting and segregation does not seem unconceivable, even more considering the recent discoveries discussed above.

4.8.3 – Ubiquitin fusion proteins: ANUBL1

The transcript I named *anubl1* contains an ubiquitin domain and a Zinc finger zf-AN1. AN1-type zinc fingers are often found in proteins that contain a ubiquitin-like domain and therefore

may play a role in the ubiquitination pathway. I named the transcript *anubl1* because its inferred protein contains the same domains of the “AN1-type zinc finger and ubiquitin-like domain-containing protein” (ANUBL1) described in several animals, and these domains are located in the same position, the ubiquitin-like domain in the N-terminus and the zinc-binding domain in the C-terminus. This protein was shown to have a testis-specific expression in rats (Zhang et al. 2003). Unlike ubiquitin polyproteins and most ubiquitin fusion proteins, the N-terminal ubiquitin-like domain of ANUBL1 does not undergo proteolytic processing (see also: Linnen et al. 1993) and the exact function is still unknown.

Among nuclear genes, ANUBL1 showed the highest color reaction intensity in *R. philippinarum* *in situ* hybridization analysis (Fig. 45). ANUBL1 staining in mature sperm appeared to be higher than the acinus labeling (Fig. 45), thus suggesting an enrichment of the transcript during sperm maturation. A faint ANUBL1 staining was visible in eggs. This male-biased gene could code for a tag of spermatozoon mitochondria, that, together with other factors, may determine their fate during embryo development (see a complete discussion on the issue in section 4.11).

4.9 – Post-transcriptional regulation of sex-determining factors?

In *R. philippinarum*, all the above mentioned sex bias nuclear transcripts were found both in male and female gonads. This means that male-biased genes were present also in females and that female-biased genes were present also in males. This is not surprising. It is known that females and males are almost genetically identical, and in species without genetic sex determination they are actually identical. This implies that the vast majority of sexually dimorphic traits result from the differential expression of genes that are present in both sexes (Connallon and Knowles 2005; Rinn and Snyder 2005; Ellegren and Parsch 2007; Arnold et al. 2009). This is even more true in species lacking sexual chromosomes, as *R. philippinarum*.

Although male and female carry almost the same genome, they show differences in gene expression or use alternative splice forms (Long et al. 1995; Nuzhdin et al. 1997; McIntyre et al. 2006; Foley et al. 2007) and gender-specific transcription and/or translation occurs (Bermejo-Alvarez et al. 2010). The main differences between males and females are likely to be quantitative rather than qualitative (McIntyre et al. 2006), and genes have rarely an on/off expression, but there are thresholds to be exceeded to have effects or changes.

Further, post-transcriptional (e.g. miRNA; Mukherji et al. 2011) and post-translational (Adeli 2011; Janke and Bulinski 2011) regulation contribute to the fine-tuning of the expression. Regulation by miRNAs establishes a threshold level of target mRNA below which protein production is highly repressed, thus miRNAs can act both as a switch and as a fine-tuner of gene expression. miRNAs regulate protein synthesis in the cell cytoplasm by promoting target mRNAs degradation and/or inhibiting their translation, and they can regulate a large variety of cellular processes, from differentiation and proliferation to apoptosis (Bernstein et al. 2003; Cimmino et al. 2005; Li and Carthew 2005; Yi et al. 2008; Sluiter et al. 2010; Mukherji et al. 2011).

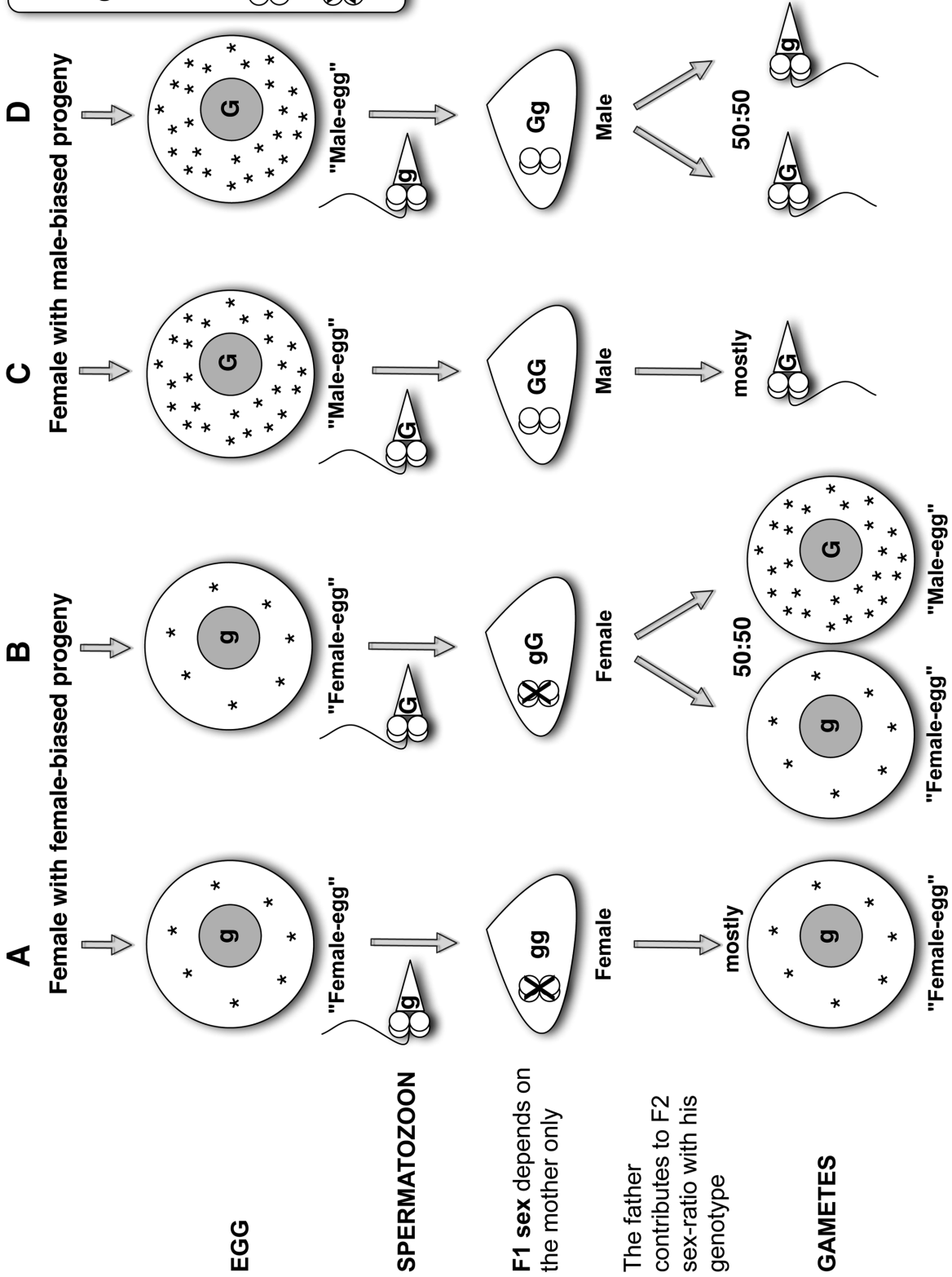
All that considered, in *R. philippinarum* I expect a post-transcriptional regulation acting to guarantee a specific translation of the proteins with a function in sex establishment only in the sex in which they are required. Obviously, the next logical step would be to study in which sex the translation to protein does actually occur.

4.10 – A sex-determination model

The finding of reproduction and ubiquitination transcripts with sex and family biases in *R. philippinarum*, led me to formulate a model (see Ghiselli et al. 2012) in which ubiquitination genes stored in female oocytes during gametogenesis would activate sex-gene expression in the early embryonic developmental stages, following the mechanism known as preformation. A simplified scheme of the model is shown in Fig. 51. Transcription factors (e.g. ubiquitination genes) would activate sex-gene expression, and the sex-differentiation process would be multifactorial and quantitative. Male development would require the crossing of a critical threshold of masculinizing transcripts (see also Kenchington et al. 2009).

Fig. 51 – (Next page) A simplified model for DUI and sex-determination. Transcription factors (e.g. ubiquitination genes) stored in female oocytes would activate sex-gene expression in early embryonic developmental stages and male development would require the crossing of a critical threshold of masculinizing transcripts. The sperm genotype contributes to F2 sex-bias. (A, B) A “female-egg” will produce a female regardless the genotype of the spermatozoon. (A) If it is fertilized by a spermatozoon with a “female-biased” genotype (g) the F1 female will produce mostly “female-eggs”. (B) If it is fertilized by a spermatozoon with a “male-biased” genotype (G) the F1 female will produce both egg types (50:50). (C, D) A “male-egg” will produce a male regardless the genotype of the spermatozoon. (C) If it is fertilized by a spermatozoon with a “male-biased” genotype (G) the F1 male will produce sperm carrying a “male-biased” genotype (G). (D) If it is fertilized by a spermatozoon with a “female-biased” genotype (g) the F1 male will produce both sperm types (50:50). The differential expression of some ubiquitination factors could regulate the fate of sperm mitochondria in the two families: degradation (A, B) or maintenance (C, D) (see also Fig. 52). Note that the genomic sex-determining factors (G and g) probably comprise more than one gene; recombination among these genes and environmental factors could account for the nearly continuous distribution of sex ratios among families.

* maleness factor
G "male-biased" genome
g "female-biased" genome
 M-type mitochondria maintenance
 M-type mitochondria elimination



4.11 – Ubiquitination factors in mitochondrial transmission

Other than having a role in sex determination, some ubiquitination factors could also be involved in mitochondrial inheritance, and their differential expression could be responsible for the different fate of sperm mitochondria in families with opposite sex bias (for example Family 1 with female bias, and Family 2 with male bias) (Fig. 51). In mammals the degradation of spermatozoon mitochondria in developing embryos involves ubiquitination of the mitochondrial membrane during spermatogenesis and the subsequent recognition and degradation of sperm mitochondria by species-specific egg factors (Sutovsky et al. 1999; Sutovsky et al. 2000; Sutovsky 2003). Following the nomenclature used for the DUI W/X/Z model (see section 1.5.5), in mammals this process can be explained as the interaction of two factors similar to W and X, the former produced during spermatogenesis and that labels the outer surface of sperm mitochondria (Ubiquitin), the latter produced during oogenesis and found in the egg cytoplasm.

Therefore, the W/X system may exist both in SMI and DUI species, but a modification of this mechanism is hypothesized to be responsible for the retention of sperm mitochondria in male embryos of DUI species (section 1.5.5).

The biased genes analyzed are good candidates to be these factors. In fact, the family-biased expression of some ubiquitination genes (see Table 3 and Ghiselli et al. 2012) can be easily linked also to the fate of sperm mitochondria. Their differential expression could be responsible for degradation vs maintenance of sperm mitochondria in families with opposite sex-ratio bias. In families with a male-bias (es. Family 2), ubiquitination factors could protect sperm mitochondria from degradation (Fig. 52A), for instance by blocking the binding of polyubiquitin chain to mitochondria, and allowing them to participate in male germ line development.

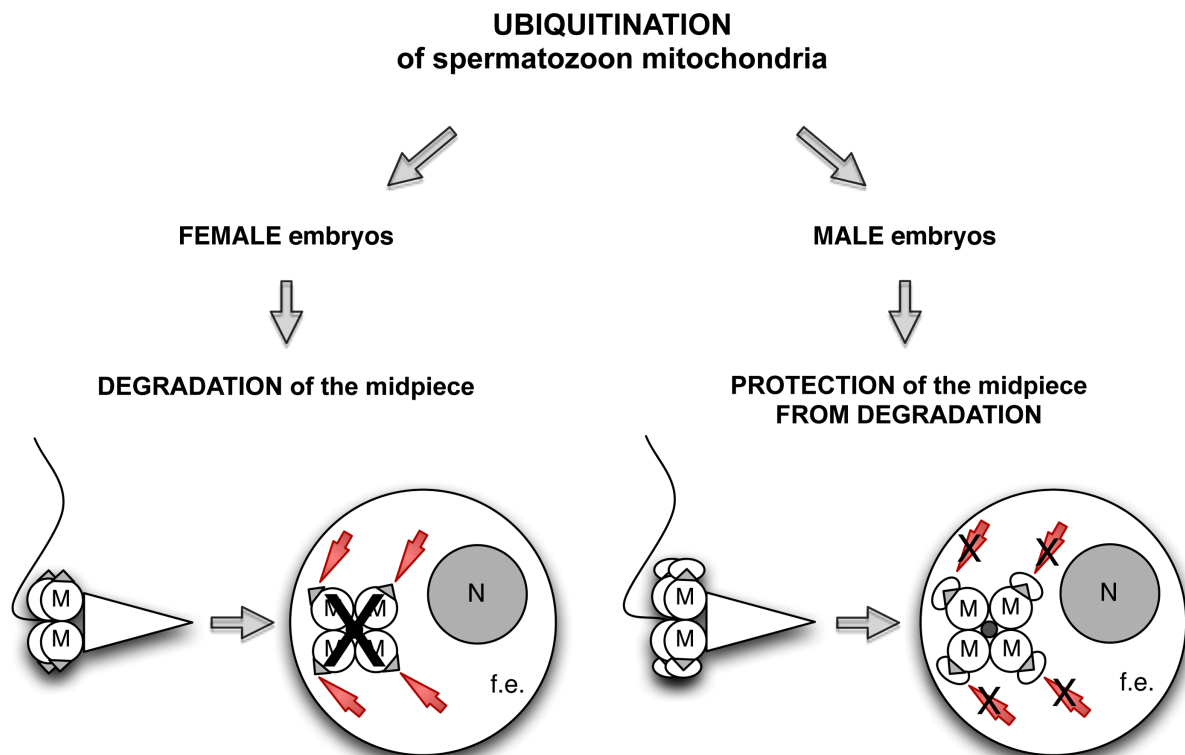
ANUBL1 may be the W factor, tagging the surface of spermatozoon mitochondrial membrane in *R. philippinarum*. This could explain why *anubl1* is equally expressed in male of families with opposite sex bias and why it has a specific expression during spermatogenesis, as in rat

(Zhang et al. 2003). Moreover, the ubiquitin-like domain in the N-terminus of its putative inferred protein points to an ubiquitin tag function as in mammals.

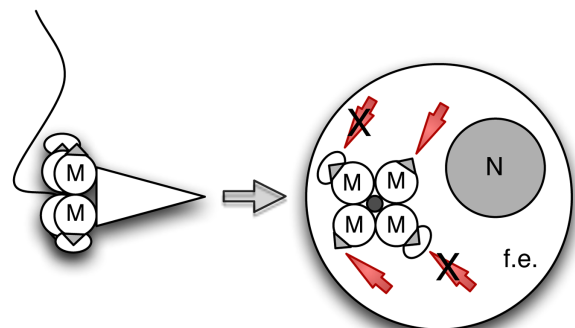
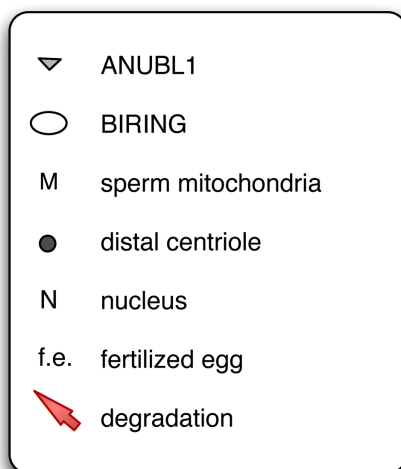
An additional factor (e.g. the inhibitor of apoptosis BIRING) would tag the spermatozoon mitochondria of male-biased family. This is consistent with the higher transcription level of *biring* in males of Family 2. Considering the function of single BIR-containing Proteins (BIRPs) in positioning factors to the spindle midzone and that the progeny of the families with a male bias (as Family 2 in this study) shows the aggregation of spermatozoon mitochondria (Fig. 21) close to the midbody (Fig. 30), a correlation between *biring* presence and the segregation of a spindle-mitochondria complex is here proposed: the higher transcription of *biring* and its presence as protein (to be verified) might allow the organization of a midbody containing M-type mitochondria, having a role in sperm mitochondria inheritance in DUI species.

Following the model mentioned in section 1.5.5, a factor Z typical of DUI species, would suppress factor X, avoiding sperm mitochondria degradation and allowing the aggregated pattern. If spermatozoon mitochondria were really coupled with masculinization, factors like Z could be transcribed by the same transcription factors that activate sex-gene expression (see section 4.10).

In conclusion, I here propose the involvement of BIRING in spermatozoon mitochondria recognition and maintenance in embryos of male-biased families. In males of female-biased families (es. Family 1) the quantity of BIRING could not be enough to nullify ANUBL1 action and guarantee the salvation of spermatozoon mitochondria, and the majority of the progeny would be female (Fig. 52B). On the contrary, in families with a male bias (es. Family 2), these proteins could protect sperm mitochondria from degradation (Fig. 52A), and the majority of the progeny would be male. All these findings are consistent with a relationship between ubiquitination, sex bias and mitochondrial inheritance.



A - MALES of male-biased families (e.g. Family 2):
more BIRING, higher probability of spermatozoon
mitochondria maintenance



B - MALES of female-biased families (e.g. Family 1):
less BIRING, less protection against degradation of
spermatozoon mitochondria

Fig. 52 – Ubiquitination factors in the transmission of spermatozoon mitochondria. In female embryos the degradation of the midpiece would be assured by ANUBL1 tag (W) and by X (red arrow) recognition after fertilization. **(A)** In males of male-biased families an additional mitochondrial tag, BIRING, could actually protect the midpiece mitochondria from degradation, also by allowing their transport to the spindle midzone and the midbody. **(B)** In males of female-biased families some sites could be prone to degradation for the less abundance of BIRING, leading to the dispersion/degradation of sperm mitochondria.

4.12 – Conclusions and perspectives

In Doubly Uniparental Inheritance (DUI) of mitochondria, during male embryo development, spermatozoon mitochondria aggregate and end up in the primordial germ cells, while they are dispersed in female embryos, but the mechanisms of the two mitochondrial segregation are still unknown. I used MitoTracker, microtubule staining and transmission electron microscopy to examine the mechanisms of distribution of sperm mitochondria in the DUI species *R. philippinarum* and an immunocytochemical analysis was performed to localize germ line determinant in early embryos. I also analyzed the gonad transcriptome of this species, searching for genes that could be involved in reproduction and sex determination. I added to the analysis an Open Reading Frame (ORF) specific of the M-type mtDNA of *R. philippinarum* that could be responsible for the maintenance/degradation of sperm mitochondria during embryo development. These transcripts were also localized in tissues using *in situ* hybridization.

As in *Mytilus* DUI species, in *R. philippinarum* the two distribution patterns were detected. Their presence in these taxa, together with their absence in species with maternal inheritance, confirms that their occurrence is related to DUI. In male embryos the midbody deriving from the mitotic spindle of the first division concurs in positioning the aggregate of sperm mitochondria on the animal-vegetal axis: in organisms with spiral segmentation this zone is not involved in cleavage, so the aggregation is maintained. Moreover, sperm mitochondria reach the same embryonic area in which also germ plasm is transferred, suggesting their contribution in male germ line formation. The finding of reproduction and ubiquitination transcripts that could be involved in *R. philippinarum* sex determination, led me to formulate a model in which ubiquitination genes stored in female oocytes during gametogenesis would activate sex-gene expression in the early embryonic developmental stages, following the mechanism known as preformation. Only gametogenetic cells were labeled by *in situ*

hybridization, proving their specific transcription in developing gametes. Other than having a role in sex determination, some ubiquitination factors could also be involved in mitochondrial inheritance, and their differential expression could be responsible for the different fate of sperm mitochondria in the two sexes.

The transcripts with a biased expression localize specifically in gametogenetic cells. The following step would be to verify the transcript translation and observe if the proteins really exist, and if they are synthesized in gametes or during embryo development. This could be done by the construction of specific antibodies, followed by western blot analysis on gonadic tissues of adult males and females and embryos in different developmental stages, and then by an immunocytochemical detection of the proteins by confocal microscopy.

The molecular regulation of mitochondrial inheritance is so far unknown. I would like to find the machinery that regulates the process, verifying the nature and structure of the specific tagging of spermatozoon mitochondria. For example, I want to confirm if MtRPH-21 is effectively translated, and study its structure and possible target (ubiquitin? motor protein such as dynein or kinesin? other molecular carriers? or adaptors to carriers?). Moreover, I want to verify the effective ubiquitination of spermatozoon midpiece by analyzing ANUBL1 localization with confocal microscopy, and investigate the possible role of BIRING in positioning spermatozoon mitochondria in developing embryos.

Finally, I am interested in understanding what is, if there is any, the peculiar function of spermatozoon mitochondria in DUI species. Some clues suggest that a specific function does exist, even if it is not already clarified. For example, I found that the male specific mitochondrial ORF-21 is transcribed only in gametogenetic cells, pointing to a specific regulation of its transcription in gonads and to a role in gamete formation. At the same time, the fact that ORF-21 transcripts were not found in surrounding tissues suggests an inactivation/silencing of M-type mtDNA in the soma. It would be really interesting to address

this point, and the construction of a cDNA library from somatic tissues could answer the question.

REFERENCES

- Abdalla FC, Cruz-Landim C (2004) Occurrence and ultrastructural characterization of “nuage” during oogenesis and early spermatogenesis of *Piaractus mesopotamicus* Holmberg, 1887 (Teleostei). *Braz J Biol* 64: 555–561.
- Adeli K (2011) Translational control mechanisms in metabolic regulation: critical role of RNA binding proteins, microRNAs, and cytoplasmic RNA granules. *Am J Physiol Endocrinol Metab* 301: E1051–E1064.
- Amikura R, Kashikawa, M, Nakamura A, Kobayashi S (2001) Presence of mitochondria-type ribosomes outside mitochondria in germ plasm of *Drosophila* embryos. *Proc Natl Acad Sci U S A* 98: 9133–9138.
- Amikura R, Sato K, Kobayashi S (2005) Role of mitochondrial ribosome-dependent translation in germline formation in *Drosophila* embryos. *Mech Develop* 122: 1087–1093.
- Andersson SGE, Zomorodipour A, Andersson JO, Sicheritz-Pontén T, Alsmark UCM, Podowski RM, Näslund AK, Eriksson A, Winkler HH, Kurland CG (1998) The genome sequence of *Rickettsia prowazekii* and the origin of Mitochondria. *Nature* 396: 133–143.
- Ashley MV, Laipis PJ, Hauswirth WW (1989) Rapid segregation of heteroplasmic bovine mitochondria. *Nucleic Acids Res* 17:7325–7331.
- Bayrer JR, Zhang W, Weiss MA (2005) Dimerization of Doublesex Is Mediated by a Cryptic Ubiquitin-associated Domain Fold – Implications for Sex-Specific Gene Regulation. *J Biol Chem* 280: 32989–32996.
- Becalska AN, Gavis EG (2010) Bazooka regulates microtubule organization and spatial restriction of germ plasm assembly in the *Drosophila* oocyte. *Dev Biol* 340: 528–538.
- Beier CL, Horn M, Michel R, Schweikert M, Görtz H-D, Wagner M (2002) The Genus *Caedibacter* Comprises Endosymbionts of *Paramecium* spp. Related to the *Rickettsiales*

- (*Alphaproteobacteria*) and to *Francisella tularensis* (*Gammaproteobacteria*). *Appl Environ Microbiol* 68: 6043–6050.
- Bermejo-Alvarez P, Rizosa D, Rathb D, Lonergan P, Gutierrez-Adana A (2010) Sex determines the expression level of one third of the actively expressed genes in bovine blastocysts. *Proc Natl Acad Sci U S A* 107: 3394–3399.
- Bernstein E, Kim SY, Carmell MA, Murchison EP, Alcorn H, Li MZ, Mills AA, Elledge SJ, Anderson KV, Hannon GJ (2003) Dicer is essential for mouse development. *Nat Genet* 35: 215–217.
- Bieliavsky N, Geuskens M (1990) Interblastomeric plasma membrane formation during cleavage of *Xenopus laevis* embryos. *J Submicrosc Cytol Pathol* 22: 445–457.
- Birky CW Jr (2001) The inheritance of genes in mitochondria and chloroplasts: laws, mechanisms, and models. *Annu Rev Genet* 35: 125–148.
- Boldogh IR, Pon LA (2006) Interactions of mitochondria with the actin cytoskeleton. *Biochimica et Biophysica Acta* 1763: 450–462.
- Boore JL (1999) Animal mitochondrial genomes. *Nucl Acids Res* 27: 1767–1780.
- Breton S, Burger G, Stewart DT, Blier PU (2006) Comparative analysis of gender-associated complete mitochondrial genomes in marine mussels (*Mytilus* spp.). *Genetics* 172: 1107–1119.
- Breton S, Beaupre HD, Stewart DT, Hoeh WR, Blier PU (2007) The unusual system of doubly uniparental inheritance of mtDNA: isn't one enough? *Trends Genet* 23: 465–474.
- Breton S, Doucet-Beaupré H, Stewart DT, Piontkivska H, Karmakar M, Bogan AE, Blier PU, Hoeh WR (2009) Comparative mitochondrial genomics of freshwater mussels (Bivalvia: Unionoida) with Doubly Uniparental Inheritance of mtDNA: gender-specific Open Reading Frames and putative origins of replication. *Genetics* 183: 1575–1589.

- Breton S, Ghiselli F, Passamonti M, Milani L, Stewart DT, Hoeh WR (2011b) Evidence for a Fourteenth mtDNA-Encoded Protein in the Female-Transmitted mtDNA of Marine Mussels (Bivalvia: Mytilidae) PLoS ONE, 6(4): e19365.
- Breton S, Stewart DT, Shepardson S, Trdan RJ, Bogan AE, Chapman EG, Ruminas AJ, Piontkivska H, Hoeh WR (2011a) Novel Protein Genes in Animal mtDNA: A New Sex Determination System in Freshwater Mussels (Bivalvia: Unionoida)? Mol Biol Evol 28: 1645–1659.
- Brooks SA (2010) Functional interactions between mRNA turnover and surveillance and the ubiquitin proteasome system. RNA, doi: 10.1002/wrna.11
- Burzynski A, Zbawicka M, Skibinski DOF, Wenne R (2003) Evidence for recombination of mtDNA in the marine mussel *Mytilus trossulus* from the Baltic. Mol Biol Evol 20: 388–392.
- Cai S, Weaver LN, Ems-McClung SC, Walczak CE (2010) Proper Organization of Microtubule Minus Ends Is Needed for Midzone Stability and Cytokinesis. Curr Biol 20: 880–885.
- Cameron SL, Johnson KP, Whiting MF (2007) The mitochondrial genome of the screamer louse *Bothriometopus* (Phthiraptera: Ischnocera): Effects of extensive gene rearrangements on the evolution of the genome. J Mol Evol 65: 589–604.
- Cao L, Kenchington E, Zouros E (2004) Differential segregation patterns of sperm mitochondria in embryos of the blue mussel (*Mytilus edulis*). Genetics 166: 883–894.
- Cao L, Shitara H, Horii T, Nagao Y, Imai H, Abe K, Hara T, Hayashi J-I, Yonekawa H (2007) The mitochondrial bottleneck occurs without reduction of mtDNA content in female mouse germ cells. Nat Genet 39: 386–390.

- Cao L, Ort BS, Mizi A, Pogson G, Kenchington E, Zouros E, Rodakis GC (2009) The control region of maternally and paternally inherited mitochondrial genomes of three species of the sea mussel genus *Mytilus*. *Genetics* 181: 1045–1056.
- Castrillon DH, Quade BJ, Wang TY, Quigley C, Crum CP (2000) The human VASA gene is specifically expressed in the germ cell lineage. *Proc Natl Acad Sci U S A* 97: 9585–9590.
- Cesari P, Pellizzato M (1990) Biology of *Tapes philippinarum*. In: *Tapes philippinarum*, biologia e sperimentazione. Ente Sviluppo Agricolo Veneto (ESAV), chapter 2.
- Chakrabarti R, Walker JM, Chapman EG, Shepardson SP, Trdan RJ, Curole JP, Watters GT, Stewart DT, Vijayaraghavan S, Hoeh WR (2007) Reproductive function for a C-terminus extended, male-transmitted cytochrome c oxidase subunit II protein expressed in both spermatozoa and eggs. *FEBS Lett* 581: 5213–5219.
- Chakrabarti R, Walker JM, Stewart DT, Trdan RJ, Vijayaraghavan S, Curole JP, Hoeh WR (2006) Presence of a unique male-specific extension of C-terminus to the cytochrome c oxidase subunit II protein coded by the male-transmitted mitochondrial genome of *Venustaconcha ellipsiformis* (Bivalvia: Unionoidea). *FEBS Lett* 580: 862–866.
- Chapman EG, Piontkivska H, Walker JM, Stewart DT, Curole JP, Hoeh WR (2008) Extreme primary and secondary protein structure variability in the chimeric male-transmitted cytochrome c oxidase subunit II protein in freshwater mussels: evidence for an elevated amino acid substitution rate in the face of domain-specific purifying selection. *BMC Evol Biol* 8: 165–181.
- Chase CD (2007) Cytoplasmic male sterility: a window to the world of plant mitochondrial-nuclear interactions. *Trends Genet* 23: 81–90.
- Chase JW, Dawid IB (1972) Biogenesis of mitochondria during *Xenopus laevis* development. *Dev Biol* 27: 504–518.
- Chuma S, Hosokawa M, Tanaka T, Nakatsuji N (2009) Ultrastructural characterization of

- spermatogenesis and its evolutionary conservation in the germline: germinal granules in mammals. *Mol Cell Endocrinol* 306: 17–23.
- Cimmino A, Calin GA, Fabbri M, Iorio MV, Ferracin M, Shimizu M, Wojcik SE, Aqeilan RI, Zupo S, Dono M, Rassenti L, Alder H, Volinia S, Liu C-G, Kipps TJ, Negrini M, Croce CM (2005) miR-15 and miR-16 induce apoptosis by targeting Bcl2. *Proc Natl Acad Sci U S A* 102: 13944–13949.
- Cogswell AT, Kenchington EL, Zouros E (2006) Segregation of sperm mitochondria in two- and four-cell embryos of the blue mussel *Mytilus edulis*: implications for the mechanism of doubly uniparental inheritance of mitochondrial DNA. *Genome* 49: 799–807.
- Conklin EG (1897) The embryology of *Crepidula*. A contribution to the cell lineage and early development of some marine gastropods. *J Morphol* 13: 1–226.
- Connallon T and Knowles LL (2005) Intergenomic conflict revealed by patterns of sex-biased gene expression. *Trends Genet* 21: 495–499.
- Cox RT, Spradling AC (2003) A Balbiani body and the fusome mediate mitochondrial inheritance during *Drosophila* oogenesis. *Development* 130: 1579–1590.
- Cree LM, Samuels DC, de Sousa Lopes SC, Rajasimha HK, Wonnapijit P, Mann JR, Dahl HH, Chinnery PF (2008) A reduction of mitochondrial DNA molecules during embryogenesis explains the rapid segregation of genotypes. *Nat Genet* 40: 249–254.
- Curole JP, Kocher TD (2002) Ancient sex-specific extension of the cytochrome c oxidase II gene in bivalves and the fidelity of doubly-uniparental inheritance. *Mol Biol Evol* 19: 1323–1328.
- Curole JP, Kocher TD (2005) Evolution of a unique mitotype-specific protein-coding extension of the cytochrome c oxidase II gene in freshwater mussels (Bivalvia: Unionoida). *J Mol Evol* 61: 381–389.

- Dalziel AC, Stewart DT (2002) Tissue-specific expression of male- transmitted mitochondrial DNA and its implications for rates of molecular evolution in *Mytilus* mussels (Bivalvia: Mytilidae). *Genome* 45: 348–355.
- Davison A (2006) The ovotestis: an underdeveloped organ of evolution. *BioEssays* 28: 642–650.
- Devauchelle N (1990) Sexual development and maturity of *Tapes philippinarum*. In: *Tapes philippinarum*, biologia e sperimentazione. Ente Sviluppo Agricolo Veneto (ESAV), chapter 3.
- Deveraux QL, Reed JC (1999) IAP family proteins — suppressors of apoptosis. *Genes Dev* 13: 239–252.
- Ding D, Whittaker KL, Lipshitz HD (1994) Mitochondrially Encoded 16S Large Ribosomal RNA is Concentrated in the Posterior Polar Plasm of Early *Drosophila* Embryos but is not Required for Pole Cell Formation. *Dev Biol* 163: 503–515.
- Diz AP, Dudley E, MacDonald BW, Pina B, Kenchington ELR, Zouros E, Skibinski DOF (2009) Genetic variation underlying protein expression in eggs of the marine mussel *Mytilus edulis*. *Mol Cell Proteomics* 8: 132–144.
- Doucet-Beaupré H, Breton S, Chapman EG, Blier PU, Bogan AE, Stewart DT, Hoeh WR (2010) Mitochondrial phylogenomics of the Bivalvia (Mollusca): Searching for the origin and mitogenomic correlates of doubly uniparental inheritance of mtDNA. *BMC Evol Biol* 10:50.
- Duckett CS, Li F, Wang Y, Tomaselli KJ, Thompson CB, Armstrong RC (1998) Human IAP-like protein regulates programmed cell death downstream of Bcl-x and L cytochrome *c*. *Mol Cell Biol* 18: 608–615.
- Dumollard R, Duchen M, Carroll J (2007) The role of mitochondrial function in the oocyte and embryo. *Curr Top Dev Biol* 77:21–49.

- Ebbert MA (1993) Endosymbiotic sex ratio distorters in insects and mites. In: Wrensh DL, Ebbert MA, editors. *Evolution and Diversity of Sex Ratio in Insects and Mites*. New York: Chapman Hall. pp. 150–191.
- Eddy EM (1975) Germ plasm and the differentiation of the germ cell line. *Int Rev Cytol* 43: 229–281.
- Eggert US, Mitchison TJ, Field CM (2006) Animal Cytokinesis: From Parts List to Mechanisms. *Annu Rev Biochem* 75: 543–66.
- Endo K, Noguchi Y, Ueshima R, Jacobs HT (2005) Novel repetitive structures, deviant protein-encoding sequences and unidentified ORFs in the mitochondrial genome of the brachiopod *Lingula anatine*. *J M Evol* 61: 36–53.
- Erkan M, Sousa M (2002) Fine structural study of the spermatogenic cycle in *Pitar rudis* and *Chamelea gallina* (Mollusca, Bivalvia, Veneridae) *Tissue Cell* 34: 262–272.
- Extavour CG, Akam M (2003) Mechanisms of germ cell specification across the metazoans: epigenesis and preformation. *Development* 130: 5869–5884.
- Fabioux C, Huvet A, Lelong C, Robert R, Pouvreau S, Daniel JY, Minguant C, Le Pennec M (2004b) Oyster *vasa*-like gene as a marker of the germline cell development in *Crassostrea gigas*. *Biochem Bioph Res Co* 320: 592–598.
- Fabioux C, Pouvreau S, Le Roux F, Huvet A (2004a) The oyster *vasa*-like gene: a specific marker of the germline in *Crassostrea gigas*. *Biochem Bioph Res Co* 315: 897–904.
- Fernandes Boaro Martins MR, de Carvalho Pinto e Silva JR (2005) Ultrastructural Aspects of Spermatids in Isogenic Black Mouse C57BL6J - Aspectos Ultraestructurales de las Espermátidas en el Ratón Negro Isogénico C57BL6. *Int J Morphol* 23: 323–328.
- Flot J-F, Tillier A (2007) The mitochondrial genomes of *Pocillopora* (Cnidaria: Scleractinia) contains two variable regions: The putative D-loop and a novel ORF of unknown function. *Gene* 401: 80–87.

- Fraser AG, James C, Evan GI, Hengartner MO (1999) *Caenorhabditis elegans* inhibitor of apoptosis protein (IAP) homologue BIR-1 plays a conserved role in cytokinesis. *Curr Biol* 9: 292–301.
- Fujiwara Y, Hatano K, Hirabayashi T, Miyazaki J-I (1994) Ubiquitin C-terminal hydrolase as a putative factor involved in sex differentiation of fish (temperate wrasse, *Halichoeres poecilopterus*). *Differentiation* 56: 13–20.
- Garesse R, Vallejo CG (2001) Animal mitochondrial biogenesis and function: a regulatory cross-talk between two genomes. *Gene* 263: 1–16.
- Garrido-Ramos MA, Stewart DT, Sutherland BW, Zouros E (1998) The distribution of male-transmitted mitochondrial DNA types in somatic tissues of blue mussels: implications for the operation of doubly uniparental inheritance of mitochondrial DNA. *Genome* 41: 818–824.
- Geller JB, Carlton JT, Powers DA (1993) Interspecific and intrapopulation variation in mitochondrial ribosomal DNA sequences of *Mytilus* spp. (Bivalvia: Mollusca). *Mol Mar Biol Biotechnol* 2: 44–50.
- Ghiselli F, Milani L, Chang PL, Hedgecock D, Davis JP, Nuzhdin SV, Passamonti M (2012) *De Novo* Assembly of the Manila clam *Ruditapes philippinarum* Transcriptome Provides New Insights into Expression Bias, Mitochondrial Doubly Uniparental Inheritance and Sex Determination. *Mol Biol Evol*, doi: 10.1093/molbev/msr248
- Ghiselli F, Milani L, Passamonti M (2011) Strict sex-specific mtDNA segregation in the germline of the DUI species *Venerupis philippinarum* (Bivalvia Veneridae). *Mol Biol Evol* 28: 949–961.
- Gilbert SF (2000) *Developmental Biology*. 6th edition. Sunderland (MA): Sinauer Associates.

- Ginalski K, Rychlewski L, Baker D, Grishin NV (2004) Protein structure prediction for the male-specific region of the human Y chromosome. *Proc Natl Acad Sci U S A* 101: 2305–2310.
- Giribet G, Wheeler WC (2002) On bivalve phylogeny: a high-level phylogeny of the mollusk class Bivalvia based on a combined analysis of morphology and DNA sequence data. *Inv Biol* 121: 271–324.
- Gissi C, Iannelli F, Pesole G (2008) Evolution of the mitochondrial genome of Metazoa as exemplified by comparison of congeneric species. *Heredity* 101: 301–320.
- Glotzer M (2009) The 3Ms of central spindle assembly: microtubules, motors and MAPs. *Nat Rev Mol Cell Bio* 10: 9–20.
- Gogusev J, Duchambon P, Hory B, Giovannini M, Goureau Y, Sarfati E, Drüeke TB (1997) Depressed expression of calcium receptor in parathyroid gland tissue of patients with hyperparathyroidism. *Kidney Int* 51: 328–336; doi:10.1038/ki.1997.41
- Gönczy P, Echeverri G, Oegema K, Coulson A, Jones SJ, Copley RR, Duperon J, Oegema J, Brehm M, Cassin E, Hannak E, Kirkham M, Pichler S, Flohrs K, Goessen A, Leidel S, Alleaume A-M, Martin C, Özlü N, Bork P, Hyman AA (2000) Functional genomic analysis of cell division in *C. elegans* using RNAi of genes on chromosome III. *Nature* 408: 331–336.
- Gustafson EA, Wessel GM (2010) Vasa genes: emerging roles in the germ line and in multipotent cells. *Bioessays* 32: 626–637.
- Hansen D, Pilgrim D (1999) Sex and the single worm: sex determination in the nematode *C. elegans*. *Mech Dev* 83: 3–15.
- Hay B, Ackerman L, Barbel S, Jan LY, Jan YN (1988a) Identification of a component of *Drosophila* polar granules. *Development* 103: 625–640.

- Hay B, Jan LY, Jan YN (1988b) A protein component of *Drosophila* polar granules is encoded by *vasa* and has extensive sequence similarity to ATP-dependent helicases. *Cell* 55: 577–587.
- Hejnal A (2010) A Twist in Time—The Evolution of Spiral Cleavage in the Light of Animal Phylogeny. *Integr Comp Biol* 50: 695–706.
- Hertig AT, Adams EC (1967) Studies on the human oocyte and its follicle. I. Ultrastructural and Histochemical Observations on the Primordial Follicle Stage. *J Cell Biol* 34: 647–675.
- Hicke L (2001) Protein regulation by monoubiquitin. *Nature Rev Mol Cell Biol* 2: 195–201.
- Hinds MG, Norton RS, Vaux DL, Day CL (1999) Solution structure of a baculoviral inhibitor of apoptosis (IAP) repeat. *Nature Struct Biol* 6: 648–651.
- Hodgkin J (1987) A genetic analysis of the sex-determining gene, *tra-1*, in the nematode *Caenorhabditis elegans*. *Genes Dev* 1: 731–745.
- Hoeh WR, Stewart DT, Guttman SI (2002) High fidelity of mitochondrial genome transmission under the doubly uniparental mode of inheritance in freshwater mussels (Bivalvia: Unionoidea). *Evolution* 56: 2252–2261.
- Hoeh WR, Stewart DT, Sutherland BW, Zouros E (1996) Multiple origins of gender—associated mitochondrial DNA lineages in bivalves (Mollusca: Bivalvia). *Evolution* 50: 2276–2286.
- Hunter S, Apweiler R, Attwood TK, Bairoch A, Bateman A, Binns D, Bork B, Das U, Daugherty L, Duquenne L, Finn RD, Gough J, Haft D, Hulo N, Kahn D, Kelly E, Laugraud A, Letunic I, Lonsdale D, Lopez R, Madera M, Maslen J, McAnulla C, McDowall J, Mistry J, Mitchell A, Mulder N, Natale D, Orengo C, Quinn AF, Selengut JD, Sigrist CJA, Thimma M, Thomas PD, Valentin F, Wilson D, Wu CH, Yeats C (2009) InterPro: the integrative protein signature database. *Nucleic Acids Res* 37 (Database Issue), D211–D215.

- Hurst GDD, Hurst LD, Majerus MEN (1997) Cytoplasmic sex-ratio distorters. In: O'Neil SL, Hoffmann AA, Werren JH, editors. *Influential Passengers: Inherited Microorganisms and Invertebrate Reproduction*. UK: Oxford University Press. pp. 125–154.
- Iida T, Kobayashi S (1998) Essential role of mitochondrially encoded large rRNA for germ-line formation in *Drosophila* embryos. *Proc Natl Acad Sci U S A* 95: 11274–11278.
- Ikenishi K (1998) Germ Plasm in *Caenorhabditis elegans*, *Drosophila* and *Xenopus*. *Develop. Growth Differ* 40: 1–10.
- Illmensee K, Mahowald AP, Loomis MR (1976) The ontogeny of germ plasm during oogenesis in *Drosophila*. *Dev Biol* 49: 40–65.
- Isaeva VV, Reunov AA (2001) Germ Plasm and Germ-line Cell Determination: The Role of Mitochondria. *Russ J Mar Biol* 27: S8–S14.
- Janke C, Bulinski JC (2011) Post-translational regulation of the microtubule cytoskeleton: mechanisms and functions. *Nat Rev Mol Cell Biol* 12: 773–86.
- Joazeiro CA, Weissman AM (2000) RING finger proteins: mediators of ubiquitin ligase activity. *Cell* 102: 549–552.
- Kakoi S, Kin K, Miyazaki K, Wada H (2008) Early Development of the Japanese Spiny Oyster (*Saccostrea kegaki*): Characterization of Some Genetic Markers. *Zool Sci* 25: 455–464.
- Kaplan J, Calame K (1997) The ZIN/POZ domain of ZF5 is required for both transcriptional activation and repression. *Nucleic Acids Res* 25: 1108–1116.
- Katayama M, Zhong Z, Lai L, Sutovsky P, Prather RS, Schatten H (2006) Mitochondrial distribution and microtubule organization in fertilized and cloned porcine embryos: Implications for developmental potential. *Dev Biol* 299: 206–220.

- Kenchington E, MacDonald B, Cao L, Tsagkarakis D, Zouros E (2002) Genetics of mother-dependent sex ratio in blue mussels (*Mytilus* spp.) and implications for doubly uniparental inheritance of mitochondrial DNA. *Genetics* 161: 1579–1588.
- Kenchington EL, Hamilton L, Cogswell A, Zouros E (2009) Paternal mtDNA and Maleness Are Co-Inherited but Not Causally Linked in Mytilid Mussels. *PLoS ONE* 4:e6976.
- Khalturin K, Anton-Erxleben F, Sassmann S, Wittlieb J, Hemmrich G, Bosch TCG (2008) A novel gene family controls species-specific morphological traits in *Hydra*. *PLoS Biol* 6: e278.
- Khalturin K, Hemmrich G, Fraune S, Augustin R, Bosch TCG (2009) More than just orphans: are taxonomically-restricted genes important in evolution? *Trends Genet* 25: 404–413.
- Kloc M, Bilinski S, Chan AP, Allen LH, Zearfoss NR, Etkin LD (2001) RNA localization and germ cell determination in *Xenopus*. *Int Rev Cytol* 203: 63–91.
- Kloc M, Bilinski S, Etkin LD (2004) The Balbiani body and germ cell determinants: 150 years later. *Curr Top Dev Biol* 59: 1–36.
- Kloc M, Etkin LD (2005) RNA localization mechanisms in oocytes. *J Cell Sci* 118: 269–282.
- Kloc M, Larabell C, Chan AP, Etkin LD (1998) Contribution of METRO pathway localized molecules to the organization of the germ cell lineage. *Mech Dev* 75: 81–93.
- Knaut H, Pelegri F, Bohmann K, Schwarz H, Nuesslein-Volhard C (2000) Zebrafish vasa RNA but not its protein is a component of the germ plasm and segregates asymmetrically before germline specification. *J Cell Biol* 149: 875–888.
- Kobayashi S, Amikura R, Mukai M (1998) Localization of Mitochondrial RNA in Germ Plasm of *Xenopus* Embryos. *Curr Biol* 8: 1117–1120.
- Kobayashi S, Amikura R, Okada M (1993) Presence of Mitochondrial Large Ribosomal RNA Outside Mitochondria in Germ Plasm of *Drosophila melanogaster*. *Science* 260: 1521–1524.

- Kobayashi T, Kajiura-Kobayashi H, Nagahama Y (2000) Differential expression of vasa homologue gene in the germ cells during oogenesis and spermatogenesis in a teleost fish, tilapia, *Oreochromis niloticus*. *Mech Dev* 99: 139–142.
- Koebornick K, Pieler T (2002) Gli-type zinc finger proteins as bipotential transducers of Hedgehog signaling. *Differentiation* 70: 69–76.
- Kogo N, Tazaki A, Kashino Y, Morichika K, Orii H, Mochii M, Watanabe K (2011) Germ-line mitochondria exhibit suppressed respiratory activity to support their accurate transmission to the next generation. *Dev Biol* 349: 462–469.
- Komiya T, Itoh K, Ikenishi K, Furusawa M (1994) Isolation and characterization of a novel gene of the DEAD Box protein family which is specifically expressed in germ cell of *Xenopus laevis*. *Dev Biol* 162: 354–363.
- Kondo R, Satta Y, Matsuura ET, Ishiwa H, Takahata N, Chigusa SI (1990) Incomplete maternal transmission of mitochondrial DNA in *Drosophila*. *Genetics* 126: 657–663.
- Kotaja N, Bhattacharyya SN, Jaskiewicz L, Kimmins S, Parvinen M, Filipowicz W, Sassone-Corsi P (2006) The chromatoid body of male germ cells: Similarity with processing bodies and presence of Dicer and microRNA pathway components. *Proc Natl Acad Sci U S A* 103: 2647–2652.
- Kotaja N, Sassone-Corsi P (2007) The chromatoid body: a germ-cell-specific RNA-processing centre. *Nat Rev Mol Cell Bio* 8: 85–90.
- Kranz AM, Tollenaere A, Norris BJ, Degnan BM, Degnan SM (2010) Identifying the Germline in an Equally Cleaving Mollusc: *Vasa* and *Nanos* Expression During Embryonic and Larval Development of the Vetigastropod *Haliothis asinina*. *J Exp Zool Part B* 314: 1–13.
- Kulkarni M, Smith HE (2008) E1 Ubiquitin-Activating Enzyme UBA-1 Plays Multiple Roles throughout *C. elegans* Development. *PLoS Genetics* 4: e1000131.

- Kuznicki KA, Smith PA, Leung-Chiu WM, Estevez AO, Scott HC, Bennett KL (2000) Combinatorial RNA interference indicates GLH-4 can compensate for GLH-1; these two P granule components are critical for fertility in *C. elegans*. *Development* 127: 2907–2916.
- Kvist L, Martens J, Nazarenko AA, Orell M (2003) Paternal leakage of mitochondrial DNA in the great tit (*Parus major*). *Mol Biol Evol* 20: 243–247.
- Laemmli UK (1970) Cleavage of structural proteins during the assembly of the head of bacteriophage T4. *Nature* 227: 680–685.
- Laipis PJ, Van de Walle MJ, Hauswirth WW (1988) Unequal partitioning of bovine mitochondrial genotypes among siblings. *Proc Natl Acad Sci U S A*. 85: 8107–8110.
- Lasko F, Ashburner M (1988) The product of the *Drosophila* gene *vasa* is very similar to eucaryotic initiation factor-4A. *Nature* 335: 611–617.
- Lee T, Ó Foighil D (2004) Hidden Floridian biodiversity: mitochondrial and nuclear gene trees reveal four cryptic species within the scorched mussel, *Brachidontes exustus*, species complex. *Mol Ecol* 13: 3527–3542.
- Lerit DA, Gavis ER (2011) Transport of Germ Plasm on Astral Microtubules Directs Germ Cell Development in *Drosophila*. *Curr Biol* 21: 439–448.
- Li F, Ambrosini G, Chu EY, Plescia J, Tognin S, Marchisio PC, Altieri DC (1998) Control of apoptosis and mitotic spindle checkpoint by survivin. *Nature* 396: 580–584.
- Li X, Carthew RW (2005) A microRNA mediates EGF receptor signaling and promotes photoreceptor differentiation in the *Drosophila* eye. *Cell* 123: 1267–1277.
- Li X, Yang Y, Ashwell JD (2002) TNF-RII and c-IAP1 mediate ubiquitination and degradation of TRAF2. *Nature* 416: 345–347.
- Linnen JM, Bailey CP, Weeks DL (1993) Two related localized mRNAs from *Xenopus laevis* encode ubiquitin-like fusion proteins. *Gene* 128: 181–188.

- Liu H-P, Mitton JB, Wu SK (1996) Paternal mitochondrial DNA differentiation far exceeds maternal DNA and allozyme differentiation in the fresh water mussel *Anodonta grandis grandis*. *Evolution* 50: 952–957.
- Longo FJ (1987) *Fertilization*. New York: Chapman and Hall.
- MacArthur H, Houston DW, Bubunenko M, Mosquera L, King ML (2000) DEADSouth is a germ plasm specific DEAD-box RNA helicase in *Xenopus* related to eIF4A. *Mech Dev* 95: 291–295.
- Maeda I, Kohara Y, Yamamoto M, Sugimoto A (2001) Large-scale analysis of gene function in *Caenorhabditis elegans* by high-throughput RNAi. *Curr Biol* 11: 171–176.
- Matova N, Cooley L (2001) Comparative Aspects of Animal Oogenesis. *Dev Biol* 231: 291–320.
- Matsumoto L, Kasamatsu H, Piko L, Vinograd J (1974) Mitochondrial DNA replication in sea urchin oocytes. *J Cell Biol* 63: 146–159.
- Maurizii MG, Cavaliere V, Gamberi C, Lasko P, Gargiulo G, Taddei C (2009) Vasa protein is localized in the germ cells and in the oocyte-associated pyriform follicle cells during early oogenesis in the lizard *Podarcis sicula*. *Dev Genes Evol*, doi: 10.1007/s00427-009-0295-7
- McIntyre LM, Bono LM, Genissel A, Westerman R, Junk D, Telonis-Scott M, Harshman L, Wayne ML, Kopp A, Nuzhdin SV (2006) Sex-specific expression of alternative transcripts in *Drosophila*. *Genome Biol*, 7:R79.
- Mignotte F, Tourte M, Mounolou JC (1987) Segregation of mitochondria in the cytoplasm of *Xenopus* vitellogenic oocytes. *Cell* 60: 97–102.
- Milani L, Ghiselli F, Passamonti M (2012) Sex-linked mitochondrial behavior during early embryo development in *Ruditapes philippinarum* (Bivalvia Veneridae) a species with the Doubly Uniparental Inheritance (DUI) of mitochondria. *J Exp Zool Part B*, in press.
- Miller LK (1999) An exegesis of IAPs: salvation and surprises from BIR motifs. *Trends Cell*

- Biol 9: 323–328.
- Mochizuki K, Nishimiya-Fujisawa C, Fujisawa T (2001) Universal occurrence of the vasa-related genes among metazoans and their germline expression in *Hydra*. *Dev Genes Evol* 211: 299–308.
- Mock KE, Brim-Box JC, Miller MP, Downing ME, Hoeh WR (2004) Genetic diversity and divergence among freshwater mussel (*Anodonta*) populations in the Bonneville Basin of Utah. *Mol Ecol* 13: 1085–1098.
- Monchois V, Abergel C, Sturgis J, Jeudy S, Claverie J-M (2001) *Escherichia coli* ykfE ORFan gene encodes a potent inhibitor of C-type lysozyme. *J Biol Chem* 276: 18437–18441.
- Mortazavi A, Williams BA, McCue K, Schaeffer L, Wold B (2008) Mapping and quantifying mammalian transcriptomes by RNA-seq. *Nat Methods* 5: 621–628.
- Mukherji S, Ebert MS, Zheng GX, Tsang JS, Sharp PA, van Oudenaarden A (2011) MicroRNAs can generate thresholds in target gene expression. *Nat Genet*, 43: 854–859.
- Nakao H (1999) Isolation and characterization of a *Bombyx* vasa-like gene. *Dev Genes Evol* 209: 316–321.
- Negri I, Franchini A, Gonella E, Daffonchio D, Mazzoglio PJ, Mandrioli M, Alma A (2009) Unravelling the *Wolbachia* evolutionary role: the reprogramming of the host genomic imprinting. *Proc R Soc B* 276: 2485–2491.
- Notredame C, Abergel C (2003) Using T-Coffee to assess the reliability of multiple sequence alignments. In: Andrade MA, editor. *Bioinformatics and Genomes*. Wymondham, UK: Horizon Scientific Press. pp. 27–49.
- Notredame C, Higgins DG, Heringa J (2000) T-Coffee: A novel method for fast and accurate multiple sequence alignment. *J Mol Biol* 302: 205–217.

- Obata M, Kamiya C, Kawamura K, Komaru A (2006) Sperm mitochondrial DNA transmission to both male and female offspring in the blue mussel *Mytilus galloprovincialis*. *Dev Growth Differ* 48: 253–261.
- Obata M, Komaru A (2005) Specific location of sperm mitochondria in mussel *Mytilus galloprovincialis* zygotes stained by MitoTracker. *Dev Growth Differ* 47: 255–263.
- Obata M, Sano N, Kimata S, Nagasawa K, Yoshizaki G, Komaru A (2010) The proliferation and migration of immature germ cells in the mussel, *Mytilus galloprovincialis*: observation of the expression pattern in the *M. galloprovincialis vasa*-like gene (*Myvlg*) by in situ hybridization. *Dev Genes Evol* 220: 139–149.
- Obata M, Shimizu M, Sano N, Komaru A (2008) Maternal Inheritance of Mitochondrial DNA (mtDNA) in the Pacific oyster (*Crassostrea gigas*): a Preliminary Study Using mtDNA Sequence Analysis with Evidence of Random Distribution of MitoTracker-Stained Sperm Mitochondria in Fertilized Eggs. *Zool Sci* 25: 248–254.
- Ogawa M, Amikura R, Akasaka K, Kinoshita T, Kobayashi S, Shimada H (1999) Asymmetrical Distribution of Mitochondrial rRNA into Small Micromeres of Sea Urchin Embryos. *Zool Sci* 16: 445–451.
- Olivo PD, Van de Walle MJ, Laipis PJ, Hauswirth WW (1983) Nucleotide sequence evidence for rapid genotypic shifts in the bovine mitochondrial DNA D-loop. *Nature* 306: 400–402.
- Parvinen M (2005) The chromatoid body in spermatogenesis. *Int J Androl* 28: 189–201.
- Passamonti M (2007) An unusual case of gender-associated mitochondrial DNA heteroplasmy: the mytilid *Musculista senhousia* (Mollusca Bivalvia). *BMC Evol Biol* 7 Suppl 2:S7.
- Passamonti M, Ghiselli F (2009) Doubly Uniparental Inheritance: Two Mitochondrial Genomes, One Precious Model for Organelle DNA Inheritance and Evolution. (Review). *DNA Cell Biol* 28: 79–89.

- Passamonti M, Scali V (2001) Gender-associated mitochondrial DNA heteroplasmy in the venerid clam *Tapes philippinarum* (Mollusca Bivalvia). *Curr Genet* 39: 117–124.
- Paweletz N (2001) Walther Flemming: pioneer of mitosis research. *Nature Rev Mol Cell Biol* 2: 72–75.
- Peruquetti RL, Taboga SR, de Souza Santos LR, de Oliveira C, de Azeredo-Oliveira MTV (2011) Nucleolar cycle and chromatoid body formation: Is there a relationship between these two processes during spermatogenesis of *Dendropsophus minutus* (Amphibia, Anura)? *Micron* 42: 87–96.
- Piano F, Schetter AJ, Mangone M, Stein L, Kempfues KJ (2000) RNAi analysis of genes expressed in the ovary of *Caenorhabditis elegans*. *Curr Biol* 10: 1619–1622.
- Pickart CM (2000) Ubiquitin biology: an old dog learns an old trick. *Nature Cell Biol* 2: E139–E141.
- Piko L, Taylor KD (1987) Amounts of mitochondrial DNA and abundance of some mitochondrial gene transcripts in early mouse embryos. *Dev Biol* 123: 364–374.
- Rajagopalan S, Balasubramanian MK (2002) *Schizosaccharomyces pombe* Bir1p, a nuclear protein that localizes to kinetochores and the spindle midzone, is essential for chromosome condensation and spindle elongation during mitosis. *Genetics* 160: 445–456.
- Rawson PD, Hilbish TJ (1995) Evolutionary relationships among the male and female mitochondrial DNA lineages in the *Mytilus edulis* species complex. *Mol Biol Evol* 12: 893–901.
- Raz E (2000) The function and regulation of *vasa*-like genes in germ-cell development. *Genome Biol* 1: REVIEWS1017.1–1017.6
- Ren J, Shi M, Liu R, Yang Q-H, Johnson T, Skarnes WC, Du C (2005) The Birc6 (Bruce) gene regulates p53 and the mitochondrial pathway of apoptosis and is essential for mouse embryonic development. *Proc Natl Acad Sci U S A* 102: 565–570.

- Reunov A (2006) Structures related to the germ plasm in mouse. *Zygote* 14: 231–238.
- Reunov A, Isaeva V, Au D, Wu R (2000) Nuage constituents arising from mitochondria: Is it possible? *Develop Growth Differ* 42: 139–143.
- Rinn JL, Snyder M (2005) Sexual dimorphism in mammalian gene expression. *Trends Genet* 21: 298–305.
- Rongo C, Lehmann R (1996) Regulated synthesis, transport and assembly of the *Drosophila* germ plasm, *Trends Genet* 12: 102–109.
- Russell L, Frank B (1978) Ultrastructural characterization of nuage in spermatocytes of the rat testis. *Anat Rec* 190: 79–97.
- Saavedra C, Reyero MI, Zouros E (1997) Male-dependent doubly uniparental inheritance of mitochondrial DNA and female-dependent sex-ratio in the mussel *Mytilus galloprovincialis*. *Genetics* 145: 1073–1082.
- Saccone C, Attimonelli M, Sbisà E (1987) Structural elements highly preserved during the evolution of the D-loop-containing region in vertebrate mitochondrial DNA. *J Mol Evol* 26: 205–211.
- Saffman EE, Lasko P (1999) Germline development in vertebrates and invertebrates. *Cell Mol Life Sci* 55: 1141–1163.
- Salghetti SE, Caudy AA, Chenoweth JG, Tansey WP (2001) Regulation of transcriptional activation domain function by ubiquitin. *Science* 293: 1651–1653.
- Salvesen GS, Duckett CS (2002) IAP proteins: blocking the road to death's door. *Nat Rev Mol Cell Biol* 3: 401–410.
- Schaeren-Wiemers N, Gerfin-Moser A (1993) A single protocol to detect transcripts of various types and expression levels in neural tissue and cultured cells: in situ hybridization using digoxigenin-labelled cRNA probes. *Histochemistry* 100: 431–440.

- Schmitz G, Heimerl S, Langmann T (2004) Zinc finger protein ZNF202 structure and function in transcriptional control of HDL metabolism. *Curr Opin Lipidol* 15: 199–208.
- Shang P, Baarends WM, Hoogerbrugge J, Ooms MP, van Cappellen WA, de Jong AAW, Dohle GR, van Eenennaam H, Gossen JA, Grootegoed JA (2010) Functional transformation of the chromatoid body in mouse spermatids requires testis-specific serine/threonine kinases. *J Cell Sci* 123: 331–339.
- Shao Z, Shannon G, Chaga OY, Lavrov DV (2006) Mitochondrial genome of the moon jelly *Aurelia aurita* (Cnidaria, Scyphozoa): A linear DNA molecule encoding a putative DNA-dependant DNA polymerase. *Gene* 381: 92–101.
- Shimada M, Kanematsu K, Tanaka K, Yokosawa H, Kawahara H (2006) Proteasomal ubiquitin receptor RPN-10 controls sex determination in *Caenorhabditis elegans*. *Mol Biol Cell* 17: 5356–5371.
- Shitara H, Hayashi JI, Takahama S, Kaneda H, Yonekawa H (1998) Maternal inheritance of mouse mtDNA in interspecific hybrids: segregation of the leaked paternal mtDNA followed by the prevention of subsequent paternal leakage. *Genetics* 148: 851–857.
- Shoubridge EA, Wai T (2007) Mitochondrial DNA and the mammalian oocyte. *Curr Top Dev Biol* 77: 87–111.
- Silke J, Vaux DL (2001) Two kinds of BIR-containing protein — inhibitors of apoptosis, or required for mitosis. *J Cell Sci* 114: 1821–1827.
- Skibinski DO, Gallagher C, Beynon CM (1994a) Mitochondrial DNA inheritance. *Nature* 368: 817–818.
- Skibinski DO, Gallagher C, Beynon CM (1994b) Sex-limited mitochondrial DNA transmission in the marine mussel *Mytilus edulis*. *Genetics* 138: 801–809.
- Skop AR, Liu H, Yates J III, Meyer BJ, Heald R (2004) Dissection of the Mammalian Midbody Proteome Reveals Conserved Cytokinesis Mechanisms. *Science* 305: 61–66.

- Sluijter JPG, van Mil A, van Vliet P, Metz CHG, Liu J, Doevendans PA, Goumans M-J (2010) MicroRNA-1 and -499 regulate differentiation and proliferation in human-derived cardiomyocyte progenitor cells. *Arterioscler Thromb Vasc Biol* 30: 859–868.
- Smiraglia DJ, Kulawiec M, Bistulfi GL, Gupta SG, Singh KK (2008) A novel role for mitochondria in regulating epigenetic modification in the nucleus. *Cancer Biol Ther* 7: 1182–1190.
- Söderström KO, Parvinen M (1976) Transport of material between the nucleus, the chromatoid body and the Golgi complex in the early spermatids of the rat. *Cell Tissue Res* 168: 335–342.
- Speliotes EK, Uren A, Vaux D, Horvitz HR (2000) The survivin-like *C. elegans* BIR-1 protein acts with the Aurora-like kinase AIR-2 to affect chromosomes and the spindle midzone. *Mol Cell* 6: 211–223.
- Starostina NG, Lim JM, Schvarzstein M, Wells L, Spence AM, Kipreos ET (2007) A CUL-2 ubiquitin ligase containing three FEM proteins degrades TRA-1 to regulate *C. elegans* sex determination. *Dev Cell* 13: 127–139.
- Sun C, Cai M, Gunasekera AH, Meadows RP, Wang H, Chen J, Zhang H, Wu W, Xu N, Ng SC, Fesik SW (1999) NMR structure and mutagenesis of the inhibitor-of-apoptosis protein XIAP. *Nature* 401: 818–822.
- Sun J, Shang X, Tian Y, Zhao W, He Y, Chen K, Cheng H, Zhou R (2008) Ubiquitin C-terminal hydrolase-L1 (Uch-L1) correlates with gonadal transformation in the rice field eel. *FEBS J* 275: 242–249.
- Sutherland B, Stewart DT, Kenchington E, Zouros E (1998) The fate of paternal mitochondrial DNA in developing female mussels, *Mytilus edulis*: implications for the mechanism of doubly uniparental inheritance of mitochondrial DNA. *Genetics* 148: 341–347.

- Sutovsky P (2003) Ubiquitin-dependent proteolysis in mammalian spermatogenesis, fertilization, and sperm quality control: killing three birds with one stone. *Microsc Res Tech* 61: 88–102.
- Sutovsky P, Moreno RD, Ramalho-Santos J, Dominko T, Simerly C, Schatten G (1999) Ubiquitin tag for sperm mitochondria. *Nature* 402: 371–372.
- Sutovsky P, Moreno RD, Ramalho-Santos J, Dominko T, Simerly C, Schatten G (2000) Ubiquitinated sperm mitochondria, selective proteolysis, and the regulation of mitochondrial inheritance in mammalian embryos. *Biol Reprod* 63: 582–590.
- Sutovsky P, Navara CS, Schatten G (1996) Fate of the Sperm Mitochondria, and the Incorporation, Conversion, and Disassembly of the Sperm Tail Structures during Bovine Fertilization. *Biol Reprod* 55: 1195–1205.
- Swartz SZ, Chan XY, Lambert JD (2008) Localization of Vasa mRNA during early cleavage of the snail *Ilyanassa*. *Dev Genes Evol* 218: 107–113.
- Theologidis I, Fodelianakis S, Gaspar MB, Zouros E (2008) Doubly uniparental inheritance (DUI) of mitochondrial DNA in *Donax trunculus* (Bivalvia: Donacidae) and the problem of its sporadic detection in Bivalvia. *Evol Int J Org Evol* 62: 959–970.
- Tourte M, Mignotte F, Mounolou JC (1984) Heterogeneous distribution and replication activity of mitochondria in *Xenopus laevis* oocytes. *Eur J Cell Biol* 34: 171–178.
- Tsang WY, Lemire BD (2002) Mitochondrial genome content is regulated during nematode development. *Biochem Biophys Res Commun* 291: 8–16.
- Tsunekawa N, Naito M, Sakai Y, Nishida T, Noce T (2000) Isolation of chicken vasa homolog gene and tracing the origin of primordial germ cells. *Development* 127: 2741–2750.
- Tyler SEB, Kimber SJ (2006) The dynamic nature of mollusc egg surface architecture and its relation to the microtubule network. *Int J Dev Biol* 50: 405–412.

- Uren AG, Beilharz T, O'Connell MJ, Bugg SJ, van Driel R, Vaux DL, Lithgow T (1999) Role for yeast inhibitor of apoptosis (IAP)- like proteins in cell division. *Proc Natl Acad Sci U S A* 96: 10170–10175.
- Uren AG, Wong L, Pakusch M, Fowler KJ, Burrows FJ, Vaux DL, Choo KHA (2000) Survivin and the inner centromere protein INCENP show similar cell-cycle localization and gene knockout phenotype. *Curr Biol* 10: 1319–1328.
- Venetis C, Theologidis I, Zouros E, Rodakis GC (2006) No evidence for presence of maternal mitochondrial DNA in the sperm of *Mytilus galloprovincialis* males. *Proc Biol Sci* 273: 2483–2489.
- Venetis C, Theologidis I, Zouros E, Rodakis GC (2007) A mitochondrial genome with a reversed transmission route in the Mediterranean mussel *Mytilus galloprovincialis*. *Gene* 406: 79–90.
- Verhagen AM, Coulson EJ, Vaux DL (2001) Inhibitor of apoptosis proteins and their relatives: IAPs and other BIRPs. *Genome Biol* 2: REVIEWS3009.
- Volodina N, Denegre JM, Mowry KL (2003) Apparent Mitochondrial Asymmetry in *Xenopus* Eggs. *Dev Dynam* 226: 654–662.
- Wang G, Yan S (1992) Mitochondrial DNA content and mitochondrial gene transcriptional activities in the early development of loach and goldfish. *Int J Dev Biol* 36: 477–482.
- Weissman AM (2001) Themes and variations on ubiquitylation. *Nature Rev Mol Cell Biol* 2: 169–178.
- Williamson A, Lehmann R (1996) Germ Cell Development in *Drosophila*. *Annu Rev Devel Biol* 12: 365–391.
- Woods FH (1931) History of the germ cells in *Sphaerium striatinum* (Lam.). *J Morphol* 51: 545–595.
- Wylie C (1999) Germ cells. *Cell* 96: 165–174.

- Xu J (2005) The inheritance of organelle genes and genomes: patterns and mechanisms. *Genome* 48: 951–958.
- Yi R, Poy MN, Stoffel M, Fuchs E (2008) A skin microRNA promotes differentiation by repressing ‘stemness’. *Nature* 452: 225–229.
- Zhang XD, Gou DW, Miao SY, Zhang JC, Zong SD, Wang LF (2003) Cloning and characterization of a novel rat gene RSD-7 differentially expressed in testis. *Zhongguo Yi Xue Ke Xue Yuan Xue Bao. Acta Academiae Medicinae Sinicae.* 25: 289–293.
- Zhang YZ, Ouyang YC, Hou Y, Schatten H, Chen DY, Sun QY (2008) Mitochondrial behavior during oogenesis in zebrafish: A confocal microscopy analysis. *Develop Growth Differ* 50: 189–201.
- Zhou RR, Wang B, Wang J, Schatten H, Zhang YZ (2010) Is the mitochondrial cloud the selection machinery for preferentially transmitting wild-type mtDNA between generations? Rewinding Müller’s ratchet efficiently. *Curr Genet* 56: 101–107.
- Zouros E (2000) The exceptional mitochondrial DNA system of the mussel family Mytilidae. *Genes Genet Syst* 75: 313–318.
- Zouros E, Oberhauser Ball A, Saavedra C, Freeman KR (1994a) Mitochondrial DNA inheritance. *Nature* 368: 818.
- Zouros E, Oberhauser Ball A, Saavedra C, Freeman KR (1994b) An unusual type of mitochondrial DNA inheritance in the blue mussel *Mytilus*. *Proc Natl Acad Sci U S A* 91: 7463–7467.

Papers published during the three years of my PhD

Doubly Uniparental Inheritance (DUI):

- Breton S, Ghiselli F, Passamonti M, **Milani L**, Stewart DT, Hoeh WR (2010) Evidence for a Fourteenth mtDNA-Encoded Protein in the Female-Transmitted mtDNA of Marine Mussels (Bivalvia: Mytilidae). PLoS ONE, 6(4): e19365.
- Ghiselli F, **Milani L**, Passamonti M (2011) Strict sex-specific mtDNA segregation in the germline of the DUI species *Venerupis philippinarum* (Bivalvia Veneridae). Molecular Biology and Evolution, 28: 949-961.
- Passamonti M, Ricci A, **Milani L**, Ghiselli F (2011) Mitochondrial genomes and Doubly Uniparental Inheritance: new insights from *Musculista senhousia* sex-linked mitochondrial DNAs (Bivalvia Mytilidae). BMC Genomics, 12: 442. doi:10.1186/1471-2164-12-442.
- Ghiselli F, **Milani L**, Chang PL, Hedgecock D, Davis JP, Nuzhdin SV, Passamonti M (2012) *De Novo* Assembly of the Manila clam *Ruditapes philippinarum* Transcriptome Provides New Insights into Expression Bias, Mitochondrial Doubly Uniparental Inheritance and Sex Determination. Molecular Biology and Evolution, 29: 771-786.
- **Milani L**, Ghiselli F, Maurizii MG, Passamonti M (2011) Doubly Uniparental Inheritance of Mitochondria as a Model System for Studying Germ Line Formation. PLoS ONE, 6(11): e28194.
- **Milani L**, Ghiselli F, Passamonti M (2012) Sex-linked mitochondrial behavior during early embryo development in *Ruditapes philippinarum* (Bivalvia Veneridae) a species with the Doubly Uniparental Inheritance (DUI) of mitochondria. Journal of Experimental Zoology Part B, in press.

Reproductive biology, speciation mechanisms and description of stick insects (Phasmida):

- **Milani L**, Scali V, Passamonti M (2009) The *Clonopsis gallica* puzzle: Mendelian species, polyploid parthenogens with karyotype re-diploidisation and clonal androgens in Moroccan stick insects. *Journal of Zoological Systematics and Evolutionary Research*, 47: 132-140.
- Scali V, **Milani L** (2009) New *Clonopsis* stick insects from Morocco: the amphigonic *C. felicitatis* sp.n., the parthenogenetic *C. soumiai* sp.n., and two androgenetic taxa. *Italian Journal of Zoology*, 76: 291-305.
- **Milani L**, Ghiselli F, Pellecchia M, Scali V, Passamonti M (2010) Reticulate evolution in stick insects: the case of *Clonopsis* (Insecta Phasmida). *BMC Evolutionary Biology*, 10: 258.
- Scali V, **Milani L**, Passamonti M (2010) *Clonopsis gallica*, a stick insect parthenogen exploiting different egg maturation mechanisms over its range. *Invertebrate Reproduction and Development*, 54:143-150.
- Scali V, **Milani L**, Passamonti M (2012) Revision of the stick insect genus *Leptynia*: description of new taxa, speciation mechanism and phylogeography. *Contributions to Zoology*, 81: 25-42.